Understanding the independent and combinatory effects of radiation therapy and doxorubicin on endothelial cell function – the role of JNK

Gillian Hargrave

A thesis submitted in fulfilment of the requirements for the degree of Doctor of Philosophy

Strathclyde Institute of Pharmacy and Biomedical Sciences

University of Strathclyde

2017

‘This thesis is the result of the author’s original research. It has been composed by the author and has not been previously submitted for examination which has led to the award of a degree.’

Signed:
Date:

Acknowledgements

I would firstly like to thank my supervisors Robin Plevin and Marie Boyd for giving me the opportunity to undertake my PhD within SIPBS and for guiding me through my research and writing my thesis. I would also like to thank the British Heart Foundation for providing the funding for my research.

Several people helped me greatly throughout my research including Katy, who I would like to thank for her patience and guidance. I would also like to thank Tony for his help during my project. A massive thank you to Rachel for making my time in the lab more enjoyable and being a friend that I could talk to. I would also like to acknowledge the rest of my lab team for all of their support.

Lastly, I would like to thank my family for getting me through this very challenging time.

Poster Communications

84th European Atherosclerosis Congress, Congress Innsbruck, Austria, 29th May-1st June 2016.

4th British Heart Foundation Fellows Meeting, Queen's College, Cambridge, UK, 28-29th September 2015.

British Society for Cardiovascular Research Autumn Meeting 'Cardiovascular Signalling in Health and Disease', University of Reading, UK, 8-9th September 2014.

Publications

Hargrave, G. (2014). Understanding the effects of cancer radiation therapy on endothelial cell dysfunction – the role of NFκB/JNK. *Heart.* **100**:A7.

Abstract

A number of epidemiological studies have associated anticancer therapy with an increased risk of cardiovascular disease in later life, a concern for patient long-term survival. Survivors of childhood cancer, previously administered radiotherapy, display chronic arterial damage including endothelial cell dysfunction, a defining feature of atherosclerosis (Brouwer *et al*., 2013). This thesis aimed to characterise the effects of radiation therapy (X-rays) and the cardiotoxic chemotherapeutic drug doxorubicin, alone or in combination, on coronary artery endothelial cell viability and function. The role of stress-activated c-Jun N-terminal kinase (JNK) in therapy-mediated endothelial cell dysfunction was also elucidated.

Survival assays, employed to assess the effects of single-agent therapy, demonstrated that doxorubicin causes concentration-dependent death of human coronary artery endothelial cells (HCAECs) and X-irradiation inhibits HCAEC clonogenic survival dose-dependently. Using fluorescence-activated cell sorting (FACS), the ability of doxorubicin to arrest HCAECs in the radiosensitive G2/M phase of the cell cycle after a period of 24 hours was identified. Nonetheless, when doxorubicin and X-rays were used in combination, synergy between the two agents was not observed, an additive effect on HCAEC clonogenic survival was detected at the specific concentration (1 μM doxorubicin) and dose (1 Gy X-rays) studied. JNK was moderately activated by doxorubicin and played a partial role in the G2/M arrest of HCAECs by doxorubicin. Surprisingly, X-irradiation poorly activated JNK, thus JNK does not appear to play a major role in endothelial cell dysfunction post-therapy with these anticancer agents.

The data collated in this thesis provides an insight into the endothelial cell dysfunction and death elicited by anticancer agents, doxorubicin and X-rays, contributing to vascular wall destruction and development of atherosclerosis post-cancer therapy.

Table of contents

List of figures

Abbreviations

7-AAD	7-aminoactinomycin D
ApoE	Apolipoprotein E
ANOVA	Analysis of variance
APC	Allophycocyanin
AT	Ataxia telangiectasia
ATM	Ataxia telangiectasia mutated
ATP	Adenosine triphosphate
ATR	Ataxia telangiectasia and RAD-3-related protein
Bad	Bcl-2-associated death promoter
Bax	Bcl-2 homologous antagonist/killer
Bcl-2	B-cell lymphoma 2
BSA	Bovine serum albumin
CAD	Coronary artery disease
cdc	Cell division cycle
CDK	Cyclin-dependent kinase
CHK	Checkpoint kinase
CI	Combination index
DMEM	Dulbecco's modified eagle medium
DMSO	Dimethyl sulfoxide
DN	Dominant negative
DNA	Deoxyribonucleic acid
DSB	Double-strand break
DTT	Dithiothreitol
EBM-2	Endothelial Basal Medium-2
ECL	Enhanced chemiluminescence
EDTA	Ethylenediaminetetraacetic acid
EGF	Epidermal growth factor
EGFR	Epidermal growth factor receptor
Em-max	Emission maximum

ERK	Extracellular regulated kinase
Ex-max	Excitation maximum
FACS	Fluorescence-activated cell sorting
FBS	Fetal bovine serum
FCS	Fetal calf serum
FGF	Fibroblast growth factor
FITC	Fluorescein isothiocyanate
GA-1000	Gentamycin Sulfate Amphotericin-B
GAPDH	Glyceraldehyde 3-phosphate dehydrogenase
GSH	Glutathione sepharose
GST	Glutathione-S-transferase
Gy	Gray
H_2O_2	Hydrogen peroxide
HCAECs	Human coronary artery endothelial cells
HUVECs	Human umbilical vein endothelial cells
ICAM-1	Intercellular adhesion molecule-1
IFN-γ	Interferon-gamma
IGF	Insulin-like growth factor
IL-1β	Interleukin-1β
IOERT	Intraoperative electron radiation therapy
IR	Irradiation
JNK	c-Jun N-terminal kinase
KO	Knockout
LAD	Left anterior descending coronary artery
LDL	Low density lipoprotein
MAPK	Mitogen-activated protein kinase
MAPKK/MEK	MAP kinase
MAPKKK/MEKK	MAP kinase kinase
MCF-7	Michigan Cancer Foundation-7
MEM	Minimum essential medium
MMP	Metalloproteinase

mRNA	Messenger ribonucleic acid
miRNA	MicroRNA
MTT	3-(4,5-dimethylthiazol-2-yl)-2,5-diphenyltetrazolium bromide
NAC	N-acetylcysteine
NO	Nitric oxide
oxLDL	Oxidised low-density lipoprotein
PBS	Phosphate buffered saline
PDGF	Platelet-derived growth factor
PE	Phycoerythrin
PECAM-1	Platelet endothelial cell adhesion molecule-1
PI	Propidium iodide
PI3K	Phosphatidylinositol 3-kinase
PKC	Protein kinase C
PMSF	Phenylmethanesulfonyl fluoride
Q	Quadrant
REF	Radiation enhancement ratio
RIP	Receptor interacting protein
RNA	Ribonucleic acid
ROS	Reactive oxygen species
SAPK	Stress-activated protein kinase
SDS	Sodium dodecyl sulphate
SDS-PAGE	Sodium dodecyl sulphate polyacrylamide gel electrophoresis
S.E. mean	Standard error of the mean
Ser	Serine
SF	Surviving fraction
SP600125	Anthra[1, 9-cd]pyrazol-6(24)-one
SSB	Single-strand break
TEMED	N, N, N', N'-tetramethylenediamine
Thr	Threonine
TNF-α	Tumour necrosis factor-alpha
TOPO-II	Topoisomerase- II

Tyr	Tyrosine
UVC	Ultraviolet type C
UVW	Human glioblastoma cell line
VCAM-1	Vascular cell adhesion molecule-1
VEGF	Vascular endothelial cell growth factor
VSMC	Vascular smooth muscle cell
WT	Wild-type

Chapter 1:

General introduction

1.1 Introduction

Cardiovascular disease is the principal cause of mortality worldwide, as acknowledged by the World Health Organisation (WHO). Recent data collated by the American Heart Association (AHA) revealed that cardiovascular disease was accountable for 31.5% of deaths worldwide in 2013, equivalent to 17.3 million fatalities (Benjamin *et al*., 2017). Cardiovascular disease is a severe economic burden, costing the United States between 2012 and 2013 $316.1 billion in direct healthcare costs and indirect loss of future productivity (Benjamin *et al*., 2017). Numerous epidemiological studies have identified an increased risk of cardiovascular disease in patients previously administered anticancer therapy (Haugnes *et al*., 2010, Killander *et al*., 2014), this is of great concern in both the fields of cardiovascular biology and oncology. Improved cancer treatment methods have enabled greater patient survival rates however this has amplified the population of patients at risk of developing late-onset cardiovascular disease. Thus, understanding the link between anticancer therapy and cardiovascular disease, such as atherosclerosis, is essential to improve patient long-term survival, this is the focus of this thesis.

1.2 Pathogenesis of atherosclerosis

Atherosclerosis, a disease of medium and large-sized arteries, contributes to hypertension, coronary heart disease and thrombosis leading to potentially fatal myocardial infarction or stroke (Sun *et al*., 2013[1]). Key events involved in the pathogenesis of atherosclerosis have been studied extensively over the last few decades. Before 1970, lipid-associated atherosclerosis dominated researchers perceptions of arterial damage. Further research between the 1970s and 1980s identified excessive smooth muscle proliferation as a key event in assembly of the atherosclerotic plaque. However, during the last few decades cumulative investigations have established a role for endothelium dysfunction and consequential chronic inflammation in atherogenesis (Libby. 2002).

1.2.1 The role of endothelium dysfunction in atherosclerosis

Atherosclerosis development progresses slowly within arterial lumens and is characterised by a continual local inflammatory response. Vascular endothelial cells form a mono-layer throughout the interior of the cardiovascular system where they perform a critical role in vascular homeostasis. Physiological roles of endothelial cells include sustaining relaxed vessel tone, by secreting factors such as nitric oxide (NO) and preventing oxidative stress (Sitia *et al*., 2010). Additionally, the endothelium controls blood clotting, aids immune responses via neutrophil recruitment and regulates fluid filtration (Rajendran, *et al.*, 2013). Exposure of the endothelium to a range of insults such as oxidative stress, hyperglycemia and shear stress can promote dysregulation of endothelial cell function (Sun *et al*., 2013[1]). Dysfunctional endothelial cells preferentially exhibit pro-inflammatory and pro-thrombotic characteristics with diminished control of vascular relaxation (Rajendran *et al*., 2013). Individuals with a high risk of developing cardiovascular disease have been shown to exhibit dysfunctional endothelium before presenting clinical symptoms of atherosclerosis (Sitia *et al*., 2010). These patients display limited responses to the vasodilators bradykinin and acetylcholine (Sitia *et al*., 2010). Therefore, abnormal functioning of endothelial cells is strongly implicated in atherosclerosis progression.

Injury to the endothelium initiates a cascade of damaging events. Noxious stimuli provoke increased expression of adhesion molecules on endothelial cells which bind leukocytes (Sun *et al*., 2013[1]). In the 1990s, Li *et al*., originally identified that rabbits fed a cholesterol-rich diet display increased focal endothelial expression of vascular cell adhesion molecule-1 (VCAM-1) in their ascending aorta after 7 days (Li *et al*., 1993). Thereafter Scalia *et al*., demonstrated that intracellular adhesion molecule-1 (ICAM-1) and P-Selectin, in addition to VCAM-1, are upregulated on the intestinal microvascular endothelium of rabbits fed a high cholesterol diet (Scalia *et al*., 1998). E-selectin is a further adhesion molecule implicated in leukocyte interactions with damaged endothelium (Libby. 2002). Captured leukocytes migrate between the junctions of injured endothelial cells, a process recognized as diapedesis, and enter the underlying tunic intima. Endothelial cell death, as a result of apoptosis or non-apoptotic mechanisms such as necrosis, diminishes the integrity of the endothelial

barrier facilitating transmigration of monocytes during atherogenesis (Rombouts *et al*., 2013). The membrane blebs of apoptotic endothelial cells are rich in oxidized phospholipids, which promote the adhesion of monocytes, and phosphatidylserine, a pro-coagulant, is expressed on the membrane of apoptotic endothelial cells encouraging thrombus formation (Rombouts *et al*., 2013). Furthermore, the expulsion of intracellular inflammatory mediators during endothelial necrotic cell death contributes to the inflammatory environment at the atherogenic site (Libby. 2002, Rombouts *et al*., 2013). The increased permeability of the endothelium, as a result of endothelial cell contraction or cell death, enables low-density lipoprotein (LDL) particles to amass within the arterial wall, as illustrated in Figure 1.1 (Sun *et al*., 2013[1]). Monocytes occupying the arterial intima evolve features of macrophages by increasing expression of scavenger receptors which promote internalisation of oxidised lipoproteins (oxLDL) leading to the formation of macrophage foam cells (Libby. 2002). The preliminary study by Li *et al*., found that rabbits fed an atherogenic diet for three or more weeks accrued intimal lesions comprised of macrophages expressing class II major histocompatibility antigen (MHC-II) (Li *et al*., 1993). Foam cells accumulate and replicate within the atheroma and secrete further inflammatory factors such as cytokines, growth factors and metalloproteinases, thus amplifying the local inflammatory response (Libby. 2002).

Lesion development requires proliferation of smooth muscle cells within the underlying tunica media, construction of a lipid core and assembly of a collagen rich fibrous cap (Sun *et al*., 2013[1]). Vascular complications, such as angina, arise as the atherosclerotic plaque enlarges, narrowing lumen diameter and disturbing blood flow. Additionally, thrombosis due to rupture of the plaque can cause myocardial infarction or stroke. The chronic inflammatory environment is reported to inhibit production of collagen by smooth muscle cells and accumulated macrophages at the atheroma generate matrix metalloproteinases (MMPs) which degrade collagen (Libby. 2002). Peter Libby and his team reported increased MMP-2 and MMP-9 expression at human atherosclerotic lesions localized to the fibrous cap, shoulders of the lesion and at the base of the lipid core; an increase in MMP-2 and MMP-9 activity was also detected

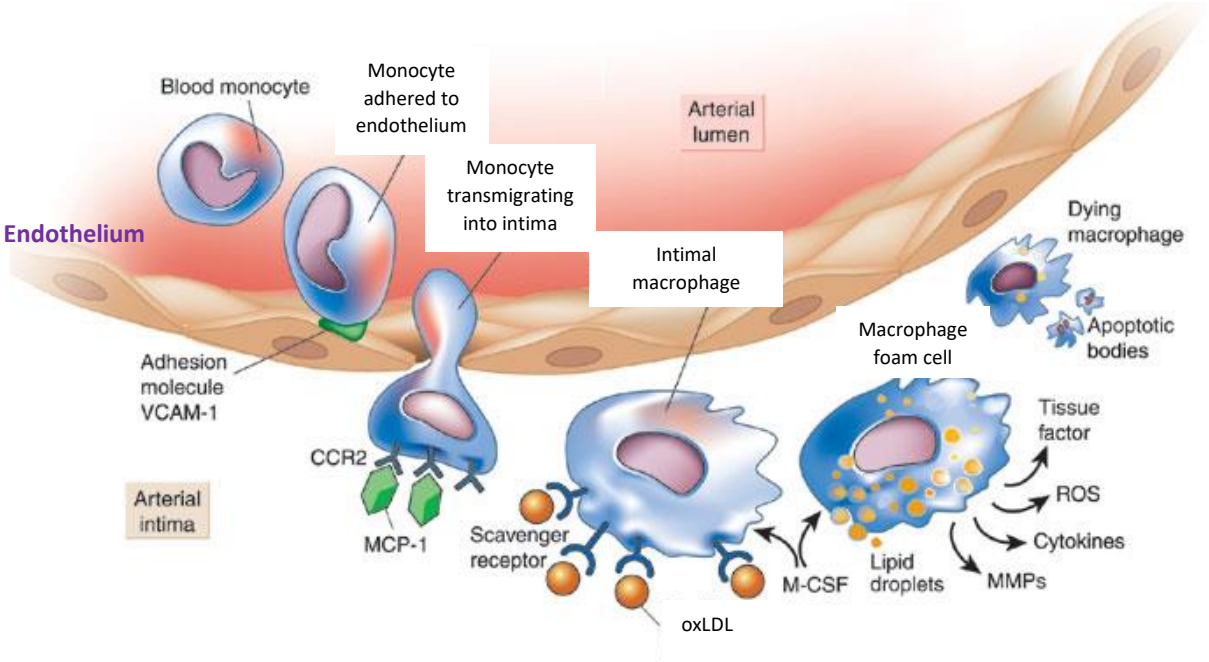

(adapted from Libby. 2002)

Figure 1.1: Overview of the sequential events involved during early atherogenesis. Post-insult the structure of the endothelium is compromised and endothelial cells increase adhesion molecule expression. Luminal monocytes adhere to adhesion molecules and transverse through the perturbed endothelial barrier into the arterial intima. Migration of monocytes (diapedesis) requires a chemoattractant gradient established by the presence of chemokines within the arterial intima such as monocyte chemotactic protein-1 (MCP-1). Diapedesis precedes uptake of oxidized lipoproteins (oxLDL) by macrophages resulting in the generation of foam cells which secrete strong inflammatory mediators.

within these regions (Galis *et al*., 1994). Interstitial collagenase (MMP-1) was also found to reside in the luminal endothelium encasing the plaque, implicating collagenases in extracellular matrix degradation too (Galis *et al*., 1994). Consequently, the structure of the fibrous cap is compromised and liable to rupture (Libby. 2002). Atherosclerotic lesions occur at locations experiencing disturbed blood flow such as vessel branch points hence rupture of the arterial plaque is highly probable. It is evident that the development of atherosclerosis is multi-factorial with potentially fatal outcomes.

1.3 Radiotherapy

Radiation therapy is a widely-used tool for the control and eradication of cancerous tumours, including breast malignancies, but it is linked to cardiovascular damage in treated patients. Prior to 1950, low-voltage X-ray generators, employed for radiotherapy, had restricted depth-dose capacity thus exposure to the heart and surrounding vessels was limited (Sardo *et al*., 2012). In the 1950s, the invention and use of megavoltage generators resulted in increased radiation exposure to the heart, the cardiovascular complications of radiotherapy became evident in the 1960s but the magnitude of radiotherapy toxicity to the heart was only universally recognised in the 1990s (Sardo *et al*., 2012). New radiotherapy techniques have been devised to minimise non-target tissue exposure such as high energy beams, contouring techniques and more-recently respiratory-gated radiotherapy (Becker-Scheibe *et al*., 2016, Sardo *et al*., 2012). Taylor *et al*., observed a decline in the total mean radiation dose to the left anterior descending coronary artery (LAD) in women treated with tangential radiotherapy for left-sided breast cancer over the last several decades as a result of improved radiotherapy techniques; 31.8, 21.9 and 7.6 Gy for women treated in the 1970s, 1990s and 2006 respectively (Taylor *et al*., 2008). Today cancer treatment strategies are tailored to specific patient requirements in order to achieve the best clinical outcome, with least adverse effects to normal tissue. However, some exposure to the heart and vasculature is unavoidable particularly during radiation therapy for left-sided breast cancer (Becker-Scheibe *et al*., 2016, Sardo et al., 2012).

1.3.1 Radiotherapy-related cardiovascular disease

Worldwide epidemiological studies have reported an association between radiotherapy treatment for cancer and cardiovascular disease. Studying survivors of the atomic bomb in Hiroshima post-nuclear disaster provided vital evidence that radiation exposure detrimentally affects the vasculature. Elevated mortality from cardiovascular disease has been reported in survivors of the atomic bomb (Hayashi *et al.,* 2005). A study of 2436 survivors exposed to up to 2 Gy radiation reported increased blood concentrations of the inflammatory cytokine interferon-γ in survivors (IFNγ) (Hayashi *et al*., 2005). This study was conducted greater than 50 years post-disaster occurrence thus proving that radiation can promote a chronic inflammatory environment within the vasculature. The altered vessel environment was associated with elevated erythrocyte sedimentation rate, a marker for atherosclerosis, further highlighting the link between radiation and a pro-atherosclerotic vessel environment (Hayashi *et al*., 2005).

In relation to cardiovascular disease as a consequence of radiation therapy for cancer, breast cancer radiotherapy is strongly linked with cardiac damage due to the close proximity of the heart and breast tissue. Data gathered from approximately 90,000 Swedish women treated with radiotherapy for breast cancer found equivalent death rates from cancer in women treated with left or right breast tumours (Darby *et al*., 2003). However, fatalities from cardiovascular disease were greater in women treated for left-sided breast tumours, relative to right-sided (Darby *et al*., 2003). Targeting the left breast with radiotherapy results in a higher radiation dose to heart, consequently promoting greater cardiovascular damage and cardiovascular-related death.

There is also grave concern about radiotherapy treatment of children and young adults and long-term damaging radiation effects. Hodgkin's lymphoma is predominantly diagnosed in individuals under the age of thirty (Wethal *et al*. 2014). Wethal *et al.*, conducted a study which evaluated lasting damaging effects of radiotherapy in Hodgkin's lymphoma survivors. Hodgkin's lymphoma survivors assessed were treated at the Norwegian Radium Hospital from 1980 to 1988 with

mantle field radiotherapy, some patients were also administered anthracycline chemotherapy treatment including doxorubicin (Wethal *et al*., 2014). Radiotherapy was delivered in 1.8 or 2 Gy fractions with a cumulative dose of 40 Gy administered (Wethal *et al*., 2014). A follow up, 18 to 27 years post-treatment, assessed the prevalence of atherosclerotic lesions in pre-cranial arteries, such as the left and right subclavian arteries and common carotid arteries, by CT angiography. These investigations revealed that the number of atherosclerotic lesions in 43 Hodgkin's lymphoma survivors was doubled relative to 43 non-irradiated control subjects, 141 and 73 lesions respectively (Wethal *et al*., 2014). Therefore, this study concluded that radiotherapy promotes internal vascular damage, promoting atherosclerosis development. Numerous other studies have identified a link between the use of radiotherapy, alone or in combination with chemotherapy, for the treatment of cancer and abnormal functioning of the cardiovascular system (Table 1.1). Hence it is critically important to understand the mechanisms responsible for altered vessel function following radiotherapy, including modifications of cellular function within arteries.

1.3.2 Mechanisms of radiotherapy toxicity

Cancer radiotherapy techniques expose patients to hazardous levels of ionizing radiation. The amount of energy deposited in human tissue is referred to as the 'absorbed dose', this is quantified in dose units called gray (Gy) (Brenner *et al*., 2007). The unit gray is identified as one joule of radiation energy per one kilogram of living tissue (Baker *et al*., 2011). To estimate the harm a patient may suffer post-radiation exposure, the weighted measurement 'effective dose' is referred to, this varies with different types of radiation and is quantified in the unit called Sievert (Sv) (Baker *et al*., 2011, Brenner *et al*., 2007). X-rays and γ-rays are the predominant types of ionizing radiation applied in medicine, for both types of radiation Gy and Sv are equal (1 Gy is equivalent to 1 Sv) (Borghini *et al.,* 2013). Ionizing radiation is a highly energetic form of electromagnetic radiation which can eject orbital electrons from atoms resulting in the formation of extremely reactive ions (Brenner *et al*., 2007). X-rays targeted at cells can react with water molecules resulting in the formation of hydroxyl radicals which cause damage to DNA structure (Brenner *et al*., 2007). DNA

Cancer type	Treatment	Time post-treatment	Risk of cardiovascular disease	Study
Unilateral testicular cancer	**Radiotherapy**	**13-28 years** (average 19 years)	**2.3-fold increased risk of atherosclerotic disease event** (compared to surgery alone)	**Haugnes *et al.*, 2010**
	Radiotherapy + Chemotherapy (primarily cisplatin based)		**4.8-fold increased risk of atherosclerotic disease event** (compared to surgery alone)	
Hodgkin's Disease	**Radiotherapy** (mediastinal) *(*4 patients also a administered anthracycline)	**≥ 5 years**	**42.6% of patients had at least one valve abnormality**	**Adams *et al*., 2004**
Acute Lymphoblastic Leukemia (ALL)	**Chemotherapy alone**	**average 20.8 years**	**0% of patients displayed hypertension**	
	Radiotherapy + Chemotherapy		**6.3% of patients displayed hypertension** (1.4% of control subjects displayed hypertension)	**Geenen *et al*., 2010**
Wilm's tumour	**Chemotherapy alone**		**4% of survivors presented with hypertension**	
	Radiotherapy + Chemotherapy		**21.6% of survivors presented with hypertension** (1.4% of control subjects)	
Breast cancer	*Pre-menopausal** **Chemotherapy alone**	**25 years**	**0% of patient deaths due to heart disease**	**Killander *et al*., 2014**
	Radiotherapy + Chemotherapy (cyclophosphamide)		**0.8% of patient deaths due to heart disease** (4 cases)	
	*Post-menopausal** **Chemotherapy alone**		**10.5% mortality from heart disease**	
	Radiotherapy + Chemotherapy (tamoxifen)		**18.4% mortality from heart disease**	

Table 1.1: Epidemiological evidence of radiotherapy-related cardiovascular disease.* post-masectomy

damage includes both single and double-strand DNA breaks, DNA strand cross-linkage and base oxidation (Parylps *et al.*, 2012). DNA double-strand breaks (DSB) are recognized as the most lethal, as they are least easily repaired, however they occur in much lower frequency post-radiation exposure than single-stand breaks (SSB) and base damage (Parylys *et al*., 2012). Thus, the fatal effects of multiple minor DNA modifications appear to be underestimated. X-rays may also directly interact with and ionize molecules of the DNA double helix to promote damage (Brenner *et al*., 2007). Unsuccessful repair of DNA fractures beneficially halts cancer cell division, however resultant gene mutations from radiation-induced DNA damage can promote secondary cancers (Brenner *et al*., 2007). Despite the unwanted effects of DNA damage, ionizing radiation is an essential tool in the treatment of cancer patients, it damages DNA and a high radiation dose can be directly targeted at a specific location in the body (Chorna *et al*., 2004).

1.3.3 Radiation-induced atherosclerosis

The association between radiation exposure and atherosclerosis has been implicated by several experimental studies. ApolipoproteinE$^{-/-}$ (ApoE$^{-/-}$) mice are a useful tool to study radiation-associated atherosclerosis development (Gabriels *et al*., 2012). Cholesterol levels are raised in these mice and they incur atherosclerosis associated with aging, hence dissimilar results observed between the irradiated mice and control ApoE$^{-/-}$ mice can only be accounted for by radiation exposure. Gabriels *et al*., found a significantly elevated presence of coronary atherosclerotic lesions in the mid-part of the heart 20 weeks after local heart X-irradiation with 16 Gy (Gabriels *et al*., 2012). Stewart *et al*., observed an increase in the number of both male and female ApoE$^{-/-}$ mice with carotid artery lesions densely populated with leukocytes following X-irradiation (14 Gy) (Stewart *et al*., 2006). In this study both male and female ApoE$^{-/-}$ mice populations displayed abnormal, swollen endothelial cells in the carotid artery 22 weeks after exposure of the neck region to 14 Gy radiation (Stewart *et al*., 2006). Stewart *et al*., identified that the use of a single dose of 14 Gy is not clinically relevant and aim to elucidate the effect of daily, fractionated 2 Gy radiation doses on atherosclerosis development. More *in vivo* research is required to establish the effects of therapy-relevant doses on the endothelium.

Experimental research focusing on the cellular effects of ionizing radiation on endothelial cell function has investigated endothelial cell adhesion molecule expression as it is a key event in atherogenesis. Exposure of human umbilical vein endothelial cells (HUVECs) to 2 Gy X-rays significantly elevated the number of cells expressing E-selectin (20-fold increase after 4 hours) (Hallahan *et al*., 1996). ICAM-1 transcription was also instigated by exposure to ionising radiation with maximum expression reached 24 hours after exposure. Studies have also generated evidence relating radiation exposure and impaired endothelial cell relaxant functions. Following pre-contraction of neck cervical arteries with noradrenaline, acetylcholine-induced arterial relaxation was inhibited by approximately 67% in irradiated patient arteries compared to control arteries (Sugihara *et al.*, 1999). This study also observed significant thickening of the tunica media of irradiated arteries compared to controls, mean tunica media thickness for irradiated and control arteries were 315.3 μm and 225.3 μm respectively (Sugihara *et al*., 1999). Collectively these results demonstrate an altered structure at the radiation-exposed arterial wall with associated endothelial cell dysfunction.

Unexpectedly some evidence suggests that low therapeutic doses of radiation have a protective effect by inhibiting atherosclerosis development. Exposure to doses less than 1 Gy have been shown to attenuate E-selectin expression hence reducing leukocyte-endothelial cell interactions (Stewart *et al*., 2013). Additionally, hypercholesterolaemic mice which experienced whole body exposure of less than 0.5 Gy displayed less atherosclerotic lesions than before irradiation (Mitchel *et al*., 2011). However, irradiation of hypercholesterolaemic animals with 2 Gy or higher has been shown to increase atherosclerotic plaque numbers (Stewart *et al*., 2013). These findings suggest that only doses above 2 Gy promote the pathogenesis of atherosclerosis and are associated with radiation-induced cardiovascular disease such as myocardial infarction and stroke. This assumption is contradicted by data from survivors of the atomic bomb. Increased deaths from cardiovascular disease were observed in survivors exposed to between 0 and 4 Gy irradiation (Senkus-Konefka *et al*., 2007). Furthermore, as previously incited, an increased inflammatory phenotype was observed in atomic bomb survivors exposed to up to 1.5 Gy radiation (Hayashi *et*

al., 2005). Overall these findings illustrate a clear link between radiation exposure and atherosclerosis, more research is required to establish the potential harmful effects of modern radiotherapy techniques where patients experience low radiation exposure.

1.4 Doxorubicin

Modern cancer treatment involves the use of radiotherapy or chemotherapy or both used in combination, there is considerable evidence for chemotherapy-mediated cardiovascular disease too. Anthracycline chemotherapeutic agents are predominantly employed for breast cancer treatment in North America and in Europe, breast cancer survival rates of greater than 70% have been attributed to the use of anthracycline chemotherapeutic drugs post-surgery (Kanno *et al*., 2014, Mandilaras *et al.*, 2015). Doxorubicin hydrochloride, trade name 'Adriamycin', is the most extensively administered anthracycline antibiotic and is utilised in the treatment of lymphomas, soft tissue sarcomas, haematological cancers and endocrine resistant or metastasised breast cancer (Kanno *et al*., 2014, Kim *et al*., 2009 and Spallarossa *et al*., 2010). Doxorubicin hydrochloride (referred hereafter as doxorubicin), and related anthracylines including daunorubicin and epirubicin, are generated by the bacterium *Streptomyces peucetius var. caesius* (Octavia *et al.*, 2012). Doxorubicin was initially isolated from this bacterium in 1967, and became a useful cancer cell killing agent thereafter (Carvalho *et al*., 2014).

Doxorubicin administered intravenously displays rapid distribution and uptake by tissues succeeded by slow elimination via liver metabolism and biliary excretion (Barpe *et al*., 2010, Ryu *et al*., 2014). The initial distribution half-life of doxorubicin in mice and humans is approximately 5 and 11 minutes respectively (Patel *et al*., 2013). Doxorubicin principally exerts its cytotoxic properties by provoking cancer cell apoptosis (Kim *et al*., 2009). Doxorubicin has several distinct mechanisms of action to promote cancer cell death: 1) doxorubicin intercalates between DNA bases on adjacent strands preventing DNA replication and cancer cell division (as depicted in Figure 1.2), 2) doxorubicin inhibits the enzyme topoisomerase-II (TOPO-II), a nuclear enzyme responsible for cleaving both strands of the DNA double helix to correct

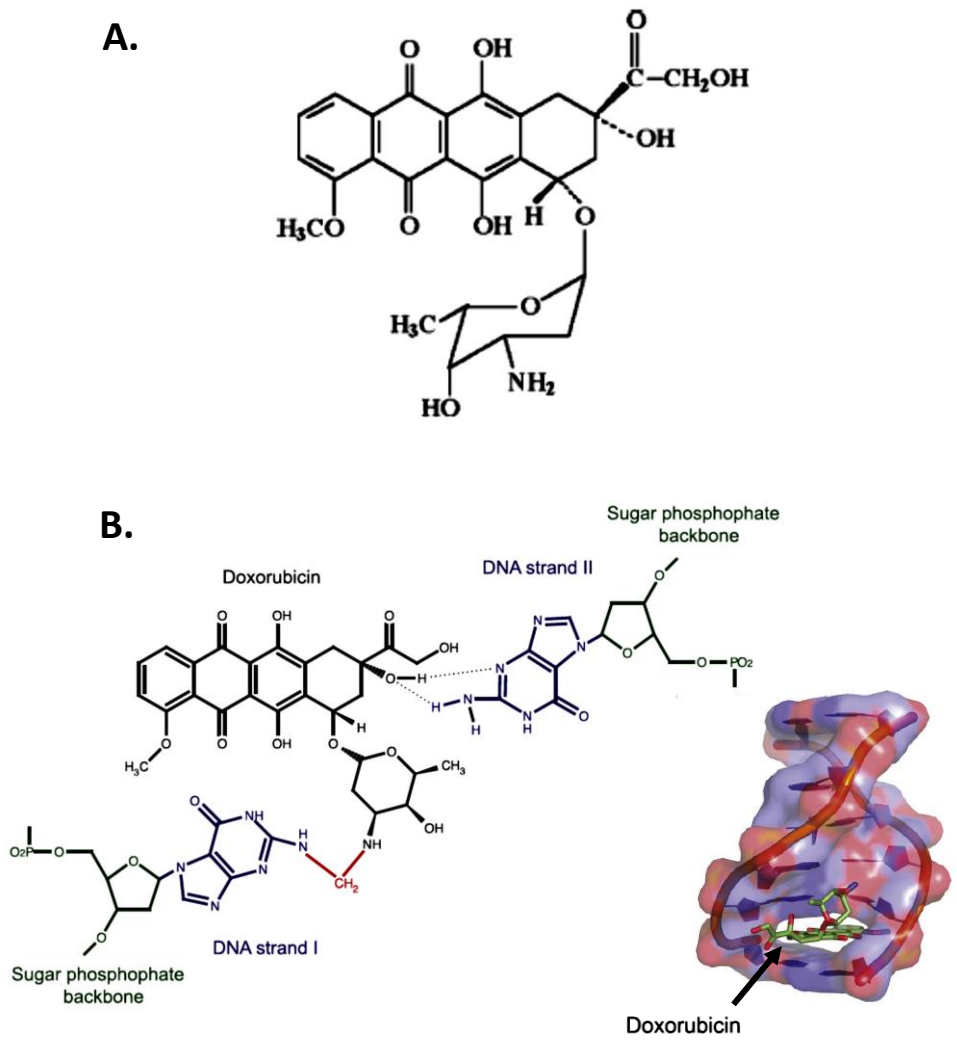

(adapted from Trevisan and Poppi, 2003, Yang *et al*., 2014)

Figure 1.2: Intercalation of doxorubicin within the DNA double helix. A) The chemical structure of doxorubicin depicts a fluorescent napthacenedine core connected at C7 to a hydrophilic aminoglycosidic side chain. **B)** Doxorubicin interacts with DNA by forming a covalent bond with a guanine on one DNA strand (red line) and forming hydrogen bonds with a guanine on the opposite strand (dotted lines).

DNA supercoils and tangles, 3) doxorubicin promotes the production of free radicals which cause oxidative damage to DNA bases (Kim *et al*., 2003, Osman *et al.*, 2012). During free radical production, doxorubicin is oxidized to a semiquinone radical via one-electron addition, catalysed by NAD(P)-oxidoreductases (Ryu *et al*., 2014, Yang *et al*., 2014). Semiquinone radicals react rapidly with oxygen, resulting in the generation of superoxide and hydrogen peroxide (Yang *et al*., 2014). Doxorubicin is not selective for specifically cancer cell DNA therefore the deleterious effects of doxorubicin are not strictly limited to cancer cells and normal cells can be damaged too. In a study by Ren *et al*., investigating the pharmacokinetics of doxorubicin, intratumoral injection of murine H22 hepatoma- bearing mice with doxorubicin (20 mg/kg), an administration method exercised to ensure highest drug concentration at the tumour site, found doxorubicin to be present in lung, liver, spleen, kidney and heart tissue (Ren *et al*., 2014). Hence the use of doxorubicin in cancer patients is associated with several adverse effects such as nausea, vomiting, alopecia, impaired immune function and cardiac toxicity (Octavia *et al*., 2012).

1.4.1 Doxorubicin-mediated cardiovascular damage

Cardiac damage, including cardiomyopathies such as congestive heart failure, pericarditis and sudden cardiac death, is a major limiting factor for the clinical use of doxorubicin (Octavia *et al*., 2012, Yang *et al*., 2013). Interestingly, the detrimental cardiac effects have been observed 10 to 15 years post-doxorubicin treatment, highlighting the chronic damaging effects of doxorubicin (Octavia *et al.*, 2012). Doxorubicin-induced injury to the myocardium is understood to be caused by primarily apoptosis of cardiomyocytes (Chang *et al*., 2011). In experimental studies, doxorubicin promoted the death of chick cardiomyoctes in a time and concentration-dependent manner, 1 µM doxorubicin was shown to cause significant cardiomyocyte death 24 hours post-treatment (Chang *et al*., 2011). Moreover, Seemann *et al*., revealed that treatment of human cardiac myocytes with doxorubicin (up to 250 µg/ml) for 3 days attenuated cardiomyocyte viability in a dose-dependent manner (Seemann *et al*., 2013). During further *in vivo* research by Seemann *et al*., cardiac fibrosis was observed in male C57BL/6 mice treated with doxorubicin (4 mg/kg weekly for 3 weeks), confirming the cardiac toxicity of doxorubicin (Seemann *et al*., 2013).

Several intracellular mechanisms have been proposed to account for doxorubicin-induced death of cardiomyocytes, including the generation of reactive oxygen species (Thorn *et al*., 2011, Chang *et al*., 2014). Doxorubicin metabolism in the mitochondria also promotes mitochondrial deregulation, perturbing respiration and triggering the release of cytochrome-C which activates pro-apoptotic caspases (Thorn *et al*., 2011). Furthermore, an active metabolite of doxorubicin, doxorubicinol (generated by the reduction of doxorubicin by carbonyl reductases and alkoreductases), disrupts iron homeostasis by inhibiting aconitase-iron regulatory protein-1 (ACO1) and doxorubicin itself can interact with iron forming a complex which catalyses the conversion of hydrogen peroxide to extremely reactive hydroxy radicals (Thorn *et al*., 2014, Yang *et al*., 2014). Clearly, cardiac damage is an established adverse effect of doxorubicin and the mechanistics of doxorubicin-mediated cardiac toxicity are well understood.

Surprisingly knowledge of the effects of doxorubicin on the coronary vasculature, including the endothelium, is lacking. A few studies have shown that doxorubicin induces a pro-coagulant phenotype on endothelial cells of the vasculature. Swystun *et al*., demonstrated elevated plasma thrombin generation, within 5 minutes, when defibrinated plasma was incubated with doxorubicin-treated (3 µg/ml) HUVECs (Swystun *et al*., 2009). Furthermore, doxorubicin-treatment of HUVECs (3 µg/ml for 24 hours) increased tissue factor activity, measured by the conversion of Factor X to Factor Xa, and phosphatidylserine expression was raised, in a dose- and time-dependent manner, on doxorubicin-exposed HUVECs, cellular modifications involved in promoting thrombin generation (Swystun *et al*., 2009). In an earlier study, Woodly-Cook *et al*., identified inhibition of the protein C anti-coagulant by doxorubicin; doxorubicin diminished membrane expression of endothelial protein C receptor (EPCR), critical for the conversion of protein C to anti-coagulant enzyme activated protein C (APC) on HUVECs, further demonstrating the enhanced pro-coagulant properties of doxorubicin-treated endothelial cells (Woodley-Cook *et al*., 2006). The effect of doxorubicin on the vital barrier function of the endothelium has also been investigated by Wilkinson *et al.*, where doxorubicin treatment (0.1 µM for 6 hours) was found to disturb tight junctions between human dermal microvascular endothelial

cells (HDMECs), observed by staining tight junction protein zona occluden-1 (ZO-1), leading to increased permeability of the endothelial cell monolayer (Wilkinson *et al*., 2016). Wojcik *et al*., also demonstrated the effect of doxorubicin on the functional capabilities of the endothelium (Wojcik *et al*., 2015). Aortic rings from C57BL/6 mice were treated with doxorubicin (10 μM) for 30 minutes prior to pre-constriction with phenylephrine, thereafter acetylcholine-induced, endothelium-dependent relaxation of was impaired in the doxorubicin-exposed arteries (Wojcik *et al*., 2015). Understanding the intricacies of doxorubicin mediated vascular toxicity is necessary as damage to the vasculature supplying the heart has a profound influence on fatal heart events.

1.5 Combination cancer therapy

Chemotherapeutic agents, such as doxorubicin, serve as vital tools in the multi-modality treatment of cancer. Single-agent therapy often fails due to the attainment of tumour resistance thus the application of additional cytotoxic measures is required to achieve more successful outcomes (Hagtvet *et al* 2011). Chemotherapy and radiotherapy combinations, clinically termed chemoradiotherapy, initially implemented in the late 1960s are deemed superiorly efficacious relative to single therapies owing to: the ability of specific chemotherapeutic drugs to radiosensitize cancer cells, preservation of organ tissue as no pre-surgery is required and radiotherapy targets the primary site of cancer growth whereas chemotherapy kills systemic metastases, this is termed spatial co-operation (Bartelink *et al*., 2002, Neuner *et al*., 2009, Mandilaras *et al*., 2015, Seiwert *et al*., 2007). Table 1.2 details the precise functional mechanisms provided by selective cancer chemotherapeutic drugs resulting in improved cancer cell killing when used in combination with radiation. Currently, the most successful chemoradiotherapy treatment regimens for numerous cancers are being surveyed, regime options include: dose of radiation, use of fractionated radiotherapy, effective drug(s), drug concentration and delivery schedule (Kaffas *et al*., 2014).

Mechanism of action	Explanation	Example	Reference
Damage DNA/alter DNA structure	Synergistic effect with DNA damage induced by ionizing radiation	Cisplatin	Seiwert *et al*., 2007
Prevention of DNA repair	Repair of radiation-induced DNA strand breaks can be hindered by drugs which alter nucleotide/nucleoside metabolism	Gemcitabine	Seiwert *et al*., 2007
Synchronise cells in G2/M phase of cell cycle	G2/M phase most radiosensitive	Paclitaxel Taxanes	Supiot *et al.*, 2005
Affect different stage of cell cycle	Radiation yields optimum damage during mitosis, some chemotherapeutic drugs cause maximal damage during S phase (additive effect)	Doxorubicin 5-fluoruracil	Seiwert *et al*., 2007
Preferentially kill hypoxic cells	Tumour killing improved when radioresistant hypoxic cancer cells are eradicated	Mitomycin C	Seiwert *et al*., 2007
Impede angiogenesis of tumour microvasculature	Tumour growth and metastases requires construction of new blood vessels	VEGF inhibitors, e.g. Gefitinib	Zhang *et al*., 2011
Inhibit receptor tyrosine kinases	Prevent development of tumour microvasculature	Sunitinib	Zhang *et al*., 2011

Table 1.2: Reasons for the use of chemotherapeutic drugs with radiation therapy. Several mechanisms exploited by chemotherapeutic drugs, as listed above, can potentiate the damaging effects of radiation therapy when used in combination.

1.5.1 Clinically practiced combinatory treatments

Various chemo- and radiotherapy combinatory regimes are currently utilised for different cancer types. The platinum analogue, cisplatin, is the most frequently employed chemotherapeutic drug in combinatory regimes (Seiwert *et al*., 2007). Cisplatin binds to DNA nucleophilic regions and crosslinks DNA strands, inhibiting DNA replication and ablating cancer cell division (Seiwert *et al*., 2007). The presence of cisplatin within the DNA double helix at sites of radiation-induced strand breaks also hinders the ability of repair proteins to effectively restore DNA integrity (Seiwert *et al*., 2007). Consequentially, an increase in apoptotic cell death is observed and cisplatin is considered a radiosensitizer (Seiwert *et al*., 2007). A patient trial conducted by Jeremic *et al*., revealed the beneficial effect of combining cisplatin- based chemotherapy with radiation therapy for nasopharyngeal cancer. Cisplatin was delivered at a concentration of 6 mg/m^2 daily to 130 patients plus hyperfractionated radiotherapy (70 fractions, total dose 77 Gy) (Jeremic *et al*., 2000). This study reported an almost 2-fold increased survival of patients treated with chemoradiotherapy 5 years post-treatment, 25% and 46% for radiation alone and chemoradiotherapy respectively (Jeremic *et al.*, 2000). Combinatory administration of cisplatin-containing chemotherapy plus thoracic irradiation is recognised as the customary treatment for unresectable locally advanced non-small cell lung cancer (NSCLC) (Ohe *et al.*, 2004). A phase III trial by Curran *et al*., on NSCLC patients, using cisplatin and vinblastine plus radiation therapy, highlighted the differing outcomes of concurrent and sequential combinatory treatment regimes. Median patient survival duration was greater using the concurrent approach (17 months) compared to sequential (14.6 months) (Curran *et al*., 2011). Similarly, the 5-year survival was superior following concurrent chemoradiotherapy treatment compared to sequential; 16% and 10% respectively (Curran *et al.*, 2011). Notably, toxicity, such as myelosuppression and esophagitis, was more common in the concurrently treated patient group (Curran *et al*., 2011). Hence, thorough consideration is necessary when clinically developing the scheduling of drug and radiation delivery to achieve maximum patient survival with least toxicity.

Cisplatin is considered a chemotherapeutic agent employed for dated multi-agent chemoradiotherapy programmes which included cisplatin, vindesine and mitomycin C combinations (Ohe *et al*., 2004). Newer drugs have been developed, trialled and

implemented in chemoradiotherapy regimens during the last decade including doxorubicin. Doxorubicin is regularly used for the treatment of anaplastic thyroid carcinoma (ATC), a rare rapidly proliferating thyroid tumour with significant metastatic capability (Sherman *et al*., 2011). Surgical resection of ATC is often ineffective attributable to: a poorly-defined tumour outline, adherence of tumour tissue to critical organs in the neck region and metastasis is often highly prevalent at diagnosis (Sherman *et al*., 2011). Therefore, a favourable approach for the treatment of ATC is doxorubicin plus radiation therapy delivered alone or administered post-surgery (Sherman *et al*., 2011). Sherman *et al*., studied ATC patients administered weekly doses of doxorubicin (10 mg/m^2) plus concurrent radiation therapy (median total dose 57.6 Gy) - approximately 50% of patients also underwent surgery (palliative or complete resection) (Sherman *et al*., 2011). Median survival for all patients was 6 months however when the total radiation dose delivered was beyond 60 Gy, survival improved to 14.1 months (Sherman *et al*., 2011). Thus, co-administration of radiation with doxorubicin effectively prolonged ATC patient survival. Therapy for large cell lymphoma continues to be controversial however chemoradiotherapy comprising of doxorubicin is the principal therapy for early stage diffuse B-cell lymphoma (Zhang *et al*., 2013). Zhang *et al*., reported the efficacy of doxorubicin-containing chemoradiotherapy in a study of early stage anaplastic large-cell lymphoma (ALCL) adult sufferers (Zhang *et al*., 2013). Patients received routine CHOP (cyclophosphamide, doxorubicin, vincristine and prednisolone) or CHOP-like treatment (CHOP plus etoposide or bleomycin) prior to fractionated involved-field radiation therapy (average total dose was 46 Gy X-rays delivered in 2 Gy fractions) (Zhang *et al.*, 2013). Complete response rates were found to be superior after the administration of chemotherapy and radiation compared to initial administration of chemotherapy alone - 82.6 and 63% respectively (Zhang *et al*., 2013). Thus, the use of doxorubicin and X-rays in chemoradiotherapy regimes has been proven to be clinically successful.

1.5.2 Chemoradiotherapy and cardiovascular disease risk

The use of chemotherapeutic drugs and radiation in combination, while having an enhanced detrimental effect on cancer cells, may potentiate damage to non-cancerous tissue. This has been proven in long-term survivors of testicular cancer where coronary artery disease (CAD) is one of the most prevalent late toxicities; 15 to 20 years after cisplatin-based chemotherapy the absolute risk of CAD is 6 to 10% whereas post-chemoradiotherapy the absolute risk is 17% (Haugnes *et al*., 2010). Van den Belt-Dusebout *et al*., also studied CAD in survivors of testicular cancer, diagnosed between 1965 and 1995, at a median follow-up of 18 years post-therapy (van den Belt-Dusebout *et al*., 2006). Risk of CAD, more than 5 years post-diagnosis, was 1.61, 1.16 and 2.27 (standardised incidence ratios, SIR) for mediastinal radiotherapy alone, chemotherapy alone and chemoradiotherapy respectively, demonstrating increased vascular toxicity associated with combination therapy (van den Belt-Dusebout *et al*., 2006). In a study of breast cancer patients delivered adjuvant therapy post-surgery, 0.8% of patients treated with doxorubicin alone developed congestive heart failure whereas 2.6% of patients administered concomitant doxorubicin and left-breast irradiation displayed congestive heart failure (Valagussa *et al*., 1994). Furthermore, adjuvant therapy containing cyclophosphamide, methotrexate and fluorouracil (CMF) plus doxorubicin caused valvular disease in 13% of breast cancer patients but the addition of left-breast irradiation to this adjuvant therapy increased the incidence of valvular to 18% (Zambetti *et al*., 2001). In a more recent study, Magne *et al*., examined cardiac damage in 64 stage II to III breast cancer patients administered adjuvant chemotherapy (doxorubicin, docetaxel and CMF) and radiation therapy (Magne *et al*., 2009). Following treatment, there was a significant drop in LVEF (median 10%) in 21 patients however at a follow-up, median 6 years later, all patients had reclaimed their initial LVEF value, restored normal cardiac function and no cardiac events, defined as a myocardial infarction or clinical evidence of congestive heart failure, were reported (Magne *et al*., 2009). This study has performed a mid-term follow-up, 5 to 7 years, thus the damaging cardiovascular effects of chemoradiotherapy in this cohort may not have yet arisen as cardiotoxicity is typically identified decades post-therapy. On account of the independent toxic effects of radiation and doxorubicin on the

cardiovascular system, as discussed previously, the mechanistics of combined toxicity, whether toxicity heightened or unchanged, requires investigation.

1.6 The cell cycle

It is important to understand the effects of radiation therapy and chemotherapy on fundamental cellular processes such as the cell cycle. The ability of cells to survive and replicate necessitates an operational cell cycle, thereby the ability of anticancer therapies to disrupt cell cycle progression is a significant means to halt cancer growth. The damaging effects of anticancer agents are not cancer cell-specific, therefore therapy-mediated dysregulation of the cell cycle can also initiate dysfunction of normal cells.

1.6.1 Regulation of the cell cycle

The cell cycle is a tightly regulated process, proceeding in well-defined phases, as outlined in Figure 1.3. Briefly, upon mitogenic stimulation, cells enter the G1 phase, committing to the cell cycle and preparing for DNA replication. Once the DNA content has been doubled during the S phase, the G2 phase enables DNA repair to occur and the cell readies itself for mitosis (DiPaola, 2002, Kaplon *et al*., 2015). Mitosis is a stepwise process (prophase to metaphase to anaphase to telophase) where chromatids separate and the cellular DNA is divided into two daughter cells via a process known as cytokenesis (Kaplon *et al*., 2015). Understanding the control of the cell cycle has been the principal work of Sir Paul Nurse and his team since the 1970s (Nurse, 2002). In 1989 Hartwell and Weinert, demonstrated that entry into specific cell cycle stages is regulated by cell cycle checkpoints which verify DNA integrity; the late G1 checkpoint controls passage into the S phase while the G2 checkpoint enables DNA to be repaired before entry to mitosis (Hartwell and Weinert, 1989). Employing single-celled fission yeast, Nurse and Bissett, had previously shown the importance of cyclin-dependent kinase 1 (CDK1), which belongs to a family of protein kinases imperative for cell cycle control, in G1 to S phase and G2 to M phase progression (Nurse and Bissett, 1981). CDKs are associated with specific cyclin proteins in order to regulate

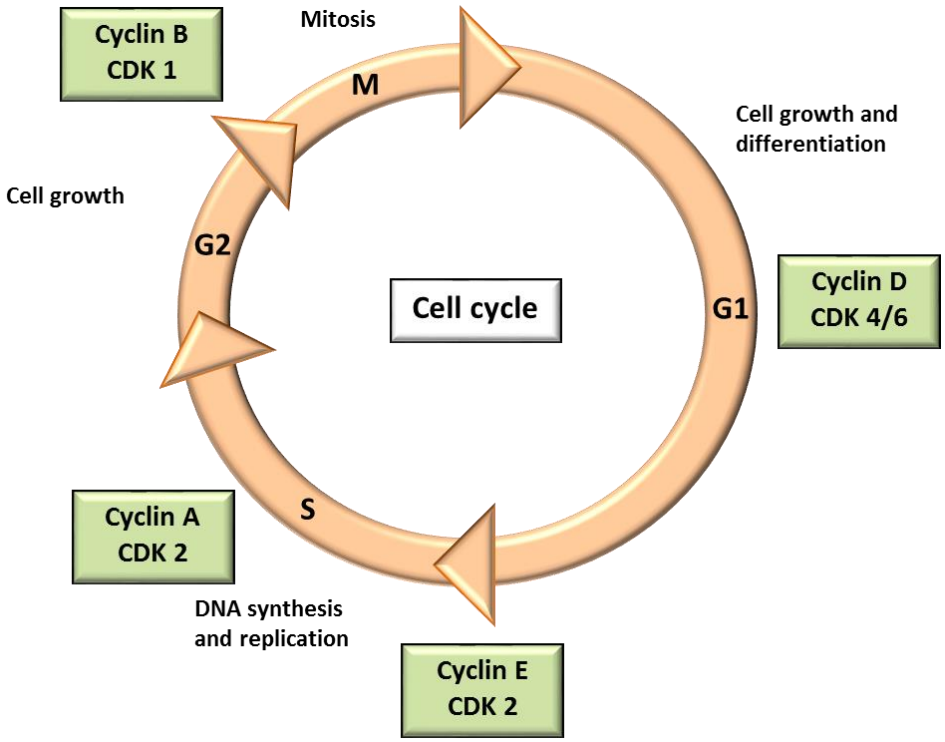

(adapted from Kaplon *et al.*, 2015)

Figure 1.3: Progression and control of the cell cycle in eukaryotic cells. The cell-cycle is a consecutive, multi-phase process consisting of an interphase (G1, S and G2) plus a mitotic phase (M). The cell cycle is controlled by cyclin-CDK heterodimers which function at precise cell cycle stages prior to mitosis.

cell cycle progression (Kaplon *et al*., 2015). Figure 1.3 details the cyclin-CDK complexes involved in regulation of particular cell cycle stages. Active cyclin D-CDK4/6 complexes, functional during the G1 phase, phosphorylate a retinoblastoma protein (pRB) leading to a reduction in the affinity of pRB for transcription factor E2F/DP, blocking the inhibitory effect of pRB on gene regulatory E2F/DP (DiPaola, 2002, Kaplon *et al*., 2015). Consequently, the transcription of genes essential for DNA replication is permitted and progression through the cell cycle can proceed (Kaplon *et al*., 2015). Later at the G1 checkpoint, cyclin E-CDK2 complexes phosphorylate pRB at further sites, resulting in irreversible transcription of genes associated with DNA synthesis during the S phase (Lapenna and Giordano, 2009). Post-G1, cyclin A-CDK2 and cyclin B- CDK1 sustain pRB in a hyperphosphorylated state, thus warranting successful cell cycle progression (Lapenna and Giordano, 2009).

1.6.2 Dysregulation of the cell cycle by anticancer agents

Eukaryotic cells have evolved intracellular control mechanisms that constrain cell cycle progression post-stress (Stewart *et al*., 2003). Genotoxic agents, such as ionizing radiation and chemotherapeutic drugs, activate the serine-threonine protein kinases ataxia telangiectasia mutated (ATM) and ataxia telangiectasia and RAD3-related protein (ATR) which are recruited to DNA lesions within minutes and signal for cell cycle arrest (Lapenna and Giordano, 2009). Transient arrest of the cell cycle is very useful post-DNA damage as it enables DNA repair processes to commence, however in cells with heavily damaged DNA permanent arrest, termed cellular senescence, can be induced or arrest can lead to the induction of apoptotic death (Korwek *et al*., 2012, Lapenna and Giordano, 2009). ATM is activated by DNA double-strand breaks (DSB) whereas ATR primarily responds to stalled replication forks but also plays a delayed role in the response to DSB (Shiloh, 2003). Figure 1.4 illustrates the events downstream of ATM and ATR leading to arrest of the cell cycle. As depicted in Figure 1.4, ATM directly or indirectly, via ATM-mediated activation of checkpoint kinase 2 (CHK2), phosphorylates and activates transcription factor p53 (Lapenna and Giordano, 2009). Subsequent transcription of CDK2 inhibitor, p21, by p53 prevents CDK2-mediated phosphorylation of pRB, prohibiting entry of the damaged cell into the S phase and prompting G1 phase arrest (DiPaola, 2002).

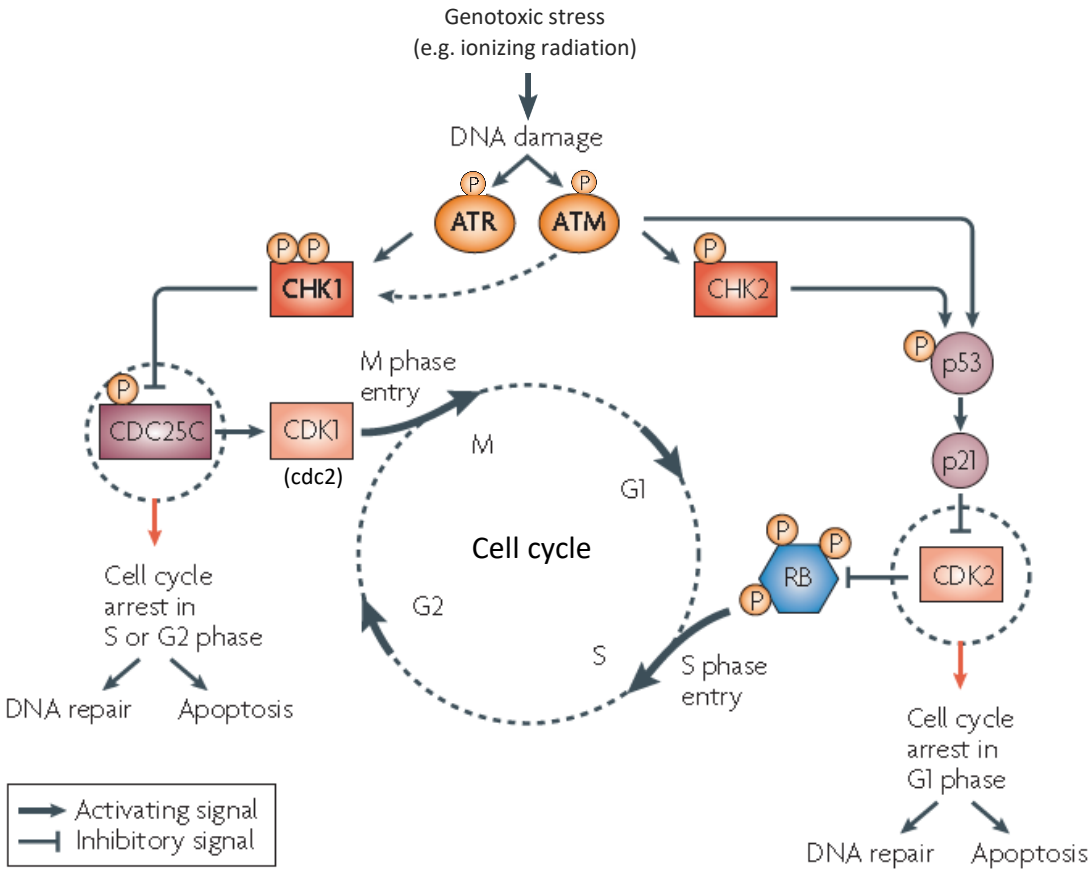

(adapted from Lapenna and Giordano, 2009)

Figure 1.4: Arrest of the cell cycle by DNA-damaging agents. ATM and ATR act as nuclear transducers post-DNA damage, generating a downstream molecular response which results in arrest of the cell cycle in the G1 or G2 phases. Arrest of the cell cycle enables damaged DNA to be repaired but if excessive damage has been acquired apoptosis is induced.

Cells which proceed beyond the S phase and incur DNA damage or had previously sustained DNA damage earlier during the cell cycle but successfully bypassed the first checkpoint (G1 checkpoint) can be arrested in G2 by ATM or ATR-mediated activation of checkpoint kinase 1 (CHK1) (Figure 1.4) (Lapenna and Giordano, 2009). CHK1 phosphorylates the phosphatase cdc25c on serine residue 216, creating a binding site for 14-3-3 proteins which sequester cdc25c in the cytoplasm, isolating cdc25c from cyclin B-CDK1 located within the nucleus (Goss *et al*., 2002). Therefore, cdc25c is unable to remove the two inhibitory phosphates located at threonine 14 and tyrosine 15 within the ATP-binding region of CDK1 (herein referred to as cdc2) (Goss *et al*., 2002, Lapenna and Giordano, 2009). Cyclin B-cdc2 resides in its phosphorylated, inactive state and entry to the M phase is obstructed; cyclin B-cdc2 has an important role in G2 to M transit by promoting structural alterations during mitosis such as nuclear lamina depolymerisation (Goss *et al*., 2002). Cells are arrested in the G2 phase, or G1 phase as previously discussed, until DNA damage has been repaired however severe DNA lesions, often induced by anticancer therapy, cannot be restored resulting in ATM/ATR-triggered apoptotic death, commonly mediated by downstream activation of p53 which regulates pro-apoptotic genes such as Bcl-2 protein family members (Korwek *et al*., 2012, Lapenna and Giordano, 2009). Hence, antineoplastic drugs can manipulate the cell cycle to promote growth arrest or programmed cell death.

A number of studies have demonstrated the distinct effects of anticancer therapies on the cell cycle machinery. Parplys *et al*., examined the effects of agents which induce differing types of DNA damage on the cell cycle in human osteosarcoma U2OS cancer cells (Parplys *et al*., 2012). Greatest phosphorylation of CHK1 was induced by agents which promoted DNA double-strand breakages including X-rays, the chemotherapeutic drug topotecan (causes one-ended DSB) and a high concentration of hydrogen peroxide (H_2O_2) (induces two-ended DSB) (Parplys *et al*., 2012). Each of the aforementioned therapies substantially inhibited DNA replication elongation whereas methyl methanesulfonate (MMS) (intra-stand cross links) and a low concentration H_2O_2 of (SSB) reduced the elongation rate to a lesser extent and mitomycin C (MMC) (base damage principally methylation) had no effect on

elongation during DNA replication (Parplys *et al*., 2012). Interestingly, extensive G2 phase arrest was observed following treatment with agents that induced strong, sustained CHK1 phosphorylation and prolonged replication elongation (X-rays, topotecan, high H_2O_2 concentration), showing that the nature and severity of DNA damage influences the cell cycle de-regulation incurred. G2 phase arrest in response to X-rays has also been observed in the murine osteoblast precursor cell line OCT-1, 4 Gy X-rays increased the G2 population after 8 hours however 48 hours post-exposure to ionizing radiation a portion of cells had resumed cell cycle progression (Lau *et al*., 2010). This suggests that G2 phase arrest provides a momentary period for DNA repair.

Doxorubicin differs from ionizing radiation regarding its damaging effects on DNA, however doxorubicin is also a known inducer of cell cycle arrest. Doxorubicin (1 μM) was shown to trigger autophosphorylation of ATM (serine residue 1981) and ATM-dependent phosphorylation of downstream effectors CHK1 and CHK2 in a human lymphoblastic cell line (BT) (Kurz *et al*., 2004). Furthermore, doxorubicin induced phosphorylation of p53 in BT cells but not ATM-deficient L3 cells, implicating doxorubicin in the activation of an ATM-mediated cascade of events leading to cell cycle arrest, unfortunately the effect of doxorubicin on cell cycle profile was not specifically investigated in this study by Kurz *et al*., (Kurz *et al*., 2004). The influence of doxorubicin on ATM- and ATR-mediated signalling has been illustrated further by Forrest *et al*., who treated HeLa cells synchronised at the G1/S boundary with a combination of doxorubicin and pivaloyloxymethyl butyrate (AN-9), AN-9 is cleaved intracellularly to formaldehyde which provides the carbon essential for the covalent linkage of doxorubicin to one of the DNA strands thus DNA adduct formation (Forrest *et al*., 2012). Post-treatment the cells were released from blockade and cell cycle progression enabled however G2/M arrest was evident in the treated cells (Forrest *et al*., 2012). Utilising siRNA knockdown of ATR, G2/M arrest induced by doxorubicin was prevented and many HeLa cells became multinucleated, suggesting that ATR-mediated arrest at G2 is important for repair of damage and successful cell division (Forrest *et al*., 2012). While ATR knockdown abrogated G2/M arrest, knockdown of ATM had no effect on G2/M blockade but increased doxorubicin-induced apoptosis (Forrest *et al*., 2012). The authors concluded that ATM, which was

recruited to discrete DNA regions post-adduct formation, is involved in the DNA damage response at the G1 phase (Forrest *et al*., 2012). The sequential molecular events leading to G1 or G2 phase arrest, as outlined in Figure 1.4, are not strictly fixed. Lupertz *et al*., observed p53 phosphorylation (serine residue 392) and increased p21 expression in Hct-116 human colorectal cancer cells treated with doxorubicin (5 μM), this was associated with G2 phase arrest, not G1, and elevated expression of the pro-apoptotic protein Bax (Lupetz *et al*., 2010). Additionally, early up-regulation of p21 was detected in the X-irradiated OCT-1 cells which subsequently achieved G2 phase arrest, as discussed earlier (Lau *et al*., 2010). Thus, the cell cycle effects of particular anticancer agents are complex and require investigation in cell-type specific settings.

1.7 Cellular signalling

Whilst the effects of radiation therapy and chemotherapeutics on endothelial cell survival may be due to direct modulation of the cell cycle machinery, evidence also indicates a direct effect of anticancer therapies on cellular signalling pathways. A complex network of signalling intermediates interacts to maintain cell function but anticancer therapies can have a disruptive effect on these signalling systems.

1.7.1 Signalling events instigated by ionizing radiation

As previously described, ionizing radiation has a detrimental effect on vascular cell function. Dysfunction of cells within the cardiovascular system is principally mediated by the activation or dysregulation of intracellular signalling pathways, it is known that exposure of cells to radiation results in the activation of specific stress-related signalling cascades. Radiation promotes the phosphorylation of tyrosine residues within the cytoplasmic domain of receptor tyrosine kinases (Zingg *et al*., 2004). Attachment of specific signalling molecules to the phosphorylated residues of receptor tyrosine kinases initiates downstream activation of signalling pathways including mitogen-activated protein kinase (MAPK) pathways and the phosphatidylinositol 3'-kinase (PI3K)/Akt pathway (Zingg *et al*., 2004). Progression of the PI3K/Akt pathway involves PI3K-mediated phosphorylation of phosphoinositides which bind downstream protein kinase Akt. Following migration to the plasma membrane, Akt is

phosphorylated at threonine residue 308 (T308), by 3-phosphoinositide-dependent kinase 1 (PDK1) (Bozulic *et al*., 2008). Once translocated to the nucleus, phosphorylation site serine 473 (S473) of Akt is targeted by DNA-dependent protein kinase (DNA-PK); DNA-PK kinase activity is initiated by radiation-induced DNA damage (Bozulic *et al*., 2008). Zingg *et al*., reported enhanced phosphorylation of Akt at S437 after irradiation of HUVECs with 2 Gy X-irradiation (Zingg *et al.*, 2004). The Bcl-2 family member Bad and human pro-caspase 9 are phosphorylated by activated Akt, impeding the pro-apoptotic role of these proteins (Zingg *et al.*, 2004). A further pro-survival pathway triggered by radiation exposure is the extracellular signal regulated kinase (ERK) pathway. Park *et al*., detected transient activation of ERK 30 minutes post-treatment of human brain microvascular endothelial cells (HHSECs) and human dermal microvascular endothelial cells (HDMECs) with 4 Gy γ-radiation (Park *et al*., 2012). Kumar *et al*., observed that exposure of HDMECS to γ-irradiation resulted in poor phosphorylation of pro-survival signalling intermediates Akt and ERK however phosphorylation of cell-death promoting MAPK kinases for example, p38 and JNK, was markedly greater (Kumar *et al*., 2004). This implies that radiation preferentially provokes a response fatal for cells.

As indicated, p38 and JNK are stress-associated MAP kinases primarily linked to cell death post-radiation treatment. HDMECs are a highly radiosensitive type of endothelial cell (Park *et al*., 2012). The p38 MAPK pathway has been shown to have a critical role in HDMEC apoptosis following exposure to γ-irradiation (10 Gy), both a p38 enzyme inhibitor (PD169316) or transfection with a dominant negative mutant of p38 protected HDMECs from cell death (Kumar *et al*., 2004). Likewise, JNK has been implicated in apoptosis of U937 human monoblastic leukemia cells and bovine aortic endothelial cells (BAECs) induced by γ-irradiation (Verheji *et al*., 1996). Furthermore, JNK-mediated cell death incited by X-irradiation has been observed in human T cell leukaemia (MOLT-4) (Enomoto *et al*., 2000). Enomoto *et al*., reported limited, transient phosphorylation of JNK in X-ray resistant Rh-1a cells (a cell line derived from human T cell leukaemia MOLT-4 cells) - approximately 31% of cells were viable 24 hours after 10 Gy X-irradiation (Enomoto *et al*., 2000). However, in MOLT-4 cells up-regulation of phosphorylated JNK was maintained and only 7% of cells survived post-irradiation (Enomoto *et al.*, 2000). Hence sustained activation of

JNK, recognised to be essential for JNK-mediated apoptosis, correlated with a reduction in MOLT-4 cell survival (Chen *et al.,* 1996, Enomoto *et al.,* 2000).

In opposition to the conclusion that JNK is a death-promoting kinase, studies have delivered evidence that JNK can promote cell survival following radiation treatment. Potapova *et al*., observed a decrease in the viability of UVC-treated T98G human glioblastoma cells expressing a dominant negative form of downstream JNK target c-Jun which is unable to be phosphorylated compared to T98G cells with functional c-Jun activity (Potapova *et al*., 2001). Likewise, the viability of T98G cells expressing a non-functional c-Jun was reduced upon treatment with other DNA damaging agents, including the chemotherapeutic drugs cisplatin and doxorubicin (Potapova *et al.,* 2001). Therefore JNK-mediated c-Jun transcriptional activity can potentially protect cells from the actions of cytotoxic agents. Clearly, radiation is able to instigate a complex network of signalling cascades. Cells respond to noxious stimuli such as radiation by either activating cell survival-promoting pathways or more often are subject to stress-related death.

1.7.2 Anthracycline-mediated activation of MAPK

Anthracycline chemotherapeutic drugs are also known to have an effect on multifaceted signalling systems within cells, including cells of the cardiovascular system. The intracellular generation of ROS upon treatment of cells with anthracycline drugs is key for DNA damage, but ROS are also known strong activators of MAPK signalling cascades (Yamada *et al*., 2012). The anthracycline chemotherapeutic drug epirubicin, also recognised to cause vascular injury such as necrotizing vasculitis, has been shown to induce p38-dependent apoptosis of pulmonary artery endothelial cells (PAECs) (Yamada *et al*., 2012). Yamada *et al.,* revealed that epirubicin-induced cell death and activation of caspase-3 and -7 was inhibited by the p38 inhibitors SB203580 and PD169316, wheras the widely utilised JNK inhibitor and ERK inhibitors, SP600125 and PD98059 respectively, had no effect on epirubicin-mediated cytotoxicity (Yamada *et al*., 2012). Thus, p38 appears to be the principal MAPK critically involved in epirubicin-mediated apoptotic responses in PAECs. Interestingly, there was only a marginal reduction in epirubicin-triggered p38

phosphorylation when PAECs were pre-treated with the antioxidants glutathione (GSH) or N-acetylcysteine (NAC), implying that p38 activation by epirubicin involves other molecular mechanisms in addition to oxidative stress such as DNA injury, inflammatory cytokine production and endoplasmic reticulum stress (Yamada *et al*., 2012). The role of p38 in anthracycline-mediated apoptosis has been proven further, treatment of H9c2 cardiac myocytes with p38 inhibitor SB203580 prior to doxorubicin treatment significantly reduced doxorubicin-mediated cytotoxicity (Guo *et al*., 2013). Likewise, SB2033580 ablated apoptosis of bone marrow-derived mesenchymal stem cells (BMSC) induced by doxorubicin (1 µM) (Yang *et al*., 2013). Clearly, p38 is an established mediator of cell death responses post-anthracycline treatment.

A single MAPK is rarely responsible for mediating the detrimental intracellular effects of anthracyclines. In the study of BMSC by Yang *et al*., the ERK inhibitor PD98059 did not prevent doxorubicin-induced apoptosis but JNK inhibitor SP600125 abolished apoptosis, implicating JNK in doxorubicin-mediated apoptosis too (Yang *et al*., 2013). Kim and Freeman. revealed that apoptosis of MCF-7 cells induced by doxorubicin (10 µg/ml), assessed by DNA fragmentation, was significantly diminished in cells transfected with constructs to knockdown JNK1 or c-Jun (Kim and Freeman. 2003). A further study by Brantley-Finley *et al*., assessing doxorubicin-induced JNK responses in KB-3 carcinoma cells reported that doxorubicin (1 µM) increased phosphorylated c-Jun expression 12-fold but pre-treatment with the widely utilised JNK inhibitor SP600125 for 1 hour prior to doxorubicin treatment marginally protected the cells from death (Brantley-Finley *et al*., 2003). The role of JNK in doxorubicin-mediated death of cancer cells is evident but requires further exploration in non-cancerous cells.

1.7.3 Biochemistry of the JNK signal transduction pathway

Initially identified as stress-activated protein kinase (SAPK) at the beginning of the 1990s (Tournier *et al*., 2013), JNK is a signalling intermediate of great scientific interest due to its contribution to various disease states such as inflammatory rheumatoid arthritis (Sumara *et al*., 2005). Since the discovery of JNK, researchers have attempted to identify the molecular mechanisms of JNK activity to further

understand how the JNK pathway can be targeted therapeutically. Three genes are responsible for JNK expression in mammalian cells; Jnk1, Jnk2 and Jnk3 (Bogoyevitch and Kobe, 2006). Ten JNK proteins can be transcribed from these genes as a result of alternative gene splicing; four splice forms from Jnk1 (JNK1α1, JNK1α2, JNK1β1, JNK1β2), four from the Jnk2 gene (JNK2α1, JNK2α2, JNK2β1, JNK2β2) and two from Jnk3 (JNK3α1, JNK3α2) (Bogoyevitch and Kobe, 2006). This leads to the generation of different size JNK proteins, either 54 kDa and 46 kDa (with a carboxy-terminal or without respectively) (Davis. 2000). Thus, there are several JNK isoforms responsible for varied cellular responses in distinct tissues, contributing to the functional complexity of JNK activation (Davis. 2000). Interestingly, both JNK1 and JNK2 are widely distributed throughout tissues of the body however JNK3 expression is limited to the brain, testes and heart (Ricci *et al*., 2004). This indicates a discrete role for JNK 3 in these tissues independent of JNK1 and JNK2 activity.

As discussed previously, JNK belongs to the MAP kinase family of signalling molecules. MAP kinase activity is primarily triggered via a three-tier kinase cascade (MAP3K to MAP2K to MAPK) (Figure 1.5). MEKK1 was the earliest MAP3K found to mediate activation of the JNK pathway (Karin and Gallagher, 2005). Numerous other contributing MAP3K have since been elucidated including MEKK2/3/4, Mixed Lineage kinases (MLK 2/3), TGF-β- activated kinase (TAK1) and Apoptosis Signal Regulating Kinases (ASK 1/2) (Karin and Gallagher, 2005). MKK4 and MKK7 are MAP2Ks, downstream of MAP3K, principally phosphorylated during transduction of the JNK cascade (Karin and Gallagher, 2005). MKK4 is dually phosphorylated at serine residue 257 (S257) and threonine residue 265 (T265) within its activation loop (T loop); MKK7 undergoes dual phosphorylation at S271 and T275 (Karin and Gallagher, 2005). Thereafter, MKK4 and MKK7 target distinct residues in the T loop of JNK, tyrosine residue 185 (Y185) and threonine residue 183 (T183) respectively (Karin and Gallagher, 2005). Dual phosphorylation of JNK at the Thr-Pro-Tyr motif, by MKK4 and MKK7, prompts a conformational change facilitating ATP binding to the JNK catalytic region, thus enabling complete activation of JNK kinase activity (Karin and Gallagher, 2005, Weston and Davis, 2002).

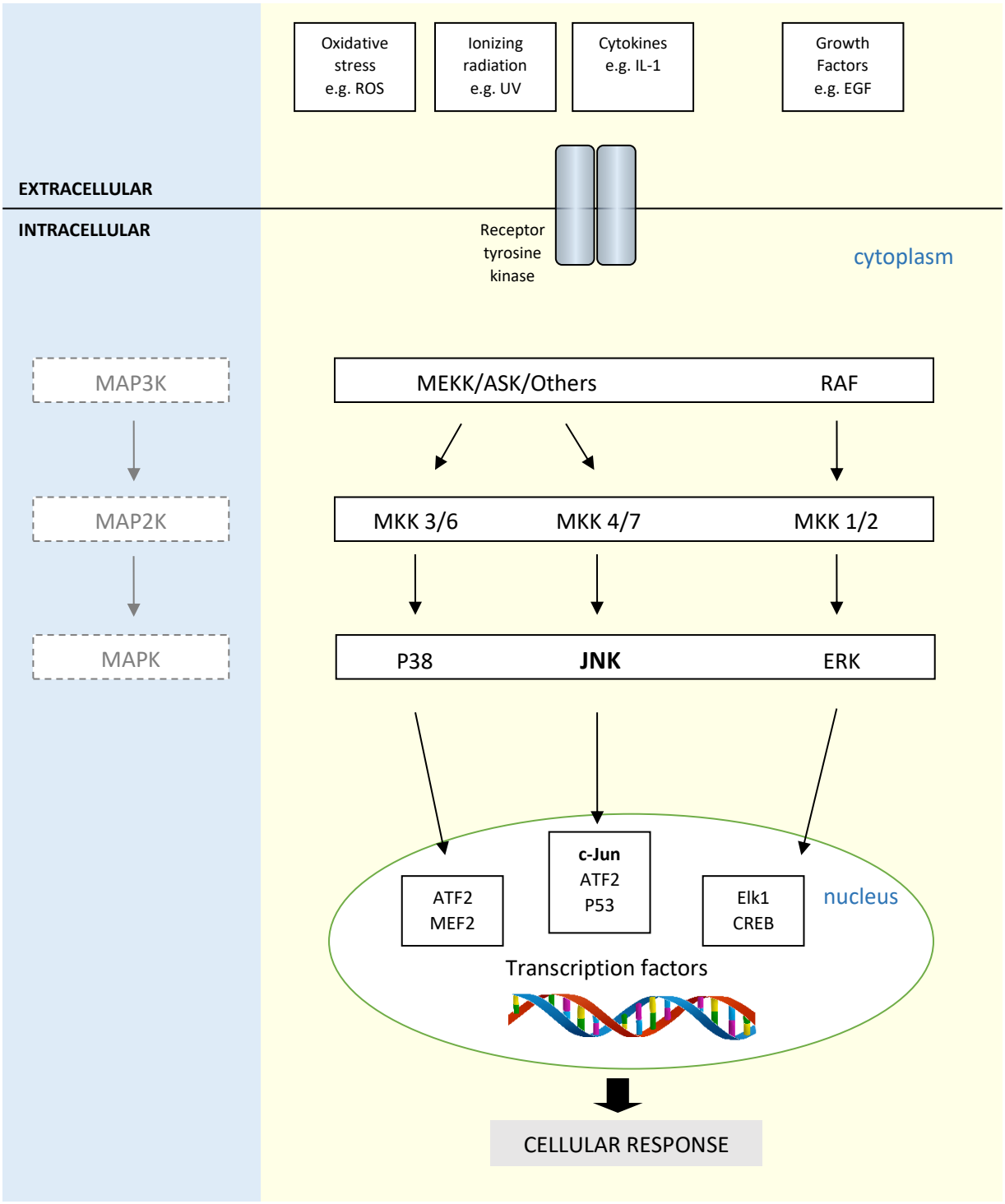

(adapted from Davis. 2000, Munshi and Ramesh, 2013)

Figure 1.5: Organisation of the MAP kinase signal transduction pathways. MAP kinase (p38, JNK and ERK) pathways are initiated in response to inflammatory cytokines, growth factors and environmental stresses such as osmotic stress and UV radiation. Upon activation, MAPK kinase kinases (MAP3Ks) phosphorylate MAPK kinases (MAP2Ks) succeeded by MAPK phosphorylation. Activated MAPK translocate to the nucleus and phosphorylate transcription factors.

JNK-mediated phosphorylation of diverse substrates results in the varied outcomes of JNK cascade transduction. A well-recognised group of JNK substrates is the AP-1 transcription factor family. AP-1 transcription factors are formed due to homo- or hetero-dimerisation of JNK, Fos and ATF proteins (Meng and Xia, 2011). AP-1 transcription factors are bZIP (basic-zipper) family members thus these dimerize through leucine zipper interactions (Karin and Gallagher, 2005). Jun proteins (c-Jun., JunB and JunD) are able to form heterodimers with Fos proteins (c-Fos, FosB, Fra-1 and Fra-2) or ATF proteins (ATF-2 and ATF-a) or homo-dimers (Leppa and Bohmann, 1999, Meng and Xia, 2011). JNK was initially detected following the observation that UV-irradiation could promote c-Jun phosphorylation (Karin ad Gallagher, 2005). JNK interacts with c-Jun by binding to a docking site, identified as the delta domain or JNK-binding domain (I_{33}-L-K-Q-S-M-T-L-N-L-A_{43}) (Bogoyevitch and Kobe, 2006, Dunn *et al*., 2002). The delta region is sited within the N-terminal transactivation region of c-Jun, enabling JNK to target phosphorylation of c-Jun serine residues 63 and 73 effectively (Karin and Gallagher, 2005). It has been proposed that JNK dimers form complexes with c-Jun homo-dimers, consequently increasing JNK-c-Jun docking interactions and stability of the complex leading to greater phosphorylation capacity of JNK (Dunn *et al.,* 2002). JNK-mediated phosphorylation of c-Jun functions to enhance transcriptional c-Jun activity (Bogoyevitch and Kobe, 2006). Similarly, dual phosphorylation of threonine residues 69 and 71 within the N-terminal transactivation domain of ATF-2 by JNK amplifies ATF-2 gene regulation (Bogoyevitch and Kobe, 2006). Jun/ATF-2 heterodimers are recognised to bind the cAMP-response element (CRE, 5'-TGACGTCA-3') permitting regulation of gene transcription (Meng and Xia, 2011).

JNK translocates to the nucleus after activation to mediate transcription factor activation, however other nuclear and non-nuclear JNK targets have been reported highlighting the complexity of JNK-triggered cellular responses. UVA treatment was found to cause JNK-mediated phosphorylation of histone H2AX (S139), a protein which localises at DNA strand breaks and is implicated in apoptosis (Al-Muhtari *et al*., 2010, Bode and Dong, 2007). Furthermore, JNK can promote apoptosis by phosphorylating mitochondrial proteins Bcl-xl (T47 and T115) and Mcl-1 (S121 and

T163), inhibiting their anti-apoptotic activity (Bogoyevitch and Kobe, 2006). Conversely, JNK can phosphorylate and impede the activity of pro-apoptotic protein Bad thus preventing apoptosis (Bode and Dong, 2007). Pro-survival kinase Akt is another target of JNK, JNK phosphorylates Akt at T450 thus promoting binding of the Akt activator PDK1 (Bogoyevitch and Kobe, 2006). This further emphasizes the variability of JNK-mediated responses.

1.7.4 Role of JNK in the pathogenesis of atherosclerosis

MAP kinase pathway activation, including JNK, has been implicated in the promotion of cardiovascular disease. ERK has been shown to contribute to cardiac hypertrophy by regulating cardiomyocyte protein expression and p38α participates in detrimental cardiac remodelling following a myocardial infarction (Muslin *et al.*, 2008). Interestingly, related MAP kinases, p38α and JNK, have been associated with stages of atherogenesis. JNK and p38α inhibitors, SP600125 and SB203580 respectively, prevented oxLDL uptake and transformation of cultured murine macrophages into foam cells (Rahaman *et al*., 2006, Zhao *et al*., 2002). Additionally, plaque formation in the inner curvature of the aorta, an area vulnerable to atherosclerosis, was reduced approximately 86% in $ApoE^{-/-}$ mice following pharmacological inhibition of JNK using SP600125, compared to controls (Wang *et al*., 2011).

A study by Ricci *et al*., reported JNK2 as the principal isoform that partakes in the promotion of atherosclerosis. JNK2 knockdown $ApoE^{-/-}$ mice, supplied a diet with elevated cholesterol, displayed reduced atherosclerosis with the number of aortic plaques decreased by approximately one half compared to control mice (Ricci *et al*., 2004). Conversely, decreased plaque formation was not observed in JNK1 knockdown $ApoE^{-/-}$ mice. In addition, foam cell generation was reduced 50% in the $ApoE^{-/-}/JNK2^{-/-}$ mice but this was not detected when assessing macrophages from $ApoE^{-/-}/JNK1^{-/-}$ mice (Ricci *et al*., 2004). This study found that serine-phosphorylation of macrophage scavenger receptor SR-A was reduced in the JNK2 knockdown mice, supporting the hypothesis that JNK2 plays a role in the uptake of oxLDL by macrophages which results in foam cell formation (Ricci *et al*., 2004). In support of a critical role for JNK2 in the pathogenesis of atherosclerosis, Osto *et al.*, found that JNK2 knockdown mice

fed a cholesterol rich diet displayed maintained aortic relaxation in response to acetylcholine but relaxation was hindered in wild type mice fed the high cholesterol diet (Osto *et al*., 2008). Therefore, JNK2 appears to contribute to the regulation of vessel tone, causing impaired endothelial cell-mediated relaxation of arteries, a key feature of atherosclerosis. Chaudhury *et al*., argued that the study by Ricci *et al*., did not investigate the involvement of JNK1 in endothelial cell dysfunction, an early feature of atherosclerosis development. Chaudhury *et al*., reported that use of siRNA to knockdown JNK1 in endothelial cells from the inner curvature of the aorta, repressed pro-apoptotic receptor interacting protein 1 (RIP1) and caspase-3 levels (Chaudhury *et al*., 2010). This outcome suggests that JNK1 plays a role in endothelial cell apoptosis at atherosclerosis-liable sites, contributing to the pathogenesis of atherosclerosis. Similarly, Amini *et al*, found that loss of JNK1 in low-density lipoprotein receptor (LDLR)-deficient mice impaired caspase-3 activation and DNA fragmentation in endothelial cells from the inner curvature of the aorta, supporting a role for the JNK1 isoform in endothelial cell apoptosis (Amini *et al*., 2014). Consequently, atherosclerotic lesion size was decreased in the aorta (Amini *et al*., 2014). Collectively these findings suggest distinct roles for JNK1 and JNK2 in vascular pathology, perhaps participating at different stages of atherosclerotic lesion development.

The specific role of JNK in endothelial cell dysfunction has been studied in further detail to establish its contribution to atherosclerosis. Al-Mutairi *et al*., found that the use of MAP kinase phosphatase-2 (MKP-2) adenovirus, which exclusively inhibited JNK activation, diminished COX-2 levels following TNFα treatment of HUVECs, implicating JNK activation in COX-2 mediated vasoconstriction (Al-Mutairi *et al*., 2010). Expression levels of ICAM-1 and VCAM-1 remained unaltered in the HUVECs transfected with MKP-2 adenovirus (Al-Mutairi *et al*., 2010). However, Wang *et al*, reported lower VCAM-1 expression in an area of the carotid artery exposed to low shear stress, when examining $ApoE^{-/-}$ mice administered JNK inhibitor SP600125, suggesting that VCAM-1 expression at atherosclerosis-prone sites is JNK-dependent (Wang *et al*., 2011). Additionally, E-selectin expression has been shown to be JNK-dependent in TNFα-treated HUVECs using a dominant negative JNK1/2 construct

(Min and Pober. 1997). As discussed previously in section 2.1, increased permeability of the endothelium is a key event during atherogenesis. JNK blockade, using SP600125, has been shown to prevent attenuated endothelial barrier function, measured by transendothelial electrical resistance (TEER), of human lung microvascular endothelial cells exposed to intermittent hypoxia, implicating a role for JNK in increased permeability of the endothelium (Makarenko *et al*., 2014). JNK is understood to regulate reorganization of endothelial cytoskeletal and junction proteins thus barrier function (Makarenko *et al*., 2014). Clearly JNK activation in endothelial cells is a mechanism responsible for altered endothelial cell function and potentially cell death - resulting in atherosclerosis at the arterial wall. JNK pathway activation following administration of anticancer therapy may contribute to late onset cardiovascular disease.

1.8 Aims

Endothelial cells respond to noxious agents by triggering a series of damaging events during the pathogenesis of atherosclerosis.

Having outlined the current state of knowledge regarding the effects of anticancer therapies, specifically X-rays and doxorubicin, on the cardiovascular system and the potential intracellular machinery responsible for deregulation of vascular cells, this thesis aims to characterise the independent and combinatory effects of X-rays and doxorubicin on endothelial cell function. Key objectives to achieve this are:

- Establish the effect of single-agent therapy on human endothelial cell viability.
- Identify the role of JNK in the response of endothelial cells to doxorubicin or X-irradiation.
- Characterise the interactive effects of doxorubicin and X-rays on endothelial cell viability.

Collectively, the severity of endothelial cell damage caused by combinatory therapy relative to single therapy will be determined, providing a greater understanding of how to tackle cancer therapy-related cardiovascular disease.

Chapter 2:
Materials and Methods

2.1 Materials

All materials were of the highest commercial grade available and obtained from Sigma-Aldrich Co. Ltd. (Dorset, UK) unless otherwise stated.

2.1.1 Cell culture reagents

Endothelial Cell Growth Medium MV2 Kit – PromoCell GmbH, (Heidelberg, Germany) (catalogue # C-22121)
Endothelial Growth Medium-2 (EGM-2) BulletKit – LONZA (Wolverhampton, UK) (catalogue # CC-3162)
Dulbecco's Modified Eagle medium (DMEM) – Gibco (distributer: Life Technologies, Paisley, UK) (catalogue # 21969-035)
Minimum Essential Media (MEM) – Gibco (distributer: Life Technologies, Paisley, UK) (catalogue # 32360-026)
Fetal Bovine Serum (FBS) – Gibco (distributer: Life Technologies, Paisley, UK) (catalogue # 10270-106)
Trypsin-EDTA – Gibco (distributer: Life Technologies, Paisley, UK) (catalogue # 15400-054)
L-glutamine – Gibco (distributer: Life Technologies, Paisley, UK) (catalogue # 25030-024)
Penicillin/Streptomycin – Gibco (distributer: Life Technologies, Paisley, UK) (catalogue # 15140-122)

2.1.2 Antibodies

Anti-P-SAPK/JNK (T183/Y185) – Cell Signalling Technology, Inc. (distributer: New England Biolabs (UK) Ltd, Herts, UK) (catalogue # 9251)
Anti-JNK – Santa Cruz Biotechnology, Inc. (distributer: Insight Biotechnology Ltd, Middlesex, UK) (catalogue # sc-571)
Anti-P-cdc2 (Y15) – Cell Signalling Technology, Inc. (distribuer: New England Biolabs (UK) Ltd, Herts, UK) (catalogue # 9111)

Anti-cdc2 – Cell Signalling Technology, Inc. (distributer: New England Biolabs (UK) Ltd, Herts, UK) (catalogue # 9112)

Anti-GAPDH (14C10) – Cell Signalling Technology, Inc. (distributer: New England Biolabs (UK) Ltd, Herts, UK) (catalogue # 2118)

Peroxidase-conjugated Goat Anti-rabbit IgG – Jackson ImmunoResearch Laboratories Inc. (distributer: Stratech Scientific Limited, Suffolk, UK) (catalogue # 111-035-144)

2.1.3 Flow cytometry reagents

Propidium Iodide – Invitrogen (distributer: Thermo Fischer Scientific Inc., Leicestershire, UK) (catalogue # P3566)

PE Annexin V Apoptosis Detection Kit – BD Biosciences (San Jose, USA) (catalogue # 559763)

BD Calibrite 3-colour Bead Kit – BD Biosciences (San Jose, USA) (catalogue # 340486)

APC Annexin V – BD Biosciences (San Jose, USA) (catalogue # 550475)

Annexin V Binding Buffer – BD Biosciences (San Jose, USA) (catalogue # 556454)

2.1.4 Miscellaneous

Recombinant Human Interleukin-1 beta (IL-1β) – Insight Biotechnology Ltd (Middlesex, UK) (catalogue # 10-1012-C)

Bovine Serum Albumin (BSA) – Fischer Scientific International, Inc. (Leicestershire, UK) (catalogue # C/8480/53)

Acrylamide – Carl Roth GmbH+Co. (Karlsruhe, Germany) (catalogue # 3029.1)

Pre-stained Molecular Weight Markers – Bio-Rad Laboratories, Inc. (Hertfordshire, UK) (catalogue # 161-0374)

Glutathione Sepharose 4B (carrier beads) – GE Healthcare Life Sciences (Buckinghamshire, UK) (catalogue # 17-0756-01)

Easytides [γ-^{32}P]ATP, 250µCi – PerkinElmer Inc. (Buckinghamshire, UK) (catalogue # NEG502A250UC)

Glacial Acetic Acid – Fischer Scientific International, Inc. (Leicestershire, UK) (catalogue # A/0400/PB17)

Methanol – VWR International Ltd. (Leicestershire, UK) (catalogue # 20847.307)

Giemsa Solution – VWR International Ltd. (Leicestershire, UK) (catalogue # 350865P)
Plasmid (containing cDNA which encodes GST-tagged truncated c-Jun N-terminus (GST-c-Jun$_{(5-89)}$)) – kind gift from J. R. Woodgett (Ontario Cancer Institute, Princess Margaret Hospital, Toronto, Canada)

2.1.5 Equipment

T_{75} Tissue Culture Flasks – Corning Inc. (New York, USA) (catalogue # 430641U)
T_{25} Tissue Culture Flasks – TPP Techno Plastic Products AG (Trasadingen, Switzerland) (catalogue # 90026)
6 cm Cell Culture Dishes – Thermo Fisher Scientific Inc. (Hempstead, UK) (catalogue # 150326)
96-well Tissue Culture Testplate – TPP Techno Plastic Products AG (Trasadingen, Switzerland) (catalogue # 92096)
Filter Paper – GE Healthcare Life Sciences (Buckinghamshire, UK) (catalogue # 3017-915)
Nitrocellulose Blotting Membrane (Hybond ECL) – GE Healthcare Life Sciences (Buckinghamshire UK) (catalogue # 10600003)
Cellophane Sheets – GE Healthcare Life Sciences (Buckinghamshire, UK) (catalogue # 80112938)
Autoradiography Film – Santa Cruz Biotechnology, Inc. (distributer: Insight Biotechnology, Middlesex, UK) (catalogue # sc-201696)
21 Gauge Needles – BD Biosciences (San Jose, USA) (catalogue # 304432)

X-RAD 225 Biological Irradiator – Precision X-Ray, Inc. (Connecticut, USA)
Bio-Rad Mini-PROTEAN 3 Electrophoresis System – Bio-Rad Laboratories, Inc. (Hertfordshire, UK)
POLARstar Omega – BMG Labtech GmbH (Ortenberg, Germany)
CL-1000 Ultraviolet Crosslinker – UVP (Jena, Germany)
BD FACSCanto – BD Biosciences (San Jose, USA)
Ultrospec 2000 Spectrophotometer – Amersham Pharmacia Biotech UK Ltd. (Buckinghamshire, UK)
JP-33 Automatic Film Processor – JPI Healthcare Co., Ltd. (New York, USA)

Hoefer Easy Breeze Gel Drier – Fischer Scientific International, Inc. (Leicestershire, UK)

2.2 Methods

2.2.1 Cell culture

All cell culture work was performed within a class II laminar flow cell culture hood, under sterile conditions**.**

2.2.1.1 Human Coronary Artery Endothelial Cells

Primary Human Coronary Artery Endothelial Cells (HCAECs) obtained from PromoCell GmbH had been isolated from both the left and right coronary artery, including the anterior descending and the circumflex branches, of a single donor. HCAECs were maintained in Endothelial Cell Growth Medium MV2 (PromoCell GmbH, Heidelberg) supplemented with 5% (v/v) Fetal Calf Serum (FCS), 5 ng/ml recombinant human Epidermal Growth Factor (hERG), 10 ng/ml recombinant human Basic Fibroblast Growth Factor (hBFGF), 20 ng/ml Insulin-like Growth Factor (R3 IGF-1), 0.5 ng/ml recombinant human Vascular Endothelial Growth Factor 165 (VEGF), 1 µg/ml Ascorbic Acid and 0.2 µg/ml Hydrocortisone as directed by PromoCell GmbH. HCAECs were incubated at 37^{o}C in a humidified atmosphere (5% CO_2/95% air) and the culture media was replaced every second day. HCAECs from the single donor were subcultivated to different passages for repetitions of experiments (i.e. different n numbers). HCAECs were utilised for experimentation between passages 2 and 7 only and subcultured using trypsinisation. Where indicated in chapter 4, figure 4.8, HCAECs were starved for 18 hours prior to stimulation in media containing the previously described constituents but lacking growth factors and containing 0.5% FBS.

2.2.1.2 Human Umbilical Vein Endothelial Cells

Primary Human Umbilical Vein Endothelial Cells (HUVECs) purchased from Cambrex (aliquot of cryopreserved HUVECs consisted of 3 pooled donors) were maintained in Endothelial Basal Medium-2 (EBM-2) (LONZA, Wolverhampton) supplemented with 10 ml (2% (v/v)) Fetal Bovine Serum (FBS), 2 ml recombinant human Fibroblast Growth Factor-B (rhFGF-B), 0.5 ml Ascorbic Acid, 0.5 ml

recombinant human Epidermal Growth Factor (rhEGF), 0.5 ml Gentamicin Sulfate Amphotericin-B (GA-1000), 0.5 ml recombinant long R Insulin-Like Growth Factor-1 (R^3-IGF-1), 0.2 ml Hydrocortisone, 0.5 ml recombinant human Vascular Endothelial Growth Factor (VEGF) and 0.5 ml Heparin (concentrations not provided by LONZA, Wolverhampton). The culture media was replaced every second day and cells were incubated in a humidified atmosphere (37ºC, 5% CO_2/95% air). HUVECs were used for experimentation between passages 2 and 6 only, using trypsin-EDTA as a detaching agent for subculturing cells.

2.2.1.3 MCF-7 breast cancer cells

Breast cancer cells from the Michigan Cancer Foundation-7 (MCF-7) human breast adenocarcinoma cell line were a kind gift from Dr Andrew Paul (SIPBS, University of Strathclyde, Glasgow). MCF-7 cells were grown in Dulbecco's Modified Eagle Medium (DMEM) (Gibco, Life Technologies, UK) containing 10% FBS, 1% L-glutamine and 1% Penicillin/Streptomycin. Cells were incubated at 37ºC in a humidified atmosphere (5% CO_2/95% air), provided fresh media every alternate day and subcultured using trypsinisation. MCF-7 cells were utilised for experimentation between passages 20 and 30.

2.2.1.4 UVW glioma cells

Human glioblastoma cell line, UVW, was kindly provided by Dr Marie Boyd (SIPBS, University of Strathclyde, Glasgow). UVW cells were maintained in Minimum Essential Medium (MEM) (Gibco, Life Technologies, UK) supplemented with 10% FBS, 1% L-glutamine and 1% Penicillin/Streptomycin at 37ºC in 5% CO_2/95% air. Trypsin-EDTA was used as a detaching agent for subculturing cells.

2.2.2 Drug preparation

Doxorubicin hydrochloride (Sigma-Aldrich Co. Ltd., UK, catalogue # D1515) was prepared in sterile dH_20 to obtain a stock concentration of 10 mM and diluted in sterile dH_20 thereafter, on the day of use, to obtain concentrations required for stimulation. Treatment of cells with an equivalent volume of dH_20 was used as a vehicle control.

SP600125 (Sigma-Aldrich Co. Ltd., UK, catalogue # S5567), a water-insoluble small-molecule inhibitor of JNK kinase activity, was dissolved in 100% DMSO to obtain a stock concentration of 20 mM. The stock concentration was further diluted with DMSO before treatment of cells. The final concentration of DMSO in the culture media was 0.1%, as described by Bennett *et al.*, and 0.1% DMSO was used as a vehicle control for SP600125 (Bennett *et al.*, 2001).

Topotecan hydrochloride hydrate (Sigma-Aldrich Co. Ltd., UK, catalogue # T2705) was prepared as a stock concentration of 1mM, dissolved in PBS. The stock was freshly diluted in DMSO before experimentation to obtain the desired concentration for treatment.

2.2.3 Irradiation exposure

X-irradiation of cells was performed using an X-RAD 225 Biological Irradiator (operating at 225 kV, 13 mA). Cells were transported to the room accommodating the X-irradiator, stored in an incubator at 37ºC, in a humidified atmosphere (5% CO_2/95% air), and only removed for irradiation/sham-irradiation. Cells were exposed to X-rays at a fixed dose rate of 2.3 Gy/min at room temperature. The lids of 6 cm dishes and 96 well plates were removed for X-ray exposure. Sham-irradiated controls were placed in the X-RAD for the equivalent duration as the longest exposure, but X-rays were not emitted. Cells were immediately returned to an incubator (37ºC, 5% CO_2/95% air) after irradiation.

2.2.4 MTT toxicity assay

Cell viability was determined by reduction of 3-(4,5-dimethylthiazol-2-yl)-2,5-diphenyltetrazolium bromide (MTT) to formazan (purple coloured) by mitochondrial NAD(P)H-dependent oxidoreductase enzymes.

Cells were seeded in 96-well microplates at 20 to 30% confluency. The following day, cells were treated in triplicate then incubated, at 37ºC in 5% CO_2/95% air, for the appropriate duration. After incubation, the media was aspirated and replaced with fresh

media. MTT (1 mg/ml) was added to each well and the microplates incubated (37ºC, 5% CO_2/95% air) for 2 hours enveloped in tinfoil. The media was subsequently removed and formazan crystals formed were solubilised by the addition of DMSO. The microplates were incubated for a further 5 minutes then absorbance readings were measured using a POLARstar Omega microplate reader, test wavelength 570 nm, reference wavelength 690 nm.

2.2.5 Clonogenic survival assay

Clonogenic survival assays were performed to evaluate prolonged effects of cancer therapy on cell survival.

2.2.5.1 Cell plating for colony formation

Cells were plated in 6 cm (diameter) dishes and incubated for 48 hours before treatment. HCAECs were 60 to 75% confluent when treated with single agent doxorubicin (48-hour treatment) and 60% confluent when treated with doxorubicin for combination experiments (48-hour treatment). All cell types were 70 to 80% confluent at time of irradiation (24-hour incubation period post-irradiation). Treated cells were maintained at 37ºC in a humidified atmosphere (5% CO_2/95% air) for a further 24 or 48 hours before re-plating for colony growth. Briefly, the cell media was discarded and cells washed with phosphate-buffered saline (PBS) [154 mM NaCl, 5.36 mM KCl, 8 mM Na_2HPO_4 and 1.46 mM KH_2PO_4, pH 7.4], followed by trypsinisation. Cells were collected in 2 ml media, transferred to a universal and disaggregated using a 21 gauge needle and syringe. Cells were counted using a haemocytometer and re-plated at 200 (UVW, HUVEC), 350 (HCAEC) and 400 (MCF-7) cells per 6 cm dish, in triplicate. Seeded cells were incubated for between 8 and 14 days, at 37ºC in 5% CO_2/95% air, to enable colony formation. HCAECs required feeding the day after plating to promote growth. Additionally, due to the sensitivity of endothelial cells, they were fed every 2/3 days during the incubation period. MCF-7 cells also required feeding every 3/4 days due to their slow colony formation.

2.2.5.2 Colony staining and analysis

To visualise colonies formed, the media was removed followed by a wash with PBS. Cells were fixed with 100% methanol (v/v) for 15 minutes, then stained with 5% Giemsa stain (v/v). The stain was removed, dishes washed with water and dried at room temperature before analysis.

Colonies were counted and averaged between replicates (colonies of insignificant size were not counted). Surviving fractions were calculated as described in Boyd *et al*., 2006 where the surviving fraction (SF) was determined by dividing the plating efficiency (number of colonies counted/number of cells seeded) of irradiated cells by non-irradiated cells.

2.2.6 Apoptosis assay

The proportion of apoptotic cells post-treatment was determined by staining with Annexin V conjugated to allophycocyanin (APC) followed by flow cytometry.

2.2.6.1 Cell collection and staining

Cells were plated in 6-well plates and maintained at 37^{o}C in 5% CO_2/95% air for a further 48 hours. Cells were treated at 70 to 80% confluency and incubated with drug for 24 hours. Thereafter all cells were collected by retaining the media, containing detached cells, and trypsinisation to harvest remaining attached cells. Cell suspensions were centrifuged (1000 r.p.m., 5 minutes) at 20^{o}C and washed with ice cold PBS. Following two further centrifugations and PBS washes, cell pellets obtained were re-suspended in 100 µl 1X Annexin V binding buffer [10 mM Hepes (pH 7.4), 140 mM NaCl and 2.5 mM $CaCl_2$] and transferred to FACS tubes. Annexin V-APC stain (5 µl) was added to each tube and vortexed. Samples were incubated for 15 minutes at 37^{o}C in 5% CO_2/95% air, protected from light. An additional 400 µl 1X Annexin V binding buffer was added to each sample prior to fluorescence-activated cell sorting (FACS).

2.2.6.2 FACS analysis

A BD FACSCanto flow cytometer was used to measure APC fluorescence (ex-max/em-max. 650/660 nm). The cell population was gated to exclude debris. Quadrant (Q) positions were set using non-stained, untreated cells. Annexin V-APC stained cells treated with H_2O_2 were used to verify signal shifts. Annexin V binds to phosphatidylserine which migrates from the inner leaf of the cell membrane to the outer edge during early stage apoptosis (Widel *et al*., 2014). Therefore two populations were identified: healthy (Annexin V negative = Q3) and apoptotic (Annexin V positive = Q4). A total of 10,000 events per sample were recorded. BD FACSDiva software was used to analyse number of events in each quadrant.

2.2.6.3 Annexin V-PE and 7-AAD double staining

Additional experiments were performed utilising Annexin V-phycoerythrin (PE) and 7-Aminoactinomycin D (7-AAD) double staining followed by flow cytometry. When membrane integrity is lost cells become permeable to 7-AAD which binds with high affinity to GC regions of DNA (Zembruski *et al*., 2012). Therefore four populations were discriminated: viable cells [PE negative/ 7-AAD negative (Q3)], early apoptotic cells [PE positive/ 7-AAD negative (Q4)], cells in late apoptosis [PE positive/ 7-AAD positive (Q2)] and necrotic cells [PE negative/ 7-AAD positive (Q1)]. A BD FACSCanto flow cytometer was used to measure PE fluorescence (ex-max/em-max. 496/578 nm) and 7-AAD fluorescence (ex-max/em-max. 488/647 nm, PerCP channel used). Compensation, performed to prevent a given fluorochrome signal from being detected by a neighbouring channel, was executed using BD Calibrite beads (unstained, PE and PerCP). Quadrant (Q) positions were set using non-stained, untreated cells. Single-colour stained cells, treated with H_2O_2, were used to verify population shifts. 10,000 events per sample were recorded. BD FACSDiva software was used to analyse the number of events in each quadrant.

2.2.7 Cell cycle analysis

Staining of cellular DNA and flow cytometry analysis of DNA content was executed to determine cell cycle status.

2.2.7.1 Cell collection and fixation

Cells were seeded in 6-well plates and then treated 48 hours later at 70% confluency. After incubation with drug for the appropriate duration, the media containing dead cells was discarded and living cells were collected by trypsinisation of remaining attached cells. Cells were collected in a 1.5 ml eppendorf and centrifuged (1200 r.p.m.) for 5 minutes at 20^{o}C. The supernatant was aspirated off and remaining cell pellet re-suspended in 150 µl PBS, then vortexed. Cells were fixed by addition of 350 µl 100% ice-cold ethanol (v/v) and incubated at 4^{o}C for 2 to 3 hours or overnight.

2.2.7.2 Cell staining and FACS analysis

Following fixation, the cell suspensions were transferred to 15 ml tubes, followed by the addition of 1 ml ice-cold PBS and centrifugation (3000 r.p.m., 10 minutes) at 4^{o}C. Supernatants were discarded and cell pellets re-suspended in 250 µl PBS and vortexed. Cell suspensions were transferred to FACS tubes and Ribonuclease A from bovine pancreas (50 µg/ml) added to digest RNA, ensuring only DNA staining. Following a 30 minute incubation in darkness, cellular DNA was stained by the addition of 13.5 µl propidium iodide (PI) (50 µg/ml). Propidium iodide fluorescence (em-max/ex-max. 533/617 nm) was measured using a BD FACSCanto flow cytometer. The cell population was gated to exclude debris and then further gated to exclude doublets. A total of 10,000 events per sample were recorded. BD FACSDiva software was used to determine the percentage of cells in G1, S and G2/M cell cycle stages by the application interval gates.

2.2.8 Western blotting

Detection of specific cellular protein expression was achieved using western blotting.

2.2.8.1 Sample preparation

Cells grown in 6 cm dishes, 12-well plates or T_{25} flasks were treated at 70 to 100% confluency. Following treatment, cells were washed once with ice cold PBS and solubilised in sodium dodecyl sulphate (SDS) sample buffer [63 mM Tris-HCl (pH 6.8), 2 mM $Na_4P_2O_7$, 5 mM EDTA, 10% (v/v) glycerol, 2% (w/v) SDS, 0.007% (w/v) bromophenol blue and 50 mM DTT]. Cells were harvested, samples boiled for 5 minutes then stored at -20^{o}C until required.

2.2.8.3 SDS-PAGE and western immunoblotting

Whole cell lysates were resolved on 7.5% or 10% polyacrylamide gels [7.5% acrylamide: 0.2% bis-acrylamide or 10% acrylaimde: 0.27% bis-acrylamide and 375 mM Tris-base, 0.1% (w/v) SDS, pH 8.8 plus 0.08% (w/v) APS and 0.08% (v/v) TEMED] of 1 mm thickness. Samples were loaded onto a stacking gel [3% acrylamide: 0.08 % bis-acrylamide and 125 mM Tris-base, 0.1% (w/v) SDS, pH 6.8 plus 0.1% (w/v) APS and 0.1% (v/v) TEMED], positioned on top of the resolving gel, and proteins were separated using Sodium Dodecyl Sulphate Polyacrylamide Gel Electrophoresis (SDS-PAGE) (Bio-Rad Mini-PROTEAN 3 electrophoresis system) at 130 V in running buffer [20 mM Tris-base, 192 mM glycine and 3.5 mM SDS]. Proteins were transferred onto nitrocellulose membranes at 300 mA for 1 hour 45 minutes in transfer buffer [20 mM Tris-base, 192 mM glycine and 20% (v/v) methanol]. The membranes were blocked in 3% or 5% (w/v) BSA in TBST [20 mM Tris-base, 150 mM NaCl and 0.1% (v/v) Tween-20, pH 7.5] for 2 hours at room temperature, orbital shaking at 46 r.p.m. Membranes were immunoblotted with primary antibodies overnight at room temperature or at 4^{o}C. Anti-phospho-JNK (Threonine 183/Tyrosine 185) antibodies were utilised at 1:1500 in 0.5% (w/v) BSA/TBST. Anti-phospho-cdc2 (Tyrosine 15) and anti-cdc2 were both used at 1:1000 in 0.3% (w/v) BSA/TBST. Following washes with TBST (3 x 5 minute washes), membranes were incubated with horseradish peroxidase-conjugated rabbit polyclonal

secondary antibodies for 1 hour 30 minutes, orbital shaking at 46 r.p.m. Blots were again washed repeatedly with TBST (3 x 5 minutes). Enhanced chemiluminescent (ECL) reagents ECL 1 [0.1 M Tris-HCl (pH 8.5), 25 M luminol and 25 M Coumaric acid] and ECL 2 [0.1 M Tris-HCl (pH 8.5) and 6.27 mM H_2O_2] were added to the membranes prior to exposure of the membranes to autoradiography film. Autoradiography films were developed and fixed using a JP-33 film processor. Protein expression was quantified by densitometry (background pixel intensity subtracted from corresponding band pixel intensity) using Scion Image software.

2.2.8.3 Nitrocellulose membrane stripping and re-probing

Membranes were stripped and re-probed post-western blotting to ensure total protein levels were equal in each well of the gel (loading control).

Membranes were incubated with stripping buffer [0.05 M Tris-HCl, 2% SDS, pH 6.7 plus 0.1 M β-mercaptoethanol] for 1 hour at 60ºC, orbital shaking at 70 r.p.m, to remove previously bound primary antibody. Membranes were repeatedly washed (4 x 10 min) with NATT [50mM Tris-base, 150 mM NaCl and 0.2% (v/v) Tween-20, pH 7.4] then immunoblotted with primary antibody overnight (anti-JNK. 1:1500, anti-GAPDH. 1:15000 in 0.5% (w/v) BSA/NATT). Membranes were probed with secondary antibody and visualised as described in section 2.2.8.2.

2.2.9 JNK activity assay

JNK activity was assessed by phosphorylation of truncated GST-c-Jun$_{(5\text{-}89)}$ which only contains the JNK phosphorylation site. Phosphorylation of truncated c-Jun by JNK was detected by incorporation of γ-^{32}P from ATP.

2.2.9.1 GST-fusion protein production

Escherichia coli (E.coli) which have been transformed with a plasmid encoding GST-c-Jun recombinant fusion proteins were stored in glycerol at -80ºC. Agar plates [10 g/L tryptone, 5 g/L NaCl and 5 g/L yeast extract] containing ampicillin (0.1 mg/ml) were prepared (engineered bacteria are ampicillin resistant). The agar plates were

streaked with this specific *E.coli* bacterial strain and incubated at 37ºC overnight to allow bacterial colony formation. The following day, the largest bacterial colony formed was collected and used to inoculate 5 ml of sterile 2XYT culture broth [16 g/L tryptone, 5 g/L NaCl and 10 g/L yeast extract] containing ampicillin (50 µg/ml). The bacteria-containing broth was incubated at 37ºC for 4 hours, orbital shaking at 180 r.p.m., to promote bacterial amplification. Subsequently, the turbid bacterial culture was added to 45 ml fresh culture broth and incubated at 37ºC overnight, orbital shaking at 180 r.p.m, for further bacterial amplification. The next day, the 50 ml bacterial culture was transferred to 450 ml of fresh culture broth containing ampicillin (50 µg/ml). Optical density of a sample of the bacterial culture was read at a wavelength of 600 nm (OD_{600}) using an Ultrospec 2000 spectrophotometer. An absorbance reading between 0.6 and 0.9 is necessary as a measure for sufficient bacterial growth. Isopropyl-D-thiogalactopyranoside (IPTG) (100 µM) was added to the bacterial culture to promote protein synthesis. The bacterial culture was incubated for a further 4 hours at 30ºC, orbital shaking at 190 r.p.m. Following this incubation period, the bacterial culture was divided equally into two 250 ml centrifuge bottles and centrifuged (10 000 g) for 4 minutes at 4ºC. The supernatant was then disposed of and bacterial pellets stored at -20ºC until required.

2.2.9.2 GST-c-Jun fusion protein purification and bead conjugation

The bacterial pellets were suspended in 12.5 ml lysis buffer [50 mM Tris-HCl, 1mM EDTA, 100 mM NaCl, pH 8.0 plus 1mM Benzamidine, 0.07% (v/v) β-mercaptoethanol, 0.4 mM PMSF, 6.6 µg/ml aprotonin, 6.6 µg/ml leupeptin and 0.66 µg/ml pepstatin A] on ice and repeatedly re-suspended to lyse the bacteria. In order to disrupt cell membrane integrity, the homogenate formed was frozen by addition to a beaker of methanol and dry ice. Once frozen, the homogenate was thawed in tepid water for 20 minutes. Bacterial cell membranes were further disrupted by using a probe sonicator (2 x 20 second bursts at 80% power then 2 x 20 second bursts at 50% power). Following the addition of 1% (v/v) Triton-X-100, the homogenate was placed on a rotary wheel for 60 minutes (4ºC). The homogenate was subsequently centrifuged (12,5000 g) for 15 minutes at 4ºC. During this period, glutathione sepharose (GSH) beads were washed twice with lysis buffer (300 g for 2 minutes). The supernatant

obtained from the homogenate centrifugation, containing GST-c-Jun fusion proteins, was added to the GSH beads and placed on a rotary wheel for 60 minutes to facilitate GSH bead to GST fusion protein binding. This was followed by centrifugation at 400 g for 3 minutes then removal of the supernatant. The beads were washed twice with lysis buffer (400 g, 3 minutes) and stored at 4^{o}C.

Various aliquots were retained at different stages of the purification process (Figure 2.1). To prepare elutions from the beads; 40 µl beads were removed, added to 200 µl glutathione elution buffer [50 mM Tris-HCl (pH 8.0), 100 mM NaCl, 0.1% (v/v) Triton-X-100 and 10 mM reduced glutathione] and placed on a rotary wheel at 4^{o}C for 60 minutes. The sample was subsequently centrifuged (13 000 g for 1 minute) and supernatant retained (elution 1). This step was repeated to obtain elution 2. A bradford assay was performed to quantitatively determine the GST-c-Jun fusion protein concentration eluted from the GSH beads. The absorbance of BSA standards (0 to 20 ug/ml) and elutions were measured at a wavelength of 595 nm using an Utrospec 2000 spectrophotometer. Thereafter, the volume of beads required to provide 20 µg/µl GST-c-Jun fusion protein per sample for the ensuing kinase assay was determined.

In addition, aliqiuots obtained for the purification process were subject to gel electrophoresis on a 10% polyacrylamide gel, ran at 130 V for 1 hour 30 minutes (Figure 2.1). The gel was stained with coomassie blue stain [40% (v/v) methanol, 10% (v/v) acetic acid and 0.1 (w/v) coomasie blue] for 1 hour 40 minutes, orbital shaking at 45 r.p.m. Destaining solution [40% (v/v) methanol and 10% (v/v) acetic acid] was used to remove any background staining (5 x 20 minute washes) and the gel was finally dried between two cellophane sheets using a Hoefer Easy Breeze Gel Drier (Figure 2.1).

	Samples obtained from purification process	Sample volume (µl)	Volume of 2X sample buffer added (µl)	Volume of 1X sample buffer added (µl)
1	Homogenate	2		38
2	Bacterial Pellet	2		38
3	Supernatant (post-centrifugation to obtain pellet)	10	10	
4	Supernatant (post-fusion protein binding to GSH beads)	10	10	
5	Wash 1	10	10	
6	Wash 2	10	10	
7	Elution 1	20	20	
8	Elution 2	20	20	
9	Beads	10	10	
10	Molecular weight marker (broad)			

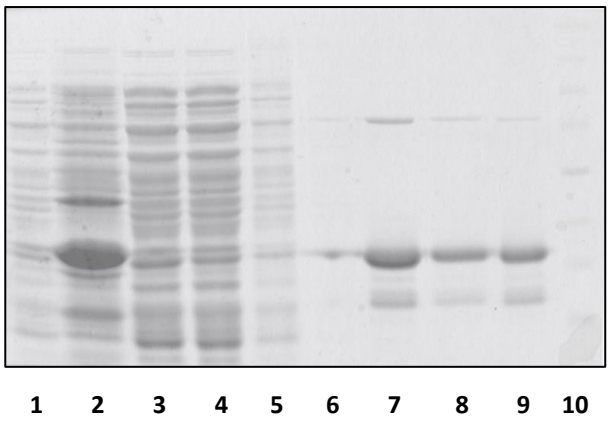

Figure 2.1: Outline of samples obtained during the generation of GST-c-Jun fusion proteins plus purification and attachment of fusion protein to glutathione sepharose beads. The table includes details of sample buffer additions before gel electrophoresis.

2.2.9.3 *In vitro* solid-phase kinase assay

Following treatment of cells plated in 6 cm dishes or 6-well plates, cells were washed twice with ice cold PBS. Cells were harvested using 300 µl solubilising buffer [20 mM Hepes-NaOH (pH 7.7), 50 mM NaCl, 0.1 mM EDTA, 1% (w/v) Triton X-100, 0.2 mM PMSF, 4 µg/ml leupeptin, 4 µg/ml aprotonin and trace Na_3VO_4, pH 7.6], transferred to a 1.5 ml eppendorf, vortexed and retained on ice to solubilise for at least 30 minutes. Glutathione sepharose (GSH) untagged carrier beads (20 µl) were washed with PBS (13 000 g centrifugation for 1 minute at 4^{o}C) prior to the addition of GST-c-Jun tagged GSH beads (2.23 µl). The beads were subsequently washed with solubilising buffer (13 000 g, 4^{o}C for 1 minute). Solubilised cellular extracts were centrifuged (13 000 g) for 5 minutes at 4^{o}C. The supernatants obtained were added to the beads and incubated at 4^{o}C overnight on a revolving wheel to pull down JNK from the cell extracts.

The following day, samples were centrifuged (13 000 g) for 1 minute at 4^{o}C and the supernatant was discarded to retain the beads. The beads were washed with solubilising buffer and kinase buffer [25 mM Hepes-NaOH (pH 7.6), 20 mM $MgCl_2$, 4.6 mM β-glycerophosphate, trace DTT and trace Na_3VO_4, pH 7.5] consecutively. [γ-^{32}P]ATP was added to cold ATP (25 µM cold ATP prepared in kinase buffer), the ATP mix was subsequently added to the samples (0.5 µCi [γ-^{32}P]ATP per sample). Samples were incubated at 30^{o}C for 30 minutes, shaking at 14 000 r.p.m. Reactions were terminated by the addition of 4X SDS sample buffer and boiling samples for 3 minutes. Samples were subsequently centrifuged (10 000 g) for 1 minute. Proteins were run on 11% ployacrylamide gels [11% acrylaimde: 0.29% bis-acrylamide and 375 mM Tris-base, 0.1% (w/v) SDS, pH 8.8 plus 0.08% (w/v) APS and 0.08% (v/v) TEMED] of 1.5 cm thickness and the gels were placed in fixer solution [20% methanol and 10% acetic acid] for at least 30 minutes. Fixed gels were dried using a Hoefer Easy Breeze Gel Drier and phosphorylated c-Jun visualised by autoradiography, using a JP-33 film processor.

2.2.10 Bystander transfer technique

The media transfer technique, transferring conditioned media from treated to untreated cells, was utilised to assess bystander signalling between cells.

This technique is based on the media transfer assay performed by Boyd *et al*., 2006. Cells plated in 6 cm dishes (HACEC, MCF-7) or T_{25} flasks (UVW) were incubated for 48 hours at 37^{o}C in a humidified atmosphere (5% CO_2/95% air) until 70% confluent. Immediately prior to irradiation, the media in each dish/flask was replaced with 1.5 ml fresh media. Cells, designated 'donor' cells, were directly irradiated and incubated for 1 hour. Thereafter, the media maintaining 'recipient' cells was removed and conditioned media from 'donor' cells transferred to the appropriate 'recipient'. The 'donor' cells were supplemented with 1.5 ml fresh media and all cells were incubated for a further 24 hours at 37^{o}C in 5% CO_2/95% air. After 24 hours, all cells were subject to a clonogenic survival assay as outlined in section 2.2.5.

2.2.11 Statistical analysis

Values are represented as mean ± standard error of the mean (S.E. mean). Data gathered was analysed using GraphPad Prism 4 analytical software. Statistically significant differences between groups were determined by one-way analysis of variance (ANOVA) (three or more group comparisons) with Dunnett's post hoc test (control vs. non-control group) or Tukey's post hoc test (non-control vs. non-control group), $p<0.05$ was deemed statistically significant.

Concentration response curves were created using GraphPad Prism 4 analytical software fitting a non-linear regression curve (sigmoidal dose-response curve with variable slope). Where indicated in the figure legend, constraints were applied (i.e. bottom of the curve constrained to 1 for data represented as fold control and top constraint set at 100 for viability experiments where data depicted as % control). A separate curve was created for each individual experiment (3 experiments analysed) and the EC_{50}/IC_{50} value attained from each curve compiled to find the mean ± S.E.mean.

Chapter 3:

Characterisation of the effects of doxorubicin on endothelial cell function – the role of JNK

3.1 Introduction

Due to the transport of doxorubicin in the bloodstream, vascular endothelial cells, providing a barrier between the blood and underlying vessel tissue, may be subject to the detrimental effects of doxorubicin leading to vascular damage. Nonetheless, the effects of doxorubicin on endothelial cells, especially coronary artery endothelial cells, are poorly defined. Current endothelial cell studies portray both cytostatic and cytotoxic properties of doxorubicin, for example, Spallarossa *et al*., identified apoptotic death of cord blood endothelial progenitor cells (EPCs) treated with 1 µM doxorubicin, whereas 0.25 µM doxorubicin induced a senescent phenotype (Spallarossa *et al*., 2010). Interestingly, inhibition of JNK activity promoted death of EPCs treated with a sub-apoptotic dose of doxorubicin (0.25 µM), suggesting a pro-survival role for JNK in endothelial cells (Spallarossa *et al*., 2010). This single study by Spallarossa *et al*., is currently the only published research investigating the contribution of JNK to doxorubicin-mediated cellular effects in endothelial cells. Therefore the role of JNK in endothelial cell responses to doxorubicin requires further exploration.

Endothelial cells from different organs display phenotypic heterogeneity and respond differently to anticancer drugs relative to their organ of origin (Maney *et al*., 2011). Maney *et al*., studied doxorubicin-treated primary endothelial cells and uncovered that doxorubicin-treated HUVECs displayed significantly greater chromatin condensation compared to porcine endocardial endothelial cells (EECs) and human aortic endothelial cells (HAECs), indicating that doxorubicin is more toxic to HUVECs than EECs and HAECs (Maney *et al.*, 2011). Additionally, immortalised EECs (hTEKT-EECs) were less affected by mitochondrial membrane-potential changes resulting in apoptosis than immortalised human hybridoma EA.hy926 cells (Maney *et al.*, 2011). Despite this, the majority of studies investigating the response of endothelial cells to anticancer agents employ HUVECs (Maney et al., 2011). At present, two papers published by Kaushal *et al*., are the only studies to report doxorubicin-related toxic effects on *in vitro* cultured HCAECs (Kaushal *et al*., 2004[1], Kaushal et l., 2004[2]). These studies report the apoptotic response of doxorubicin-treated HCAEC but do not explore further cellular changes. Hence characterisation of

the effects of doxorubicin on the functioning and survival of HCAECs is lacking, an important area of concern due to the contributory role of HCAEC dysfunction in the pathophysiology of highly prevalent coronary artery disease.

This chapter utilised HCAECs to establish the cellular effects of doxorubicin on arterial endothelial cells, located within vessels where atherosclerosis development can result in fatal heart failure. More specifically, the effect of doxorubicin on HCAEC cell cycle progression and survival was examined, plus the role of JNK in doxorubicin-mediated HCAEC dysfunction was elucidated.

3.2 Results

3.2.1 Doxorubicin-induced death of HCAECs

As mentioned previously, doxorubicin has been shown to be cytotoxic to endothelial cell types presently studied. Most studies investigating the effects of doxorubicin on endothelial cells report doxorubicin-mediated cellular death (Damrot *et al*., 2006, Maney *et al*., 2011, Spallarossa *et al*., 2010). Kaushal *et al*., detailed some of the apoptotic mechanisms of death in doxorubicin-treated HCAECs using a limited range of doxorubicin concentrations (Kaushal *et al*., 2004[1], Kaushal et l., 2004[2]). To expand on their work, this section will characterise the survival of the HCAECs acquired for this study, using a broader range of doxorubicin concentrations.

In vitro MTT toxicity assays were initially employed to assess the mitochondrial metabolic activity, an indicator of cell viability, of acutely doxorubicin-exposed HCAECs. A comparison between the survival response of HCAECs and MCF-7 breast cancer cells was investigated to understand the severity of doxorubicin-mediated endothelial cell death relative to cancer cell death. MCF-7 cells were chosen as a comparative cancer cell response as MCF-7 cells are a proven doxorubicin-sensitive cell line with multiple published studies detailing the inhibitory effect of doxorubicin on MCF-7 cell survival (Fornari *et al*., 1996, Kanno *et al*., 2014, Kim *et al*., 2003, Osman *et al*., 2012).

HCAECs and MCF-7 cells were exposed to a concentration range of doxorubicin between 0.1 and 100 μM for 8 and 24 hours to assess the early effects of doxorubicin on the survival of endothelial and cancer cells. At the earliest timepoint studied, 8 hours doxorubicin treatment, high concentrations (≥ 10 μM) of doxorubicin caused a minor but statistically insignificant reduction in HCAEC cell viability (Figure 3.1). High doxorubicin concentrations were also required to reduce MCF-7 viability [% control: 30 μM dox. 68.74 ± 7.16, $p<0.01$, n=3]. Therefore, HCAECs and MCF-7 cells exposed to low μM doxorubicin concentrations remained viable up to 8 hours after initial exposure. However, when observations were extended to 24 hours doxorubicin treatment, a concentration-dependent reduction in cell viability was observed for HCAECs and MCF-7 cells, the viability of both cell types was reduced significantly with 3 μM doxorubicin [% control: HCAEC, 63.13 ± 1.32, $p<0.01$, n=4. MCF-7, 40.81

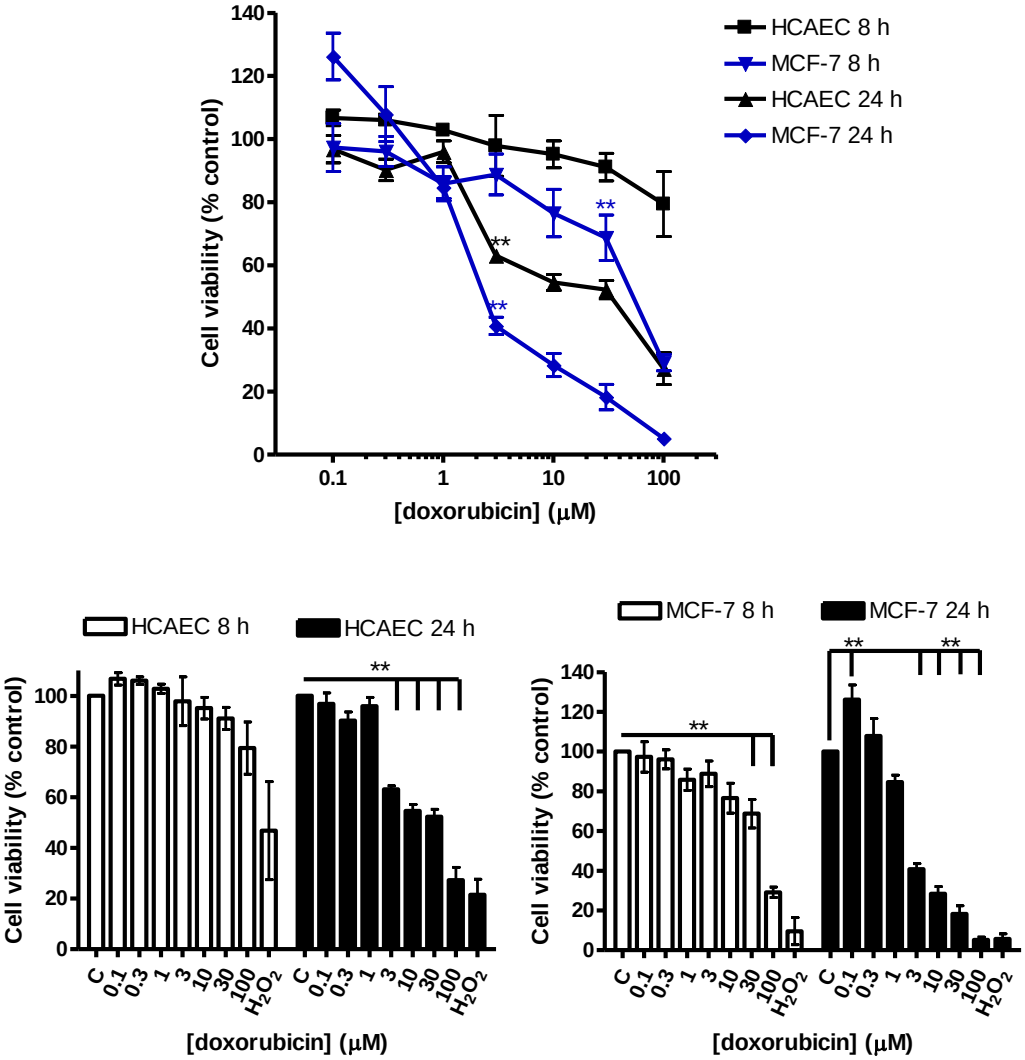

Figure 3.1: Comparison of the effect of doxorubicin on HCAEC and MCF-7 cell viability. Cell viability was assessed by MTT assay, as outlined in section 2.2.4, 8 or 24 hours post-treatment with doxorubicin. HCAECs/MCF-7 cells treated with dH_2O provided a negative control (C) and H_2O_2 (0.98 M) acted as a positive control. Values show mean ± S.E. mean, n=3 for 8 hour treatments and n=4 for 24 hour treatments. Triplicates were averaged for each experiment. ** $p<0.01$ relative to the negative control (C).

± 2.74, $p<0.01$, n=4]. MCF-7 cells were more sensitive to doxorubicin, the generation of concentration response curves confirmed that doxorubicin is more potent for MCF-7 cells than HCAECs with calculated IC_{50} values of 1.24 ± 0.27 µM and 5.82 ± 2.10 µM respectively (Figure 3.2). Thus, assessment of the viability of endothelial and cancer cells following exposure to doxorubicin revealed that this compound affects the metabolic activity of both HCAEC and MCF-7 cells, promoting loss of viable cells, but doxorubicin has a greater detrimental effect on breast cancer cells.

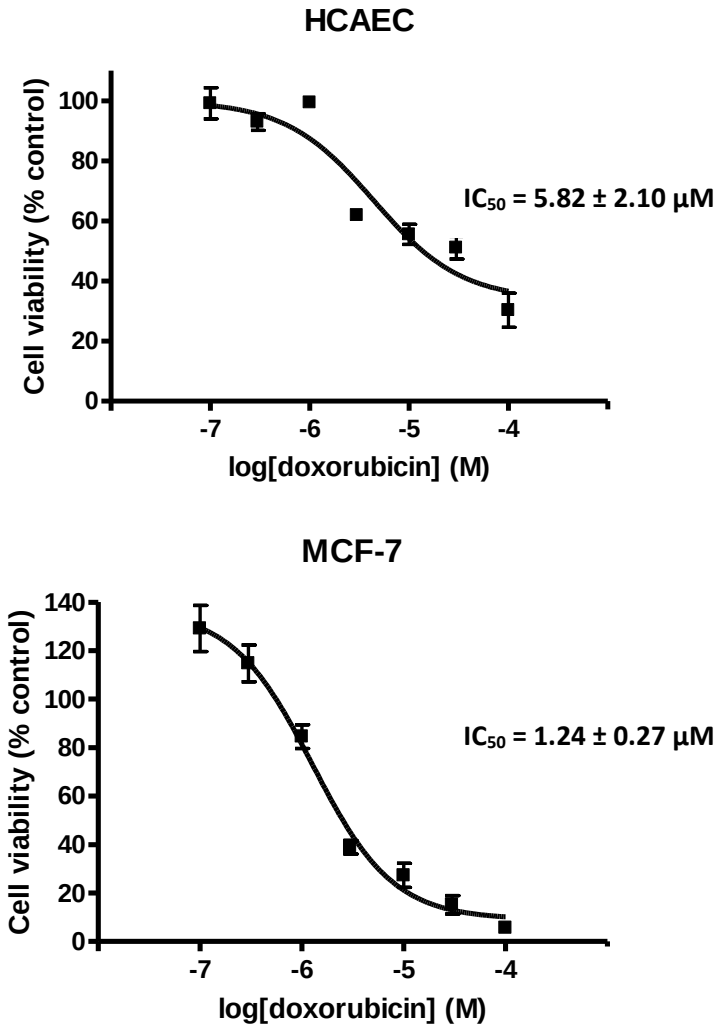

Figure 3.2: Calculation of IC_{50} values for doxorubicin-mediated reduction of HCAEC and MCF-7 cell viability after 24 hours. Each curve illustrates the average of 3 separate experiments. IC_{50} values were calculated from 3 separate curves as outlined in section 2.2.11, then averaged to discern the mean IC_{50} ± S.E.mean. An upper constraint of 100% was applied for the HCAEC response curve.

As discussed previously, doxorubicin elicits apoptotic death of endothelial cells, including HCAECs (Kaushal *et al*., 2004[2]). Kaushal *et al*., showed that doxorubicin caused DNA fragmentation and activated apoptotic regulator caspase-3 in HCAECs using experimental techniques including TUNEL assays, enzyme activity assays and western blotting (Kaushal *et al*., 2004[1], Kaushal *et al*., 2004[2]). However, their published research did not include the use of flow cytometry, a useful and widely utilised technique to study apoptotic cells which express specific markers, such as extracellular expression of membrane phospholipid phosphatidylserine which is associated with early apoptosis. Flow cytometry apoptotic studies require labelling of cells with Annexin V (binds phosphatidylserine) conjugated to a fluorophore and incubation with a membrane-permeable fluorescent DNA stain, thereby providing information about the current stage of cellular apoptotic death (early or late).

For this study, doxorubicin-treated HCAECs were labelled with Annexin V-PE and incubated with DNA stain 7-AAD, which have been used to investigate apoptosis of doxorubicin-treated lymphoid REH and myeloid K562 leukemic cell lines, epithelial colon cell line LS 174T and mononuclear cells from umbilical cord blood *in vitro* (Cheng *et al*., 2013, Chieng *et al*., 2015. Lu *et al*., 2008). Annexin V-PE/7-AAD dual staining has also been successfully used by our laboratory to study apoptosis of UVC-irradiated MDA-MB-231 breast cancer cells and TNF-α-stimulated HUVECs transfected with dominant-negative IKKβ adenovirus (Al-Mutairi *et al*., 2010), hence preliminary experiments were attempted. However, doxorubicin is autofluorescent, it has an anthraquinone chromophore constituent, with excitation and emission maximum at 480 nm and 560-590 nm respectively (de Lange *et al*., 1992). Consequently, there is spectral overlap between doxorubicin and PE (em-max. 496 nm/ex-max. 578 nm) and to a lesser extent 7-AAD (em-max. 488 nm/em-max. 647 nm). In order to examine whether intracellular doxorubicin would itself increase the number of Annexin V-PE and 7-AAD positive events detected by FACS, doxorubicin-treated but unstained cells were analysed (Figure 3.3). A concentration-dependent increase in the number of events recorded by the channels detecting PE and PerCP was observed as a shift of cells into Q2 [no. of events in Q2: control. 13.00 ± 4.00, 1 µM dox. 3354.00 ± 311.50, $p<0.01$, n=3] (Figure 3.3, Graph A). Therefore, an experiment

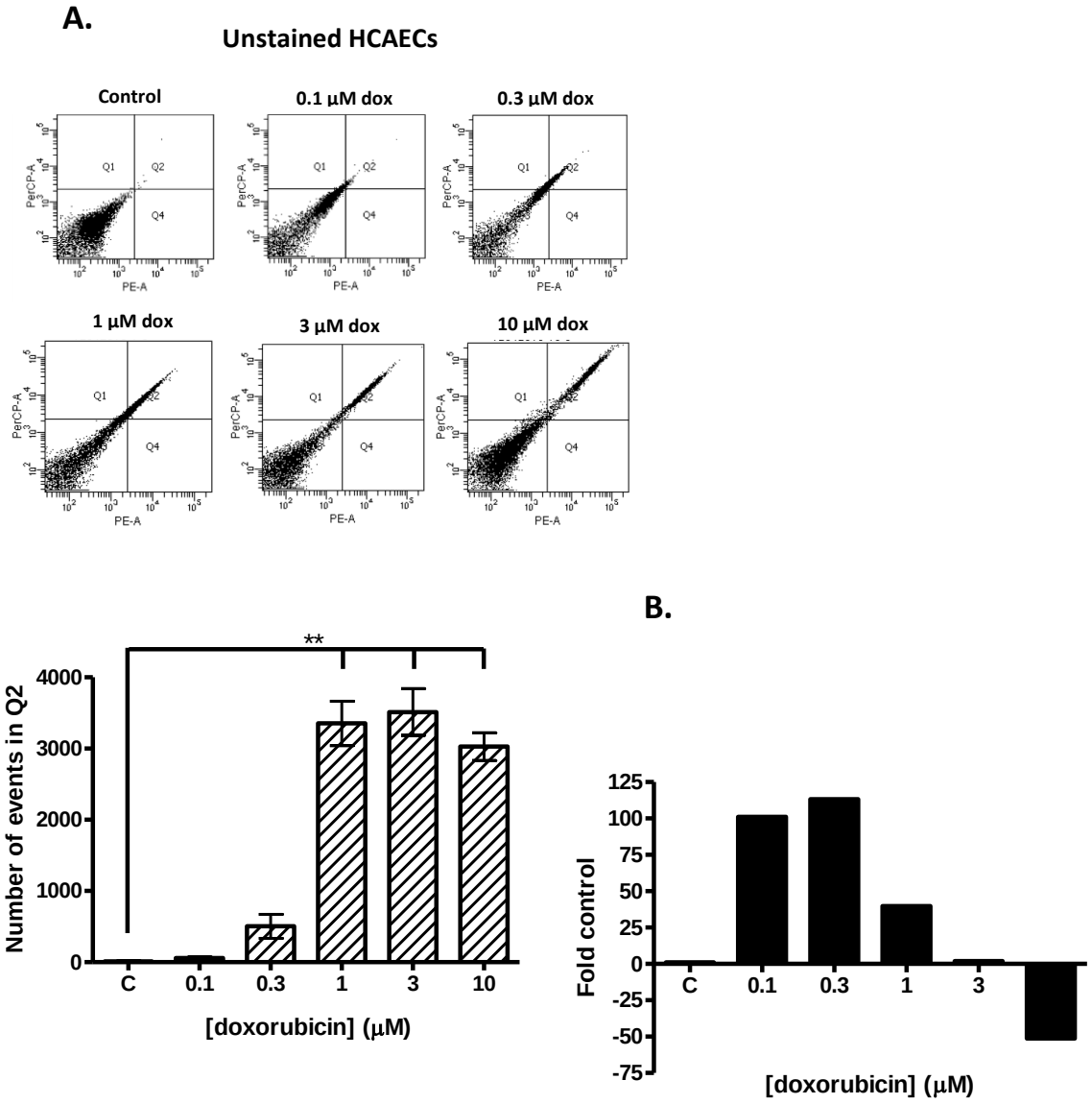

Figure 3.3: Problems using Annexin V-PE and 7-AAD to study apoptosis of HCAECs. **A.** HCAECs were treated with doxorubicin alone (no staining) and analysed by FACS 24 hours post-treatment, as detailed in section 2.2.6.3. Values represent mean ± S.E. mean, n=3. **p<0.01 compared to control (C). **B**. The number of events in Q2 generated from stained doxorubicin-treated HCAECs was normalised to the results from non-stained HCAECs. n=1.

was performed where doxorubicin-treated HCAECs stained with Annexin V-PE and 7-AAD were analysed by FACS in parallel with doxorubicin-stimulated HCAECs which remained unstained. The data for stained cells was normalised to the results for unstained cells, correcting for an increase in Q2 events caused by the stains and doxorubicin autofluroescence (Figure 3.3, Graph B). The data gathered from this single experiment demonstrated an increase in Q2 events with 0.1 and 0.3 µM doxorubicin indicating late apoptotic responses by HCAECs. However, at doxorubicin concentrations greater than 0.3 µM, normalisation of results generated diminished and negative values, indicating that the autofluoresence of doxorubicin, which significantly increased the number of events in Q2, is eclipsing any signals generated by Annexin V binding of phosphatidylserine or DNA staining by 7-AAD. Despite Annexin V-PE/7-AAD being utilised to study apoptosis of cancer cells exposed to doxorubicin (up to 6 µM) (Chieng *et al*., 2015), it is not a suitable method for this study of HCAEC apoptosis where doxorubicin concentrations up to 10 µM for 24 hours were trialled. However, these findings did verify the intracellular accumulation of doxorubicin in HCAECs with doxorubicin remaining present in HCAECs 24 hours post-treatment.

Due to Annexin V-PE being unsuitable to study apoptosis of doxorubicin-exposed HCAECs, the use of a different fluorophore conjugated to Annexin V was attempted. Annexin V-FITC is the most routinely used combination for studying doxorubicin-mediated apoptosis of cells, including endothelial cells such as HUVECs and BAECs (Chen *et al*., 2014, Peled *et al*., 2008). However, the FITC (em-max. 494 nm/em-max. 520 nm) and doxorubicin fluorescence spectrums also overlap. Doxorubicin-treated, unstained HCAECs were analysed by FACs to determine whether doxorubicin cellular accumulation would relay an increase in FITC positive events (Figure 3.4). Moreover, the effect of the doxorubicin-treated HCAECs on APC positivity was examined because the emission maximum of APC (em-max. 650 nm/em-max. 660 nm) differs more greatly from doxorubicin than FITC. Figure 3.4 depicts the effect of doxorubicin alone, without the addition of stains, on FITC and APC signal generation. The increase in the number of FITC and APC positive events generated (Q4) was concentration-dependent, however doxorubicin caused a dramatically greater increase in FITC positive events relative to APC [no. of events in Q4: 3 µM dox. FITC, 2891.00 ±

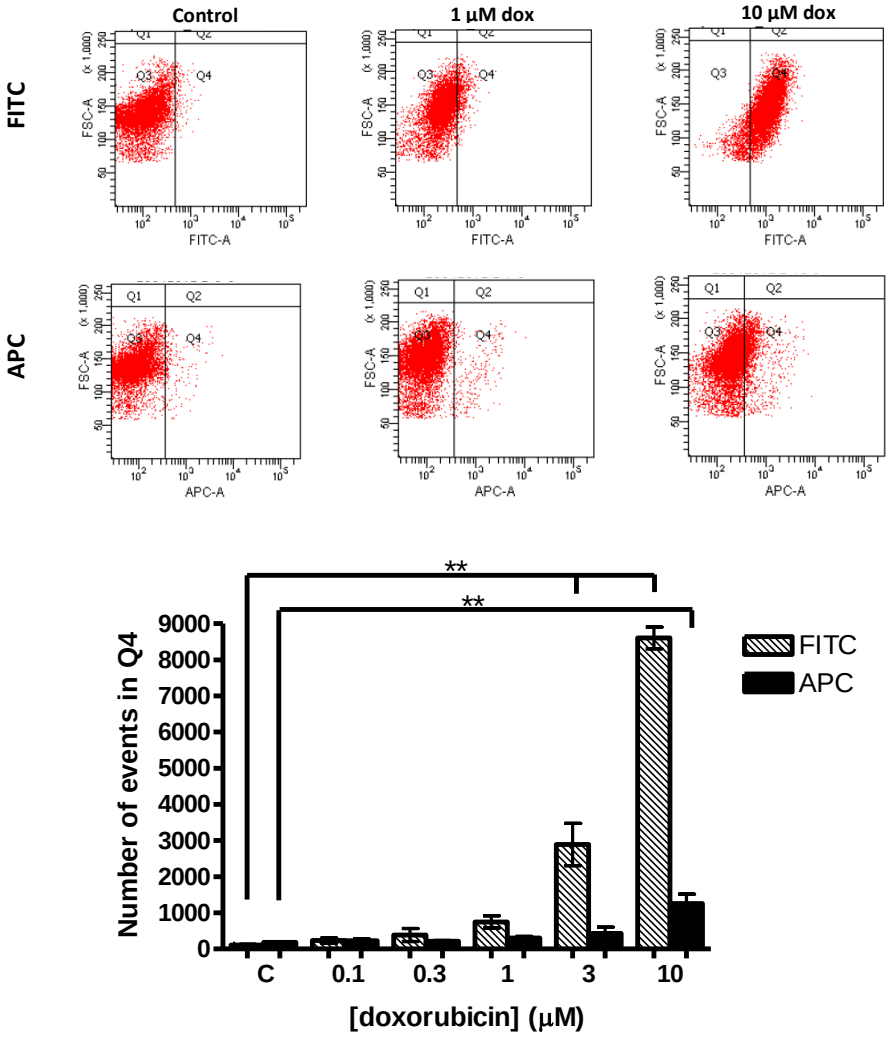

Figure 3.4: Comparison of the FITC and APC signal shift caused by doxorubicin alone. HCAECs treated with increasing concentrations of doxorubicin were analysed using FACS as described in section 2.2.6 for FITC and APC positivity. An increase in Q4 events represents an increase in the number of HCAECs emitting fluorescence at the wavelengths detected by the flow cytometer FITC and APC channels. Values depict mean ± S.E. mean, n=3. **p<0.01 compared to control.

587.50, $p<0.01$, n=3. APC, 432.50 ± 172.50, n=3]. Consequently, Annexin V-APC was selected as the tool to study apoptosis of HCAECs caused by doxorubicin.

Single staining of HCAECs with Annexin V-APC was performed to decipher apoptotic (Q4) from non-apoptotic (Q3) cells. For each experiment performed, stained and non-stained doxorubicin-treated HCAECs were analysed in parallel. Notably, addition of Annexin V-APC to un-treated (control) cells caused a shift in the population of events compared to unstained cells (Figure 3.5). Therefore, the shift caused by the stain was accounted for during normalisation of the stained results to unstained results. Figure 3.5 (Graph A) depicts the number of events in Q4 of unstained cells and stained cells after adjusting for the signal shift generated by the stain. Additionally, to correct for doxorubicin autofluorescence, Q4 events of unstained cells were subtracted from stained cells hence the true increase in Annexin V positive cells was identified. An increase in the number of Annexin V positive cells compared to control cells was determined for all doxorubicin concentrations examined, suggesting increased numbers of apoptotic cells. The increase was somewhat concentration-dependent, excluding the variable results for 0.3 µM doxorubicin, with even the lowest doxorubicin concentration studied causing a statistically significant increase in the number of Annexin V positive cells [fold control: 0.1 µM dox. 5.98 ± 0.49, $p<0.01$, n=4] (Figure 3.5, Graph B). Thus, despite no evidence for a death response in HCAECs treated with 0.1 and 0.3 µM doxorubicin using an MTT assay 24 hours post-treatment, these experiments reveal increased cellular binding of Annexin V to early apoptotic marker phosphatidylserine induced by doxorubicin concentrations in the low µM range. Perhaps extending analysis of HCAEC death beyond 24 hours treatment with doxorubicin would have exposed cytotoxic effects of low doxorubicin concentrations in the MTT assay. Jointly, the results from the MTT assays and flow cytometric analysis of Annexin V for examination of cellular apoptosis confirm that doxorubicin is a death-promoting agent, killing HCAECs in addition to cancer cells and other endothelial cell types.

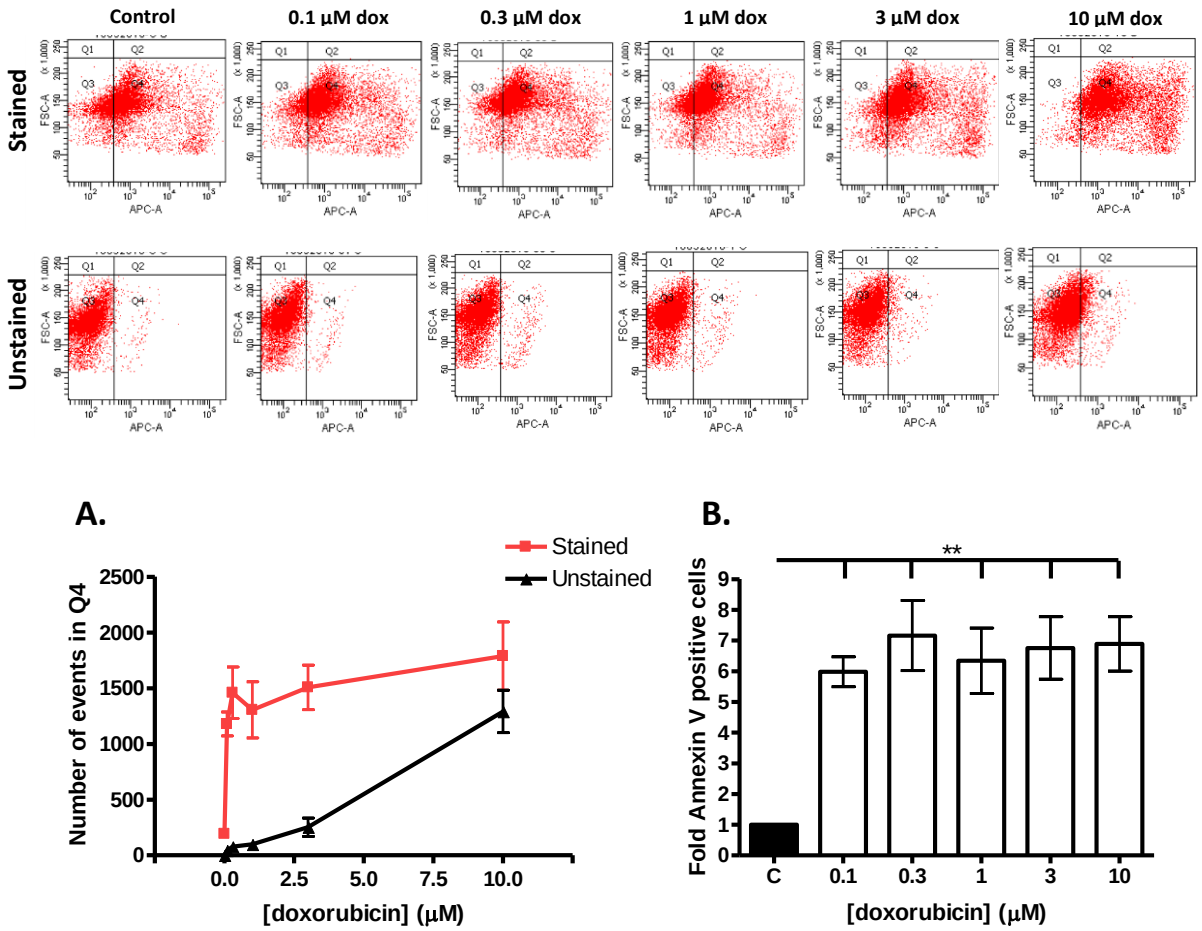

Figure 3.5: Assessment of doxorubicin-mediated HCAEC apoptosis utilising Annexin V-APC. HCAECs were exposed to increasing concentrations of doxorubicin for 24 hours then stained with Annexin V-APC or remained unstained prior to FACs analysis as described in section 2.2.6. Graph A displays the number of events in Q4 generated by doxorubicin-treated HCAECs (for stained cells (red line), the increase in the number of Q4 events caused by the Annexin V-APC stain itself was subtracted from the total number of events in Q4). Graph B illustrates the results for Annexin V-APC positive HCAECs normalised to the results for unstained HCAECs. Values show mean ± S.E. mean, n=4. **p<0.01 compared to control (C).

3.2.2 Doxorubicin-mediated cell cycle control in HCAECs

In addition to understanding the death-promoting effects of doxorubicin on HCAECs, it is important to consider the altered functionality of surviving endothelial cells at the arterial wall. Furthermore, what happens to HCAECs exposed to a concentration too low to trigger death? Cell cycle status provides key information regarding the proliferative capability of cells, this information is imperative when investigating anticancer therapies which damage DNA to inhibit cell proliferation. Therefore, the effects of doxorubicin on HCAEC cell cycle distribution were elucidated.

Analysis of cell cycle status was performed using PI staining of DNA followed by flow cytometry to determine cellular DNA content. The timescale for cell cycle changes in doxorubicin-treated HCAECs has never been characterised. Therefore, the effect of doxorubicin on HCAEC cell cycle distribution was assessed in HCAECs treated with doxorubicin for different time periods. HCAECs were not synchronised at a particular cell cycle stage prior to doxorubicin treatment to mimic the variable cell cycle status of endothelial cells exposed to doxorubicin within the vessel environment. Assessment of the cell cycle profile of HCAECs exposed to doxorubicin (0.1 to 10 μM) for 1 and 4 hours revealed no alteration of cell cycle distribution, except from a minor, statistically insignificant increase in the percentage of S phase cells when HCAECs were treated with 1 μM doxorubicin for 4 hours [fold control: 1.44 ± 0.17, n=5] (Figure 3.6), however extending analysis up to 24 hours showed marked cell cycle re-distribution. Low concentrations of doxorubicin (0.1 and 0.3 μM) promoted a statistically significant, twofold increase in the percentage of cells in the G2/M phase of the cell cycle [fold control: 0.1 μM dox. 2.01 ± 0.02, $p<0.01$, n=5], associated with a significant reduction in S phase cells [fold control: 0.1 μM dox. 0.32 ± 0.02, $p<0.01$, n=5] (Figure 3.6 cont.). On the other hand, higher doxorubicin concentrations caused a significantly greater proportion of cells to be positioned at the S phase of the cell cycle compared to control cells [fold control: 3 μM dox. 2.14 ± 0.17, $p<0.01$, n=5]. This experiment revealed that low concentrations of doxorubicin enable progression of HCAECs through the cell cycle until accumulation at G2/M, whereas higher doxorubicin concentrations block HCAECs earlier during cell cycle transition, the S phase, hindering advancement of the cells to G2 and commencement of mitotic division. Unsurprisingly, due to increased number of cells in either the S phase (high

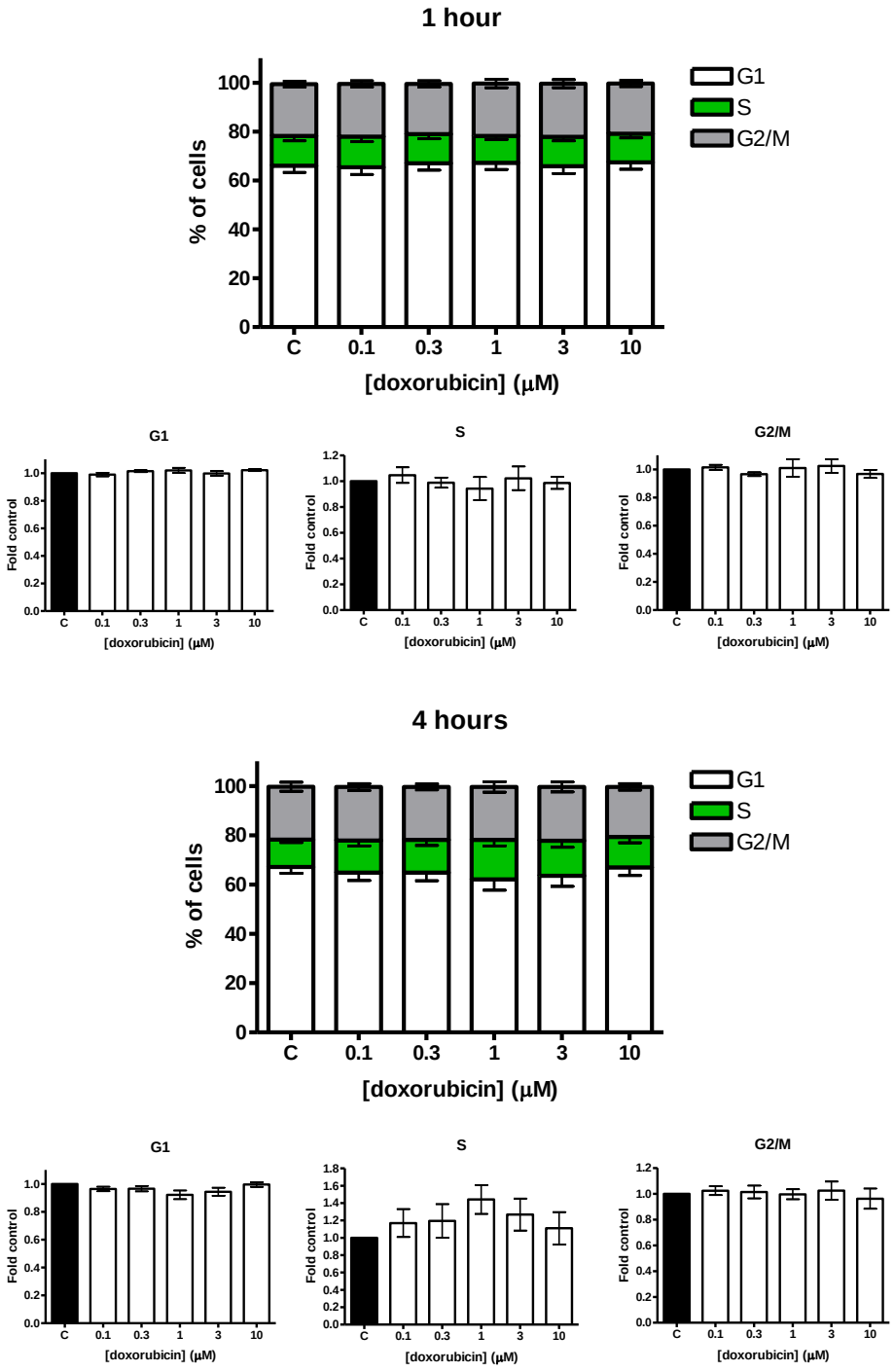

Figure 3.6: Effect of doxorubicin on HCAEC cell cycle distribution. HCAECs were treated with varying doxorubicin concentrations (50 µl) for 1 or 4 hours and cell cycle analysis performed using FACS as outlined in section 2.2.7. HCAECs treated with dH_2O (50 µl) acted as a vehicle control (C). Values represent mean ± S.E. mean, n=5.

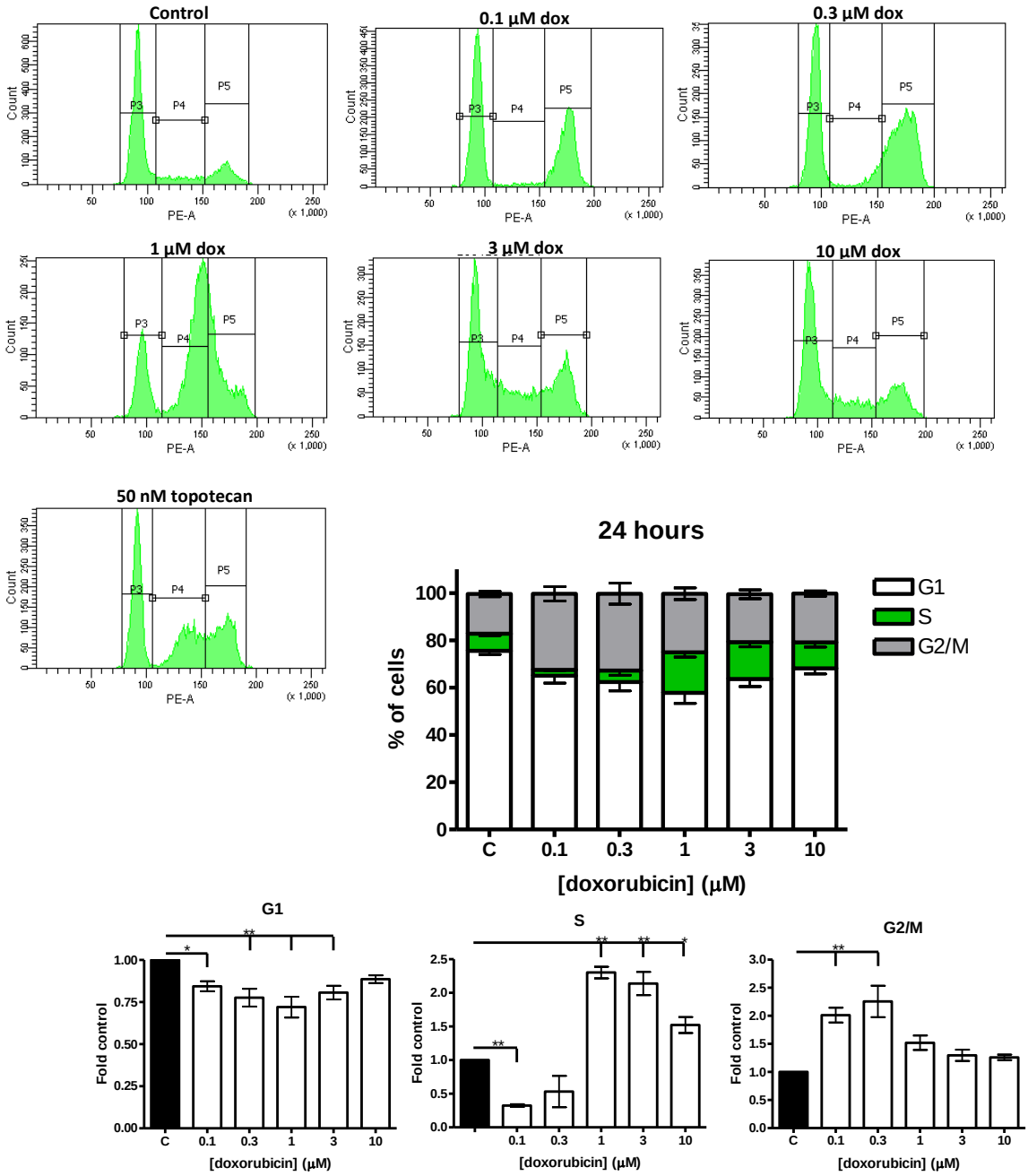

Figure 3.6 cont.: Effect of doxorubicin on HCAEC cell cycle distribution. HCAECs were treated with doxorubicin for 24 hours (treated at the same time as 1 and 4 hour stimulations) and cell cycle distribution determined by FACS as detailed in section 2.2.7. HCAECs treated with dH_20 provided a negative control (C) and chemotherapeutic drug topotecan (50 nM) acted as a standard for cell cycle re-distribution. Intervals P3, P4 and P5 represent G1, S and G2/M cell cycle stages respectively. Values represent mean ± S.E. mean, n=5. *p<0.05, **p<0.01 compared to control.

doxorubicin concentrations) or G2/M phase (low doxorubicin concentrations), all concentrations of doxorubicin caused a reduction in the percentage of cells in the G1 cell cycle stage. Of note, doxorubicin autofluorescence did not interfere with the FACS data gathered for DNA content, as tested in doxorubicin-treated HCAECs which were not stained with PI. Collectively these findings show that cell cycle progression is impeded in HCAECs exposed to doxorubicin, blockade of cell cycle progression occurred at distinct cell cycle stages, dependent on the concentration of doxorubicin.

3.2.3 JNK pathway activation in doxorubicin-treated HCAECs

As discussed previously, cellular processes resulting in growth arrest or death are tightly controlled by numerous intracellular signalling intermediates. JNK is a known regulator of cell fate as described in section 1.7.1. Having identified that doxorubicin promotes HCAEC cell cycle arrest and death, experiments were performed to characterise the response of JNK in HCAECs treated with doxorubicin.

Doxorubicin-triggered JNK pathway activation in endothelial cells is poorly defined, therefore the kinetics of JNK activation induced by recognised, strong inducers of JNK kinase activity was firstly characterised to enable a comparison between the JNK response induced by these agents and doxorubicin. Phosphorylation of JNK, a critical modification preceding JNK kinase activation, was initially investigated in UVC-irradiated HUVECs and HCAECs treated with inflammatory cytokine IL-1β by immunoblotting whole cell lysates for JNK phosphorylated at tyrosine residue 183 and threonine residue 185. Rapid phosphorylation of both JNK isoforms, p54 and p46, was observed in endothelial cells treated with UVC radiation and IL-1β, occurring within 15 minutes of treatment and reaching peak phosphorylation after 30 minutes [fold control: p54 JNK, 50.64 ± 33.32, p46 JNK, 66.05 ± 28.63, $p<0.05$, $n=3$] (Figure 3.7). Phosphorylation of JNK was transient in IL-1β treated HCAECs, with phosphorylated JNK expression depreciating quickly 45 minutes after treatment, however phosphorylated JNK levels remained up-regulated in UVC-irradiated HUVECs for at least 4 hours post-irradiation, thus showing the differential kinetics of JNK cascade activation by different agents.

In addition to understanding kinetics of JNK phosphorylation by doxorubicin relative to UVC-irradiation and IL-1β, phosphorylation of JNK in HCAECs was also compared with MCF-7 cells to investigate a potential distinctive JNK response in HCAECs, different from cancer cells. A relatively high concentration of doxorubicin (10 μM) was exploited to trigger phosphorylation of JNK and understand the kinetics of JNK phosphorylation in HCAECs and MCF-7 cells up to 24 hours post-treatment. As previously presented in Figure 3.1, 24 hours treatment with 10 μM doxorubicin caused significant death of both HCAECs and MCF-7 cells, signifying activation of

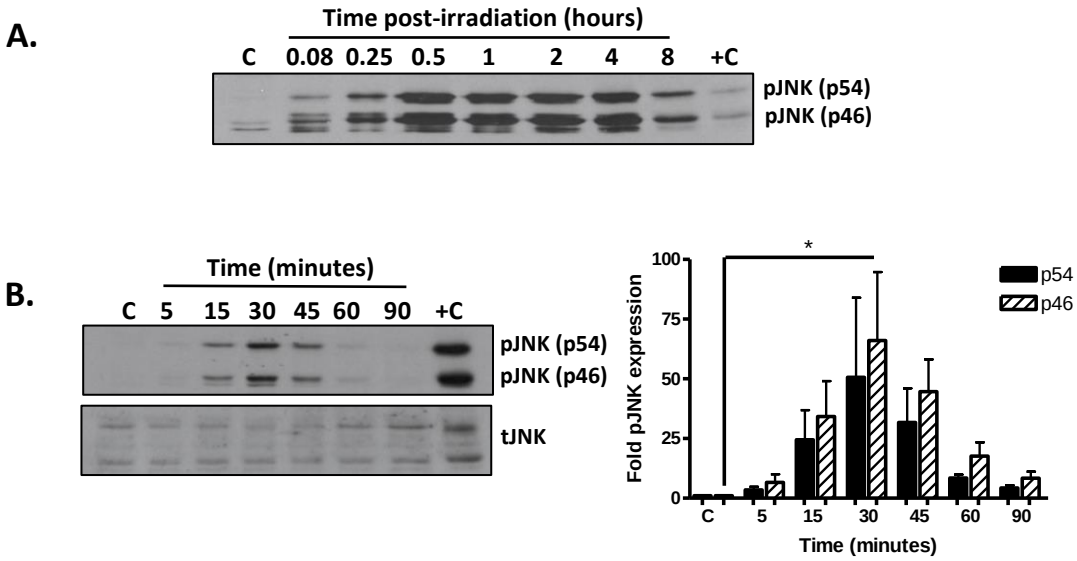

Figure 3.7: UVC radiation and IL-1-induced JNK phosphorylation in endothelial cells. A. HUVECs were exposed to 30 J/m^2 UVC radiation and phosphorylated JNK expression analysed at the identified timepoints post-irradiation (IR) by Western blotting as described in section 2.2.8. Sham-irradiated control cells (C) were harvested at the 8 hour timepoint. TNFα-treated (10 ng/ml, 15 minutes) HUVECs served as a positive control (+C). n=1. **B.** HCAECs were treated with IL-1β (10 ng/ml) for the indicated durations and phosphorylated JNK detected by Western blotting as outlined in section 2.2.8. PBS-treated HCAECS and UVC-irradiated (30 J/m^2, 30 minutes post-irradiation) HUVECs provided a negative (C) and positive control (+C) respectively (C). Values depict mean ± S.E. mean, n=3. *$p<0.05$ compared to control (C).

complex signalling systems to promote cell death which may involve stress-activated JNK.

Immunoblotting identified phosphorylation of both p54 and p46 JNK in doxorubicin-treated HCAECs and MCF-7 cells (Figure 3.8). Onset of JNK phosphorylation in HCAECs by doxorubicin was delayed compared to IL-1β and UVC-irradiation, occurring 2 hours after initial doxorubicin treatment and reaching statistical significance in HCAECs treated with doxorubicin for 4 hours [fold control: p46 pJNK, 5.12 ± 1.81, $p<0.05$, n=4] (Figure 3.8). Accounting for the large error bars, JNK phosphorylation appears to be sustained up to 24 hours post-treatment with doxorubicin. Slower than HCAECs, doxorubicin-induced phosphorylation of JNK in MCF-7 cells was delayed until 4 hours after initial doxorubicin treatment and occurred to a lesser extent than in HCAECs. Moreover, transient phosphorylation of JNK was observed in doxorubicin-exposed MCF-7 cells with maximum phosphorylation of the p46 isoform of JNK achieved in cells treated for 8 hours [fold control: p46 pJNK, 6.33 ± 1.09, $p<0.01$, n=3] (Figure 3.8). Interestingly, different isoforms of JNK were preferentially phosphorylated in the HCAECs and MCF-7 cells, p54 JNK and p46 JNK respectively. These finding imply potentially differential mechanisms of JNK activation in HCAECs and MCF-7 cells treated with doxorubicin.

From these experiments, distinct patterns of JNK activation by doxorubicin in HCAECs and MCF-7 cells have been identified, plus doxorubicin displayed slower phosphorylation of JNK than established JNK pathway activators. Phosphorylated JNK levels were up-regulated within the 24-hour period post-doxorubicin treatment, which may correlate with the cell cycle changes and death of HCAECs caused by doxorubicin.

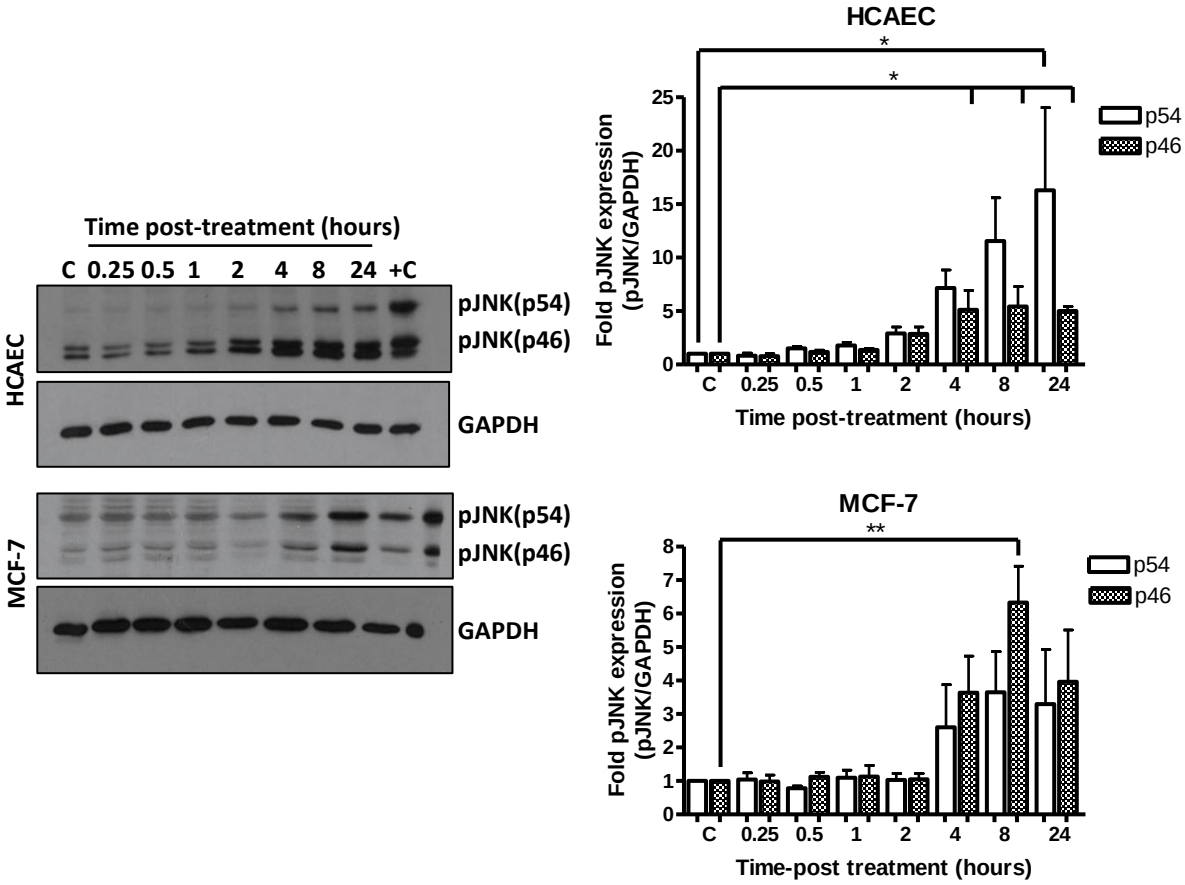

Figure 3.8: Comparison of JNK activation in doxorubicin-treated HCAECs and MCF-7 cells. Cells were treated with 10 μM doxorubicin and expression of phosphorylated JNK (pJNK) assessed by Western blotting as detailed in section 2.2.8. The upper and middle bands represent phosphorylated p54 and p46 JNK respectively. The lower band obtained is due to cross-reactivity of the antibody with phosphorylated ERK 1/2, according to the manufacture's guidelines. Phosphorylated JNK expression was normalised to the GAPDH (37 kDa) loading control. HCAECs/MCF-7 cells treated with dH_2O for 8 hours provided a negative control (C) and IL-1β-treated (10 ng/ml, 15 minutes) HCAECs/MCF-7 cells acted as a positive control (+C). Values represent mean ± S.E. mean, n=4 for HCAECs and n=3 for MCF-7 cells. *$p<0.05$, **$p<0.01$ relative to control (C).

As discerned beforehand, doxorubicin evokes HCAEC cell cycle changes and death at concentrations lower than 10 µM. Therefore, the effect of a range of doxorubicin concentrations on JNK phosphorylation in HCAECs and MCF-7 cells was examined. Cells were treated with doxorubicin for 8 hours, a timepoint identified in Figure 3.8 to show substantial phosphorylation of JNK. Increased phosphorylated JNK levels were detected in HCAECs treated with 1 µM doxorubicin [fold control: p54 pJNK, 1.94 ± 0.52, p46 pJNK, 2.52 ± 0.23, n=4] however elevated expression of phosphorylated p46 JNK was only deemed statistically significantly with doxorubicin concentrations 10 µM or higher [fold control: 10 µM dox. p46 pJNK, 5.64 ± 1.74, $p<0.01$, n=4] (Figure 3.9). Similarly, the concentration-dependent increase in JNK phosphorylation in MCF-7 cells only reached statistical significance with 30 µM doxorubicin [fold control: 30 µM dox. p54 pJNK, 4.93 ± 0.78, $p<0.05$, n=4], despite doxorubicin concentrations as low as 3 µM causing observable increased expression of phosphorylated JNK in MCF-7 cells [fold control: 3 µM dox. p54 pJNK, 2.23 ± 0.30, p46 pJNK, 5.07 ± 1.19, n=4] (Figure 3.9).

To understand the doxorubicin-induced isoform-specific phosphorylation of JNK in HCAECs in more detail, concentration-response curves were generated and EC_{50} values of 2.35 ± 0.64 µM and 1.14 ± 0.15 µM were determined for phosphorylation of p54 and p46 JNK respectively (Figure 3.10). Thus suggesting that doxorubicin is marginally more specific for the p46 JNK isoform in HCAECs. However, JNK phosphorylation in doxorubicin-treated HCAEC cells once again displayed preferential phosphorylation of p54 JNK and in MCF-7 cells p46 JNK was phosphorylated to a greater extent, further confirming favourable phosphorylation of JNK isoforms in HCAECs and MCF-7 cells. Clearly, JNK responses to doxorubicin are cell-type specific; endothelial cells displayed more rapid and sustained JNK phosphorylation compared to breast cancer cells in this study.

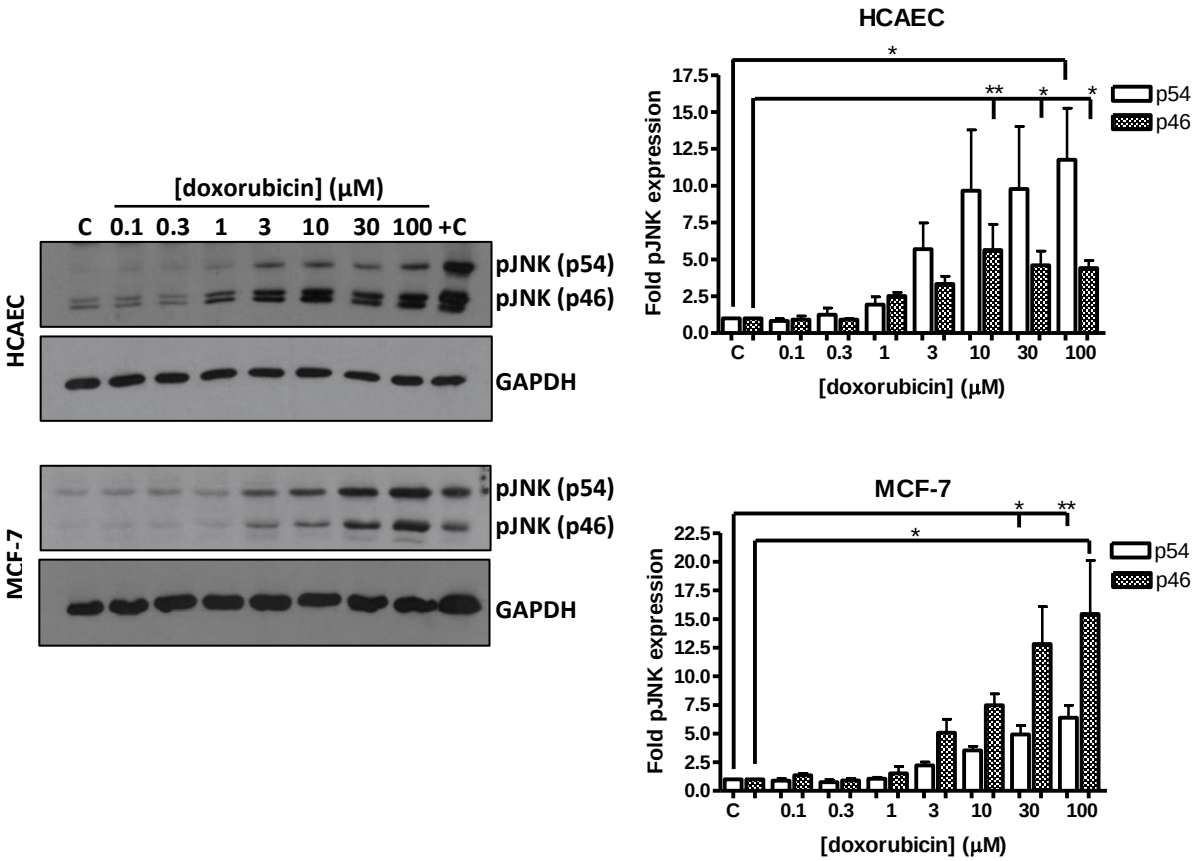

Figure 3.9: Relationship between doxorubicin concentration and phosphorylation of JNK in HCAECs and MCF-7 cells. Cells were treated with doxorubicin for 8 hours and phosphorylated JNK (pJNK) expression detected by Western blotting as outlined in section 2.2.8. HCAECs/MCF-7 cells treated with dH_2O provided a negative control (C) and IL-1β-stimulated (10 ng/ml, 15 minutes) HCAECs/MCF-7 cells provided a positive control (+C). Values represent mean ± S.E. mean., n=4. *$p<0.05$, **$p<0.01$ compared to control (C).

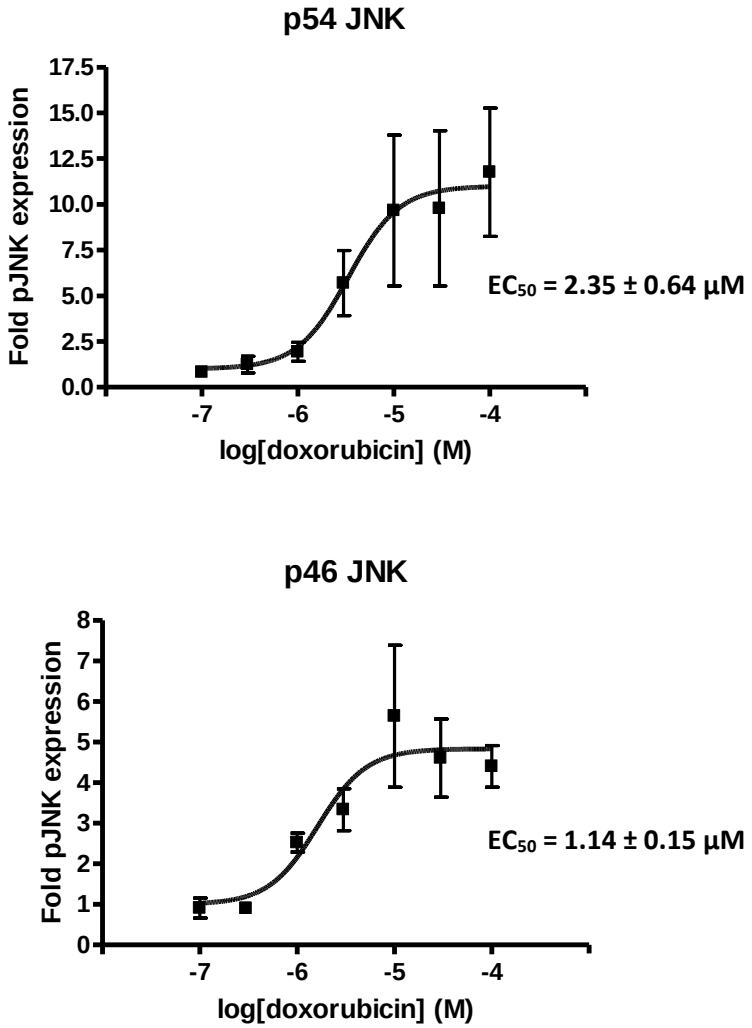

Figure 3.10: Calculation of EC_{50} values for doxorubicin-mediated phosphorylation of JNK in HCAECs. Each response curve illustrates the average of 3 separate experiments. EC_{50} values were calculated for 3 separate curves as outlined in section 2.2.11, then averaged to determine the mean EC_{50} ± S.E.mean. A lower constraint of 1 was applied for the response curves.

3.2.4 The role of JNK in doxorubicin-induced HCAEC cell cycle re-distribution

Hindered cell cycle progression has been attributed to JNK-mediated modification of cell cycle regulatory proteins, including cdc25 which is important for G2 to M cell cycle phase transition (Goss *et al*., 2003). As shown in Figure 3.9, no observable phosphorylation of JNK was detected in HCAECs treated with 0.1 and 0.3 µM doxorubicin for 8 hours, concentrations found to promote HCAEC G2/M cell cycle phase arrest in Figure 3.6. However, phosphorylation of JNK may have been identified in HCAECs if observations were prolonged to 24 hours and more sensitive kinase activity assays had been utilised. Therefore, experiments were performed to elucidate a potential mechanistic role for JNK in doxorubicin-mediated cell cycle changes in HCAECs.

The most universally applied inhibitor of JNK catalytic activity, SP600125 (anthra[1, 9-cd]pyrazol-6(24)-one) was utilised to elucidate whether JNK promotes doxorubicin-induced G2/M arrest in HCAECs (Ennis *et al*., 2005). SP600125 was originally characterised by Bennett *et al*., showing reversible competitiveness with ATP and efficacy at all JNK isoforms (Bennett *et al*, 2001). HCAECS were treated with SP600125 (10 µM) for 30 minutes prior to doxorubicin stimulation (0.1 µM), 30 minutes to 1 hour is the standard pre-incubation period denoted by published studies utilising SP600125 (Du *et al*., 2004, Li *et al*., 2016, Seok *et al*., 2008). Analysis of DNA content 24 hours after doxorubicin treatment revealed that SP600125 caused a modest but statistically significant 5.5% reduction in the percentage of doxorubicin-treated HCAECs in the G2/M phase of the cell cycle [fold dH_2O control: DMSO + dox. 1.78 ± 0.05 vs. SP + dox. 1.54 ± 0.05, $p<0.05$, n=4] (Figure 3.11). The decline in G2/M stage cells was accompanied by a significant increase in the number of cells in the S phase of the cells cycle [fold dH_2O control: DMSO + dox. 0.47 ± 0.05 vs. SP + dox. 0.86 ± 0.14, $p<0.01$, n=4]. These findings suggest that inhibition of JNK kinase activity by SP600125 hinders progression of HCAECs from the S to the G2 phase of the cell cycle in response to doxorubicin, thus implicating JNK in G2/M arrest induced by doxorubicin in HCAECs. Conversely, JNK inhibition, using SP600125, in un-stimulated HCAECs promoted cell cycle transition from the S to G2 phase, indicating that JNK impedes cell cycle progression in resting cells. Application of SP600125 itself resulted in a significant reduction of cells positioned in the S phase of the cell

cycle [fold dH_2O control: dH_2O + DMSO. 1.05 ± 0.03 vs. dH_20 + SP. 0.49 ± 0.04, $p<0.001$, n=4] and an increase in G2/M phase cells [fold dH_2O control: dH_2O + DMSO. 1.00 ± 0.02 vs. dH_20 + SP. 1.40 ± 0.08, $p<0.001$]. Therefore, JNK appears to have differential effects on the cell cycle in resting and stressed (doxorubicin-treated) HCAECs, obstructing or promoting S to G2 phase transition respectively.

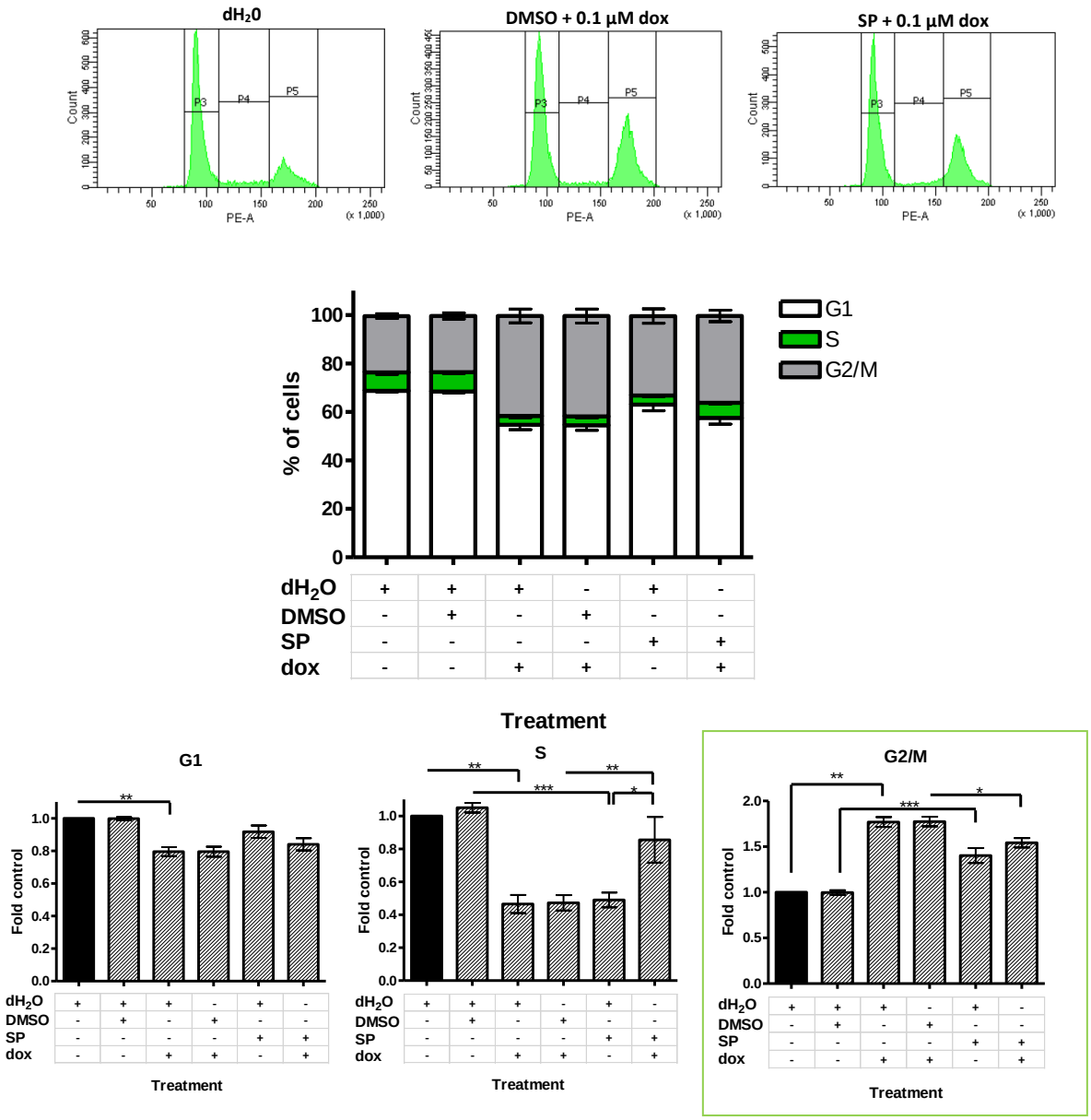

Figure 3.11: Effect of JNK inhibitor, SP600125, on doxorubicin-mediated G2/M phase arrest of HCAECs. HCAECs were treated with SP600125 (SP) (10 µM) 30 minutes prior to doxorubicin (dox) (0.1 µM) stimulation for 24 hours. Cell cycle distribution was analysed by FACS as described in section 2.2.7. Intervals P3, P4 and P5 represent G1, S and G2/M respectively. SP600125 autofluorescence did not interfere with FACS results as examined in SP600125-treated, PI unstained HCAECs. Values represent mean ± S.E. mean, n=4. *p<0.05, **p<0.01, ***p<0.001.

Investigation of the intracellular molecular alterations resulting in HCAEC cell cycle arrest by doxorubicin was attempted. Inhibition of cdc2 de-phosphorylation, a consequence of JNK-mediated phosphorylation of cdc25 in certain cell types, obstructs G2 to M phase transition hence phosphorylated cdc2 is a biomarker for arrest of cells in the G2 phase of the cell cycle (Goss *et al.*, 2003, Gutierrez *et al*., 2010). Levels of cdc2 phosphorylated at tyrosine residue 15 were measured in HCAECs treated with different doxorubicin concentrations to understand how the distinct effects of different doxorubicin concentrations on cell cycle synchronization relate to the expression of phosphorylated cdc2. Assessment of the phosphorylation of cdc2 was performed in HCAECs treated with doxorubicin for 8 hours, when considerable JNK phosphorylation was observed. Doxorubicin concentrations of 0.1 and 3 µM were found to increase the expression of phosphorylated cdc2 relative to cdc2 levels [fold control: 0.1 µM dox. 1.67 ± 0.21, 3 µM dox. 1.52 ± 0.27, n=3], but this was not statistically significant (Figure 3.12). Significant inhibition of cdc2 de-phosphorylation may have been observed if the study was extended beyond 8 hours. Figure 3.12 provides an insight into a potential altered cell cycle regulator, cdc2, post-doxorubicin treatment but more complex studies are required to fully characterise the biochemistry of HCAEC cell cycle changes caused by doxorubicin and decipher the contributory role of JNK.

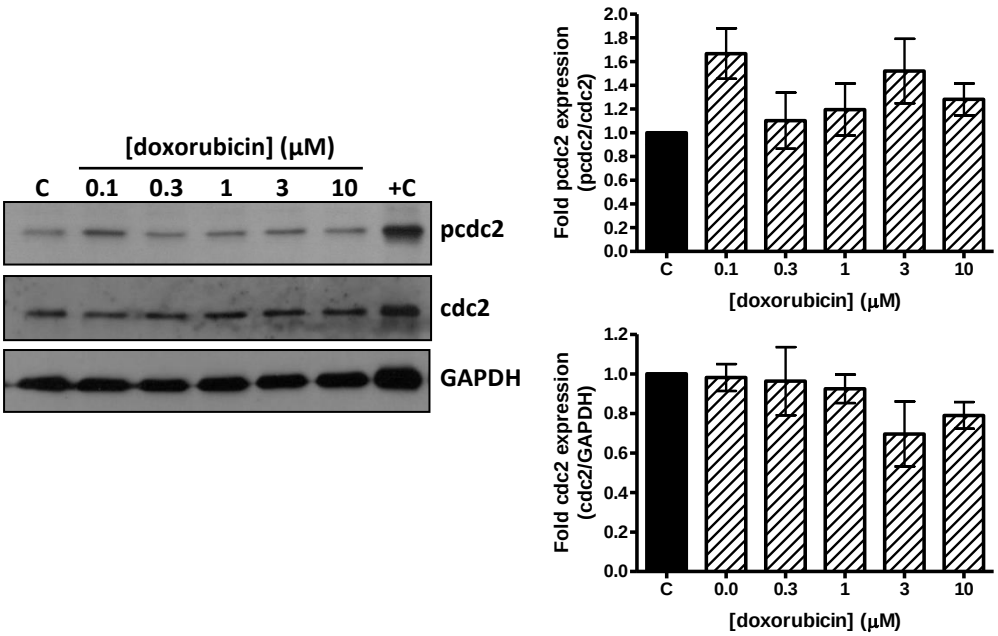

Figure 3.12: Inhibitory phosphorylation of cdc2 in doxorubicin-treated HCAECs. HCAECs were treated with doxorubicin at the indicated concentrations for 8 hours and non-phosphorylated cdc2 (34 kDa) and phosphorylated cdc2 (pcdc2) expression detected by Western blotting as outlined in section 2.2.8. Expression of pcdc2 was normalised to cdc2 levels, cdc2 expression was normalised to GAPDH (37 kDa). HCAECs treated with dH_2O provided a negative control (C) and UVC-irradiated (30 J/m^2, 30 minutes) HUVECs provided a positive control (+C). Values depict mean ± S.E. mean, n=3.

3.3 Discussion

Doxorubicin is a successful and widely utilised chemotherapeutic anthracycline drug, hindering tumour advancement by its nuclear anti-proliferative effects and the induction of cancer cell apoptosis (Kim *et al*., 2009). Doxorubicin is intravenously administered and binds to plasma proteins, chiefly albumin, displaying tri-phasic plasma elimination with half-lives of < 5 to 10 minutes, 0.5 to 3 hours and 24 to 36 hours (Ryu *et al*., 2014). Endothelial cells are at the interface of the vessel wall and bloodstream, thus this chapter aimed to explore the effects of doxorubicin on human coronary artery endothelial cells to gain a greater understating of doxorubicin-related toxicity to the vasculature.

A completely novel finding was the cell cycle arrest of specifically HCAECs, provoked by doxorubicin. Arrest of cells in the G2/M phase of the cell cycle is a recognised feature of antineoplastic anthracyclines (Stein *et al*., 2003). G2/M block serves to prevent damaged DNA from undergoing mitotic division, maintaining genomic fidelity (Gutierrez *et al*., 2010). Doxorubicin has been shown to cause G2/M arrest in colon cancer HCT-116 cells, MDA-MB-231 and MCF-7 breast cancer cells as well as non-cancerous cells such as the human fibroblast cell line F65 (Bar-On *et al*., 2007, Lee *et al*., 2005, Lupertz *et al*., 2010). Although not extensively studied, endothelial cells have also been shown to respond to doxorubicin treatment by arrest in G2/M. Spallarossa *et al*., reported G2/M arrest of cord blood EPCs treated with doxorubicin (0.25 μM) for 24 hours (Spallarossa *et al*., 2010). In this study of asynchronously growing HCAECs, a 24-hour incubation period with doxorubicin, 0.1 and 0.3 μM, also resulted in accumulation of HACECs at the G2/M phase of the cell cycle, as illustrated in Figure 3.6. Notably the lowest doxorubicin concentrations (0.1 and 0.3 μM) examined generated cell cycle block at the G2/M phase of the cell cycle whereas higher doxorubicin concentrations hindered S to G2/M phase transition, seen as S phase accumulation. The delay in S phase transit caused by the higher doxorubicin concentrations may be attributed to severe inhibition of topoisomerase II activity, the enzyme responsible for unwinding of the DNA helical structure, thus preventing DNA replication and a build-up of cells in the S phase of the cell cycle. Accordingly, doxorubicin has been shown to cause DNA replication block in HUVECs and cord

blood EPCs, observed as a concentration-dependent reduction in the incorporation of BrdU into the DNA of replicating cells 24 hours post-doxorubicin treatment (Damrot *et al*., 2006, Spallarossa *et al*., 2010), thus confirming the ability of doxorubicin to impede DNA replication in endothelial cells. Distinct cell cycle effects by differing doxorubicin concentrations has also been demonstrated in an immortalised endocardial endothelial cell line (hTERT-EEC). Maney *et al*., observed that 0.2 µM doxorubicin promoted G2/M arrest 48 hours post-treatment, conversely 1 µM doxorubicin reduced the proportion of G2/M phase positioned cells while causing a drastic increase in the sub-G1 population indicative of apoptosis (Maney *et al*., 2011). It appears that HCAECs treated with low doxorubicin concentrations experience DNA damage preventing cell entry into mitosis and subsequent cell cycle arrest but HCAECs exposed to higher concentrations of doxorubicin suffer extensive DNA damage, obstructing DNA replication and increasing the susceptibility of these cells for death as observed in Figure 3.1 at these doxorubicin concentrations.

The G2 checkpoint tightly controls progression of the cell cycle to the M phase, denying entry of cells with damaged DNA (Lapenna and Giordano, 2009). Arrest of cells at the G2 checkpoint is the result of inhibition of cdc2 de-phosphorylation as described in section 1.6.2. Therefore, initial experiments were performed to examine the levels of cdc2 phosphorylated at tyrosine residue 15 in HCAECs, a marker of G2 phase arrest. Modest inhibitory phosphorylation of cdc2 was observed in HCAECs treated with 0.1 µM doxorubicin which correlates with the G2/M phase arrest induced by this concentration of doxorubicin. However, the results from Figure 3.12 were difficult to interpret, due to inconsistencies between experiments and the timescale for observing cdc2 in its phosphorylated state was not extended beyond 8 hours. Control of the G2 checkpoint is multi-factorial, therefore numerous biochemical markers could be studied to successfully understand the molecular mechanisms responsible for G2/M arrest incited by doxorubicin. Upstream events leading to inhibition of cdc2 de-phosphorylation could be examined such as CHK1 phosphorylation, which has been observed in doxorubicin-treated HUVECs at serine residue 345, plus the subsequent phosphorylation of Cdc25 and cytoplasm sequestration of Cdc25 could be assessed (Damrot *et al*., 2006, Lapenna and Giordano, 2009). Furthermore, p53, a key player in cell cycle arrest and apoptosis following cellular stress, may contribute to cell cycle

arrest caused by doxorubicin in endothelial cells. Transcriptional regulator p53 has been closely associated with arrest of cells at the G1 checkpoint however p53 is also implicated in G2 checkpoint control by: 1) down-regulating the transcription of cyclin B1 and cdc2, 2) up-regulating the transcription of 14-3-3σ, which interacts with Cdc25 sequestering it in the cytoplasm and 3) increasing GADD45α transcription, an inducer of G2 phase arrest by preventing cyclin B-CDK1 activity (Mingo-Sion et al., 2004, Pietenpol and Stewart, 2002). A well-recognised biochemical alteration in doxorubicin-treated endothelial cells is increased p53 expression (Bruynzeel *et al*., 2007, Damrot *et al*., 2006, Kaushal *et al*., 2004[2], Lorenzo *et al.*, 2002). Bruynzeel *et al*., detected increased p53 expression 24 hours post-treatment of HUVECs with 0.75 µM doxorubicin, similarly Kaushal *et al*., observed increased p53 expression in 0.5 µM doxorubicin-treated HCAECs after 24 hours (Bruynzeel *et al*., 2007, Kaushal *et al*., 2004[2]). Thus, p53 may be an effector protein in doxorubicin-mediated cell cycle arrest in endothelial cells. Having shown that doxorubicin promoted cell cycle arrest of HCEACs, further extensive research is required to discern the molecular inputs responsible for the G2/M arrest caused by doxorubicin in HCAECs.

The stress-activated kinase pathways, including the MAPK pathways, are established cell cycle regulators, therefore their influence in doxorubicin-induced HCAEC cell cycle arrest was explored further. ERK, activated by mitogenic stimuli, is regarded as a facilitator of cell cycle progression by promoting downstream transcription of cyclin D1 and phosphorylating the inhibitory protein p27 thus targeting it for degradation and detachment from cyclin E/CDK2, enabling cyclin E/CDK2-mediated transition through the G1 checkpoint (MacCorkle and Tan, 2005, Jang *et al*., 2014). Conversely, p38, activated by cellular stressors, is linked to hindrance of cell cycle progression by phosphorylating Cdc25 B/C, hence promoting Cdc25 B/C and 14-3-3σ conjugation and sequestration in the cytoplasm, preventing G2 to M transition (Bulavin *et al*., 2001, Gutierrez *et al*., 2010). JNK is recognised as a cell survival-promoting kinase, in addition to a cell death-inducer, as discussed in section 1.7.1. In almost all resting cultured cells basal JNK activity is detected (Du *et al*., 2004). JNK promotes the survival of resting cells by positively regulating cell cycle progression as shown in numerous studies utilizing various cell types. Du *et al*., revealed that treatment of NIH-3T3 mouse fibroblasts with SP600125 (20 µM) for 24 hours resulted in an

accumulation of cells in G2/M (Du *et al*., 2004). Furthermore, SP600125-treatment (25 µM) of three breast cancer cell lines (MDA-MB-231, MCF-7 and 21PT) for 48 hours was found to promote G2/M arrest (Mingo-Sion *et al*., 2004). Using an alternative pharmacological inhibitor, JNK inhibitor IX (also known as JNKi), an ATP-competitive JNK2 and JNK3 inhibitor, Jang *et al.,* observed a concentration-dependent accumulation of Jurkat T cells in G2/M (Jang *et al*., 2014). Thus, basal JNK in resting cells appears to facilitate G2 to M transition.

In this study of HCAECs, SP600125, the most widely applied inhibitor of JNK kinase activity, was utilised to discern the role of JNK in G2/M arrest of HCAECs induced by 0.1 µM doxorubicin. SP600125, originally characterised by Bennett *et al*., at the beginning of the twenty-first century, was shown to be highly selective for JNK; 10 times more selective for JNK than upstream kinase MKK4 and 100 times more selective for JNK than other kinases such as ERK and p38-2 (Bennett *et al*., 2001). In biochemical assays, IC_{50} values of 0.04 µM were identified for SP600125 against JNK1 and JNK2 whereas in cell-based assays, the IC_{50} for SP600125-induced reduction of c-Jun phosphorylation in Jurkat T cells was between 5 and 10 µM (Bennet *et al*., 2001). Ennis *et al.*, observed reduced c-Jun phosphorylation in HMVECs treated with 10 µM SP600125 for 4 hours and in a more recent study Li *et al*., reported attenuated LPS-stimulated c-Jun phosphorylation in HUVECs pre-treated with 10 µM SP600125 for 1 hour (Ennis *et al*., 2005, Li *et al*., 2016). SP600125 has been shown to have a cytostatic effect on HMVECs rather than cytotoxic at concentrations up to 30 µM (Ennis *et al*., 2005). However, the application of SP600125 (20 µM) was linked to inhibition of cdc2 de-phosphorylation at tyrosine residue 15 in HCT116 human colorectal carcinoma cells, thus SP600125 may have a direct effect on cell cycle regulators (Kim *et al*., 2010). SP600125 at a concentration of 10 µM was chosen for this study to evaluate the role of JNK in doxorubicin-mediated cell cycle arrest in HCAECs, lessening potential SP600125-mediated off-target effects and toxicity to HCAECs.

In support of previous findings in other cell types, SP600125-treatment of unstimulated HCAECs resulted in an increase in the proportion of G2/M phase cells, as shown in Figure 3.11, suggesting that JNK is involved in G2 to M transit in resting HCAECs. However, G2/M arrest of HCAECs caused by doxorubicin was modestly

reduced by SP600125 pre-treatment, implicating a partial role for JNK in G2/M arrest induced by doxorubicin in HCAECs. In response to stress, JNK has been shown to obstruct G2 to M progression, via phosphorylation and inactivation of the phosphatase Cdc25 (Gutierrez *et al*., 2010). Gutierrez *et al*., reported that pre-treatment of HeLa cells with the JNK peptide inhibitor, JNK inhibitor VII (also known as TAT-JIP1) attenuated G2/M arrest induced by UV radiation (40 J/m^2) 24 hours post-exposure, suggesting that JNK plays a role in G2 to M blockade after UV-irradiation (Gutierrez *et al*., 2010). Thus a role for JNK in G2 to M transition in non-stressed HCAECs but G2 to M obstruction in doxorubicin-treated HCAECs has been implicated. Of note, the increase in G2/M cells after SP600125 treatment of un-stimulated cells correlated with a decrease in S phase cells, likewise the decrease in doxorubicin-arrested G2/M HCAECs by SP600125 was associated with an increase in S phase cells. These findings suggest that JNK may act as a regulator of S to G2 phase transition. Pre-treatment of human hepatoblastoma cells, HepG2, with SP600125 (20 µM, 30 minutes) potentiated S phase arrest promoted by furazolidone (FZD), a genotoxic antimicrobial agent, suggesting a role for JNK in S to G2 phase transit (Sun *et al*., 2013[2]). Progression through the S phase of the cell cycle is promoted by cyclin A-CDK2 and cyclin A-CDK1 complexes, as described in section 1.6.1. (Hochegger *et al*., 2008). JNK may modulate cyclin A-CDK to hinder S to G2 advancement, however this has not yet been defined in endothelial cells. JNK could be a regulator of S to G2 transition in addition to or rather than G2/M checkpoint control in HCAECs.

In order to definitively establish the role of JNK in HCAEC cell cycle arrest by doxorubicin, several additional pharmacological and RNA interference approaches should be attempted. For this study on HCAECs, SP600125 was the only JNK inhibitor utilised but the generation of new JNK inhibitors such as JNKi and TAT-JIP1 employed by Jang *et al*., and Gutierrez *et al*., provides additional methods to reaffirm findings. Gururajan *et al*., successfully used JNK-targeting siRNA to show that BKS-2 and WEHI-231 murine lymphoma cells transfected with siRNA against JNK have a reduced proportion of G2/M cells compared to control siRNA transfected cells (Gururajan *et al*., 2005). The effect of siRNA is only transient, therefore lentiviral knockdown of the JNK isoforms in HUVECs using stable short hairpin RNA (shRNA) was attempted by a fellow colleague, however this was unsuccessful due to functional

effects of non-target lentivirus and further optimization was required before use in functional experiments. The findings from this experiment implicate JNK in the progression of the cell cycle, from G2 to M, in resting HCAECs. However, in doxorubicin-exposed HCAECs JNK may promote G2/M arrest of HCAECs induced by doxorubicin, potentially involving JNK-mediated facilitation of S to G2 transit. Further research is required to confirm the regulatory effects of JNK on the cell cycle in HCAECs in response to doxorubicin.

Characterisation of JNK activation can provide an insight into how JNK regulates cell cycle function. At present, few studies have investigated the kinetics of JNK activation induced by doxorubicin in endothelial cells. Damrot *et al*., observed phosphorylation of JNK in HUVECs six hours after treatment with 2.5 µg/ml doxorubicin (Damrot *et al*., 2006). This study by Damrot *et al*., only depicted the phosphorylation of the p46 isoform of JNK by one doxorubicin concentration and only one timepoint post-treatment was assessed. In addition, Spallarossa *et al*., detected significantly increased expression of both p54 and p46 phosphorylated JNK after treatment of EPCs with 0.25 µM doxorubicin but this occurred rapidly, only 15 minutes after doxorubicin-treatment, which is considerably different from the 6-hour timepoint investigated by Damrot *et al*., (Spallarossa *et al*., 2010). Thus the kinetics of JNK phosphorylation in endothelial cells in response to doxorubicin are poorly defined. Phosphorylation of JNK was examined in HCAECs up to 24 hours post-doxorubicin treatment. Notably, JNK phosphorylation was delayed in doxorubicin-treated HCAECs, marginally evident 2 hours post-doxorubicin treatment, compared to UVC-irradiated and IL-1-stimulated endothelial cells which displayed peak JNK phosphorylation within 30 minutes of treatment, as observed in Figure 3.7. Rapid, transient, phosphorylation of JNK and induction of JNK1 kinase activity by UVC-irradiation has been observed in C50 keratinocytes, human embryonic fibroblast-like cells (HE49) and mouse embryonic fibroblasts (MEFs), occurring 5 minutes post-irradiation and achieving maximum JNK phosphorylation and activation 15 to 30 minutes following irradiation (Ramaswamy *et al*., 1998, Matsuda *et al*., 2000, Seok *et al*., 2008). Seok *et al*., observed JNK1-dependent phosphorylation of c-Jun, as determined by *in vitro* kinase assays, 5 minutes after UVC-irradiation (20 J/m^2) of MEFs. However, phosphorylation of c-Jun was not detectable until 5 hours post-treatment with doxorubicin (10 µg/ml),

which remained sustained until 12 hours post-doxorubicin treatment (latest timepoint investigated). Thus showing distinct kinetics of JNK activation in UV-irradiated and doxorubicin-treated cells, similar to the findings in HCAECs (Seok *et al*., 2008).

The different rates of JNK phosphorylation by UVC/IL-1 and doxorubicin in HACECs may be due to different methods of JNK activation. IL-1-mediated activation of JNK is recognised to occur via IL-1 receptor activation with subsequent MyD88 recruitment and activation of IRAK (Li *et al*., 2001, O'Neill and Dinarello, 2000). However, both UVC and doxorubicin-mediated JNK activation has been linked to DNA damage and the intracellular generation of reactive oxygen species (Ghosh *et al*., 2011, Matsuda *et al*., 2000, Seok *et al*., 2008). Similar to the findings in HCAECs, 24 hours treatment of chick cardiomyocytes with 10 μM doxorubicin increased expression of phosphorylated JNK, however when cells were simultaneously treated with doxorubicin and antioxidant baicalein (25 μM), JNK phosphorylation was significantly reduced, implicating ROS in doxorubicin-induced JNK activation (Chang *et al*., 2011). Interestingly, Seok *et al*., identified RIP, an adaptor protein involved in TNF signalling cascades, as a distinct signalling intermediate responsible for slow JNK activation by doxorubicin but not rapid JNK activation by UVC radiation (Seok *et al*., 2008). JNK-mediated phosphorylation of c-Jun by doxorubicin was attenuated in MEFs lacking functional RIP, but UVC-induced c-Jun phosphorylation was maintained, demonstrating a role for receptor interacting protein (RIP) in doxorubicin-induced JNK activation (Seok *et al*., 2008). This study also highlighted the important role of ATM in linking doxorubicin-induced DNA damage with JNK activation. Doxorubicin induces autophosphorylation of ATM at serine residue 1981, ATM-deficient fibroblasts failed to induce c-Jun phosphorylation in response to doxorubicin, implying ATM-dependent JNK phosphorylation in doxorubicin-treated MEFs (Kurz *et al*., 2004, Seok *et al*., 2008). Conversely, c-Jun phosphorylation occurred in UVC-irradiated fibroblasts lacking ATM (Seok *et al*., 2008). This single study by Seok *et al*., provides evidence of differing mechanisms of activation of JNK by doxorubicin and UVC-irradiation, leading to distinct kinetics of JNK activation.

Previous studies have demonstrated that the kinetics of JNK activation are linked to whether JNK has a pro-survival or death-promoting cellular effect, sustained JNK activation promotes cell death whereas transient JNK activation is implicated in JNK-

mediated survival responses (Chen *et al*., 1996, Sanchez-Perez *et al*., 1998, Mansouri *et al*., 2003, Seok *et al*., 2008). This phenomenon was first proposed by Chen *et al.*, in the 1990s, having identified that sustained activation of JNK1 was associated with Jurkat T cell death while transient JNK activation correlated with the proliferation of Jurkat T cells (Chen *et al*., 1996). Moreover, Mansouri *et al*., distinguished persistent JNK phosphorylation (up to 12 hours) in a cisplatin-sensitive human ovarian cancer cell line 2008 but transient phosphorylation of JNK (up to 3 hours) in cisplatin-resistant ovarian cancer 2008C13 cells (Mansouri *et al*. 2003). The study by Seok *et al*., also proved, by utilising SP600125, that persistent JNK activation by doxorubicin in MEFs was associated with cell death but transient JNK activation by alkylating agent N-methyl-N-nitro-N-nitrosoguanidine (MNNG) was not linked to the death of MEFs (Seok *et al*., 2008). A key finding from the doxorubicin-treatment of HCAECs was sustained JNK phosphorylation, up to 24 hours, after doxorubicin-treatment as illustrated in Figure 3.8. The persistent activation of JNK implicates JNK in doxorubicin-mediated death of HCAECs; death of HCAECs was observed 24 hours post-doxorubicin treatment ($\geq$ 3 μM), as deciphered by MTT toxicity assays. Unfortunately, a direct link between JNK activity and doxorubicin-mediated death of HCAECs was not elucidated in this study of HCAECs. Further characterisation of JNK activation in response to doxorubicin HCAECs should be performed using kinase activity assays to confirm that doxorubicin-mediated phosphorylation of JNK relays a functional response. The use of JNK inhibitors, such as SP600125, should also be employed to elucidate whether JNK contributes to HCAEC death. This could confirm whether JNK activation by doxorubicin is sustained in HCAECs, beyond 24 hours, leading to doxorubicin-mediated HCAEC death.

Survival of the breast adenocarcinoma cell line MCF-7 was analysed at the same time as doxorubicin-mediated HCAEC death to identify any comparable differences between doxorubicin-induced death of endothelial cells and cancer cells. Accordingly, JNK activation by doxorubicin was also investigated in MCF-7 cells to discern the role of JNK in the response of MCF-7 cells to doxorubicin. There is conflicting evidence for the role of JNK in doxorubicin-mediated cancer cell survival. JNK has been implicated in the resistance of various breast cancer cells to doxorubicin and doxorubicin-induced increased mRNA expression of an ABC transporter involved in

the resistance of cancer cells to doxorubicin, multidrug resistance-associated protein 1 (MRP1), was supressed when JNK was inhibited by SP600125 in the human small cell lung cancer cell line GLC4, implicating JNK in the protection of lung cancer cells from doxorubicin too (Kim *et al*., 2009, Shinoda *et al*., 2005). On the other hand, transfection of MCF-7 cells with dominant-negative JNK1 and c-Jun constructs resulted in reduced DNA fragmentation and cell death 24 hours after doxorubicin (10 µg/ml) treatment compared to the vector controls (Kim and Freeman. 2003). This implies a pro-apoptotic role of JNK in doxorubicin-mediated death of MCF-7 cells.

The kinetics of JNK activation in MCF-7 cells were explored in this chapter to identify potential unique JNK responses between cancer and endothelial cells, no such comparative studies between HCAECs and MCF-7 breast cancer cells have been performed to date. Kim and Freeman, detected increased phosphorylation of JNK 24 hours after doxorubicin-treatment of MCF-7 cells, likewise Kanno *et al*., observed increased levels of phosphorylated JNK 24 hours after treatment of MCF-7 cells with 10 µM doxorubicin (Kanno *et al*., 2014, Kim and Freeman, 2003). In this chapter, phosphorylation of JNK occurred slightly later in MCF-7 cells than HCAECs, 4 hours post-doxorubicin treatment; p46 phosphorylation was transient but p56 phosphorylation was sustained up to 24 hours post-doxorubicin treatment. Indeed, significant death of MCF-7 cells was observed 24 hours after doxorubicin treatment ($\geq$ 3 µM), potentially linking doxorubicin-mediated JNK phosphorylation and activation to MCF-7 cell death. Again, JNK inhibitors and knockdown strategies, which would be more easily executed in cancer cells, should be utilised to definitively decipher the role of JNK in doxorubicin-induced MCF-7 cell death. A noticeable difference between doxorubicin-induced JNK phosphorylation in HCAECs and MCF-7 cells was the preferential phosphorylation of p54 and p46 JNK respectively. Little is known about the distinct roles of the different JNK isoforms in cellular physiology and pathophysiology. The preferential phosphorylation of the specific JNK isoforms in HACECs and MCF-7 cells by doxorubicin may be partly responsible for the greater sensitivity of MCF-7 cells to doxorubicin than HCAECs, as discerned by MTT assays in Figure 3.1, however this is an assumption. The greater sensitivity of MCF-7 cells to doxorubicin than HCAECs was unexpected, Bruynzeel *et al*., demonstrated that endothelial cells (HUVECs) and cardiomyocytes (NeRCaMs) were more sensitive to

doxorubicin than A2780 and OVCAR-3 ovarian cancer cell lines. The IC_{50} values for doxorubicin-mediated apoptosis 48 hours post-treatment, as determined by flow cytometry analysis of the sub-G1 cell population, were 0.75 and 0.5 µM for HUVECs and NeRCaMs but 1.5 and greater than 10 µM for A2780 and OVCAR-3 cells (Bruynzeel *et al*., 2007). Furthermore, 0.5 µM doxorubicin induced greater time-dependent apoptosis of BAECs than PA-1 human teratocarcinoma cells, 8 hours post-treatment approximately 65% of BAECs and 10% of PA-1 cells were TUNEL positive, a measure of DNA fragmentation (Wang *et al*., 2004). This was associated with increased pro-apoptotic caspase-3 activity in BAECs compared to PA-1 cells (Wang *et al*., 2004). In both studies, the application of radical scavengers protected endothelial cells from apoptotic death caused by doxorubicin but cancer cell death was not impeded, proposing ROS-dependent doxorubicin-mediated death of endothelial cells, but a redundancy of ROS in cancer cell death induced by doxorubicin (Bruynzeel *et al*., 2007, Wang *et al*., 2004). Therefore, previous research depicts increased sensitivity of endothelial cells to doxorubicin relative to cancer cells. Cancer cells vary greatly in their sensitivity to doxorubicin, as shown by Bruynzeel *et al*., and in this study MCF-7 cells were more sensitive to doxorubicin than HCAECs (Bruynzeel *et al*., 2007). Although this is encouraging due to the desired death of cancer cells by chemotherapeutic doxorubicin over non-cancerous cells such as endothelial cells, the HCAEC cytotoxicity of doxorubicin is concerning, potentially resulting in endothelium damage.

Doxorubicin is an established cytotoxic agent to endothelial cells, as depicted by the majority of studies investigating the effects of doxorubicin on endothelial cells. Studies have predominantly used low µM range concentrations of doxorubicin (0.1 to 1 µM) to study the death of doxorubicin-treated endothelial cells (Kaushal *et al*., 2004[2], Maney *et al*., 2011, Spallarossa *et al*., 2010, Wang *et al*., 2004) but high concentrations, up to 100 µM, have also been utilised (Wojick *et al*., 2015). Plasma concentrations of doxorubicin vary greatly between individuals and differ dependent on: infusion duration, assessment time post-treatment and patient weight (Barpe *et al*., 2010, Hempel *et al*., 2002). Hempel *et al*., identified 273 µg/l doxorubicin as the geometric mean peak plasma concentration in children with acute lymphoblastic

leukemia and non-Hodgkin lymphoma after a 2-hour infusion of doxorubicin (Hempel *et al*., 2002). Barpe *et al*., reported doxorubicin plasma concentrations of 630 ± 22.1 ug/l and 39.8 ± 15.3 ug/l in female patients assessed 40 minutes and 24 hours and 40 minutes post-administration of doxorubicin respectively (Barpe *et al*., 2010). Furthermore, *in vivo* experiments on rodents delivered concentrations of doxorubicin relative to body weight, predominantly around 5 mg/kg for each infusion but increased to 15 mg/kg for studies investigating the cardiotoxic effects of doxorubicin (Kwak *et al*., 2015, Zhang *et al*., 2009). Consequently, for this study the effects of doxorubicin concentrations used by other *in vitro* studies (0.1 to 100 µM) on endothelial cells were explored.

Doxorubicin-induced death of HCAECs occurred with concentrations ≥ 3 µM, 24 hours post-treatment, a 40% reduction in cell viability was observed with 3 µM doxorubicin as depicted in Figure 3.1. However, the research performed by Kaushal *et al*., the only other research investigating the effects of doxorubicin on HCAECs, reported an approximate 40% reduction in the viability of HCAECs 24 hours after treatment with only 0.5 µM doxorubicin, assessed also by MTT toxicity assays (Kaushal *et al*., 2004[2]). In an additional study by Kaushal *et al*., 1 µM doxorubicin reduced the number of viable HCAECs by about 60% after 24 hours, therefore Kaushal *et al*., observed marked HCAEC death with lower doxorubicin concentrations than seen in this thesis (Kaushal *et al*., 2004[1]). The experimental setup by Kaushal *et al*., was almost identical to the MTT assay setup used in this study, such as continuous treatment of HCAECs with doxorubicin, the use of passage 4 or 5 cells and incubation of HCAECs in media containing 5% FBS. The poorer sensitivity of HCAECs in this study remains unclear. The research by Kaushal *et al*., showed a time-dependent reduction in cell viability caused by doxorubicin, the experiments at the beginning of this chapter were able to demonstrate concentration-dependent doxorubicin-mediated death of HCAECs. Analysis of HCAEC death by doxorubicin was expanded by Kaushal *et al*., revealing a 25.21% increase in TUNEL-positive HCAECs 24 hours post-treatment with 0.5 µM doxorubicin (Kaushal *et al*., 2004[2]). In support of these findings, doxorubicin concentrations ≥ 0.1 µM promoted Annexin V binding to HCAECs in this study, showing induction of early apoptotic marker phosphatidylserine. Thus HCAECs treated with even low µM concentrations of

doxorubicin showed signs of apoptosis induction. If observations had been extended beyond 24 hours, doxorubicin-mediated apoptotic death of HCAECs may have been observed with low µM concentrations of doxorubicin. Kaushal *et al*., also provided an insight into the mechanisms responsible for doxorubicin-mediated death of HCAECs, showing increased concentration-dependent caspase-3 activation in doxorubicin-treated HCAECs, diminished expression of pro-survival Mcl-1 and accumulation of p53 (Kaushal *et al*., 2004[1], Kaushal *et al*., 2004[2]). Therefore, Kaushal *et al*., provided a more comprehensive characterisation of doxorubicin-induced death of HCAECs, the experimental work in this thesis supports the cytotoxic effects of doxorubicin on HCAECs but further research is required to fully characterise death of HCAECs induced by doxorubicin.

Various experimental techniques have been exploited to assess doxorubicin-mediated death of endothelial cells, predominantly examining HUVECs, the cell type most frequently employed to study the effects of doxorubicin on endothelial cells, as discussed previously in section 3.1. Keltai *et al*., utilised a fluorescent nucleic acid dye, SYBR-Green, in a multi-well plate system to report a concentration-dependent reduction of attached, viable HUVECs exposed to doxorubicin (IC_{50} for 24 hour treatments = 300 ng/ml, IC_{50} for 48 hour treatments = 150 ng/ml) (Keltai *et al*., 2010). Reduced HUVEC viability was also demonstrated by Damrot *et al*., using water-soluble tetrazolium salt (WST) assays to observe a greater than 50% reduction in the viability of HUVECs treated with doxorubicin (1 µg/ml) (Damrot *et al*., 2006). Doxorubicin is recognised to cause apoptotic death of HUVECs, identified by time-dependent increases in the proportion of sub-G1 cells by FACs post-doxorubicin treatment (Lorenzo *et al*., 2002, Wu *et al*., 2002). Of note, apoptotic death of HUVECs was only observed by Lorenzo *et al*., 30 hours after the treatment of subconfluent endothelial cells, not fully confluent cell cultures (Lorenzo *et al*., 2002). Thus experiments in this thesis, investigating the death of HCAECs in response to doxorubicin, were performed using subconfluent HCAECs. Additionally, doxorubicin has been shown to cause DNA strand breakage, identified by comet assays and an increase in TUNEL-positive HUVECs post-treatment, which consequently results in apoptosis (Damrot *et al*., 2006, Wu *et al*., 2002). The molecular mechanisms responsible for the apoptotic death of doxorubicin-treated HUVECs have been

elucidated as caspase-dependent. Increased cleaved caspase-3 expression was detected by Lorenzo *et al*., 30 hours post-treatment of HUVECs with doxorubicin (500 ng/ml), which correlated with the induction of apoptosis. Moreover, pre-treatment with broad spectrum caspase inhibitor, z-VAD-FMK, prevented doxorubicin-induced DNA fragmentation and apoptosis of HUVECs (Lorenzo *et al*., 2002, Wu *et al*., 2002). Doxorubicin has also been show to activate caspase-3 and -7 in EA.hy926 cells with an EC_{50} of 2.59 ± 0.49 μM (Wojcik *et al*., 2015). *In vivo* research on doxorubicin-treated male Wistar rats (24 mg/kg cumulative dose) by Wu *et al*., also depicted increased numbers of TUNEL positive endothelial cells in myocardial sections plus increased caspase-3 expression, confirming findings from *in vitro* cultured endothelial cells (Wu *et al*., 2002). A reduction in the mRNA and protein expression of anti-apoptotic Bax family member Bcl-2 has also been identified in HUVECs, potentially contributing to the promotion of apoptosis by doxorubicin (Lorenzo *et al*., 2002, Wu *et al*., 2002). Thus several studies have conveyed the toxic effects of doxorubicin on HUVECs and provided an insight into the cellular events responsible for HUVEC death. An *in vitro* study by Monti *et al*., assessed the toxic effects of doxorubicin on endothelial cells from the coronary system surrounding the heart (Monti *et al*., 2013). Unlike the arterial endothelial cells examined in this thesis, bovine coronary venular endothelial cells (CVECs) were studied. Treatment of CVECs with doxorubicin for five days caused a concentration-dependent reduction in cell number (significant with ≥ 0.5 μM) (Monti *et al*., 2013). Dose-dependent cleavage of caspase-3 was identified 6 hours after doxorubicin treatment of CVECs and the authors concluded that doxorubicin-mediated death of CVECs was p53 but not ROS-dependent (Monti *et al*., 2013). Hence the toxic effects of doxorubicin have been demonstrated in various endothelial cell types including: BAECs, EECs, EPCs, CVECs, EA.hy926 cells and HCAECs, as discussed throughout this chapter.

Overall, the findings from this chapter have delineated the distinct responses of HCAECs to different concentrations of doxorubicin. HCAEC growth arrest was induced by doxorubicin concentrations in the low μM range (0.1 to 0.3 μM); concentrations too low to trigger cell death within 24 hours post-treatment but may eventually lead to HCAEC death in the long-term. The arrest of HCAECs in the G2/M phase of the cell cycle was also noteworthy owing to the G2/M phase of the cell cycle

being the most radiosensitive, the superior radiosensitivity of cells in the G2/M phase of the cell cycle was initially identified in the late 1960s by Sinclair and Morton using synchronized Chinese hamster cells and has been subsequently demonstrated in other cell types (Seiwert *et al*., 2007). A partial role for JNK in the cell cycle arrest of doxorubicin-treated HCAECs was identified and JNK may also have a role in doxorubicin-mediated death of HCAECs, as JNK activation was found to be sustained in doxorubicin-treated HCAECs. The death of HCAECs observed with high doxorubicin concentrations reveals the damaging effects of doxorubicin to the vasculature, endothelial cell death is associated with increased vascular permeability which is a causative factor in the development of atherosclerosis. The toxic effects of doxorubicin have been shown in other endothelial cell types, emphasising the potential of doxorubicin in the bloodstream to cause vascular damage at various anatomical sites. This chapter confirms the deregulation and death of HCAECs by doxorubicin which may promote coronary artery disease in patients.

Chapter 4:

Investigation of the survival of

X-irradiated endothelial cells

4.1 Introduction

X-rays transverse various tissues before reaching the tumour site, resulting in the unintentional exposure of normal cells to X-radiation, including endothelial cells, during radiotherapy. Different endothelial cell types exhibit varying radiosensitivities as demonstrated by Park *et al*., using γ-irradiation (^{137}Cs); human hepatic sinusoidal endothelial cells (HHSECs) were the most radiosensitive whereas human dermal microvascular endothelial cells (HDMECs) displayed the greatest resistance to ionizing radiation (Park *et al*., 2012[1]). A limited number of studies have investigated the effects of X-rays on endothelial cell function, primarily showing apoptotic death and senescence (Cervelli *et al*., 2014, Panganiban *et al*., 2013, Rombouts *et al*., 2013). Therefore, of interest in this chapter are the damaging effects of X-rays on endothelial cells, specifically coronary arterial cells which are likely to be exposed to radiation due to their close proximity to the radiation field used for breast cancer radiotherapy (Nilsson *et al*., 2016).

The effects of other forms of ionizing radiation on HCAECs have been demonstrated, including γ-rays (^{137}Cs and ^{60}Co) and β-emitters (^{188}Re) which have been shown to impair HCAEC proliferation, modify microRNA (miRNA) expression (miR-146b) plus alter the expression of proteins involved in transcription and translation and also activate signal transduction from stress-associated eukaryotic translation initiation factor 2 (eIF2α) to activating transcription factor 4 (ATF4) (Barjaktarovic *et al*., 2012, Kim *et al*., 2014, Kotzerke *et al*., 2000). Palayoor *et al*., investigated the effects of X-rays on HCAECs reporting hindered survival with a single 10 Gy X-ray dose and altered gene expression, genes involved in cell cycle control were up-regulated most greatly (Palayoor *et al*. 2014). The response of HCAECs to X-rays remains poorly understood. JNK has been implicated in cell death post-X-irradiation, primarily characterised in human T-cell leukemia (MOLT-4) cells (Enomoto *et al*., 2000), however the role of JNK in the response of endothelial cells to X-irradiation is not defined.

This chapter will investigate the survival of primary human endothelial cells, HUVECs and HCAECs, in response to X-irradiation, comparing endothelial and cancer cell

survival post-irradiation. Characterisation of the JNK response in endothelial cells exposed to X-rays was also attempted.

4.2 Results

4.2.1 Survival of X-irradiated endothelial cells

As detailed in chapter 3, section 3.2.1, MTT toxicity assays demonstrated the chemosensitivity of HCAECs to doxorubicin, therefore MTT assays were performed to assess the acute effects of X-rays on HCAEC survival. Again, MCF-7 cells were utilised as a comparative cancer cell line to compare the damaging effects of X-irradiation between endothelial and cancer cells and between primary cells and a cancer cell line. No observable reduction in the viability of HCAECs and MCF-7 was detected with MTT assays 24 hours post-exposure to X-rays (up to 10 Gy X-rays) (Figure 4.1 A). Of note, irradiated endothelial cells did not display signs of death (i.e. detachment) when examined using a microscope, but did appear morphologically different - narrower and elongated - 24 hours after exposure to the highest radiation dose (10 Gy) signifying a stress-mediated phenotypic change (Figure 4.1 B).

It is recognised that MTT assays are useful to study the cytotoxic effects of anticancer chemotherapeutic drugs but clonogenic survival assays are the preferred method to examine the survival of irradiated cancer cells (Buch *et al*., 2012). MTT assays require early, individual timepoint assessment of cell survival, whilst clonogenic assays examine cell growth and survival weeks post-irradiation, showing cells that have maintained their ability to replicate (Buch *et al*., 2012). Therefore, the results from Figure 4.1, investigating the death of X-irradiated HCAECs and MCF-7 cells by MTT assays, remain inconclusive.

Clonogenic survival assays were subsequently performed to assess the prolonged survival of X-irradiated endothelial cells. Sub-confluent cells (70 to 80%) were irradiated, incubated for 24 hours post-irradiation and then re-plated at a low density, following which colonies formed - a method adapted from Panganiban *et al*., (Panganiban *et al*., 2013). Clonogenic assays were initially attempted with HUVECs as Park *et al*., successfully demonstrated the reduced survival of X-irradiated HUVECs using clonogenic assays (Park *et al*., 2012[1]). UVW glioma cells are a relatively radiosensitive cancer cell line which was effectively employed for other clonogenic experiments and displayed radiosensitivity to X-irradiation as depicted later in chapter 6, figure 6.1. Therefore, UVW cells were analysed simultaneously with HUVECs to

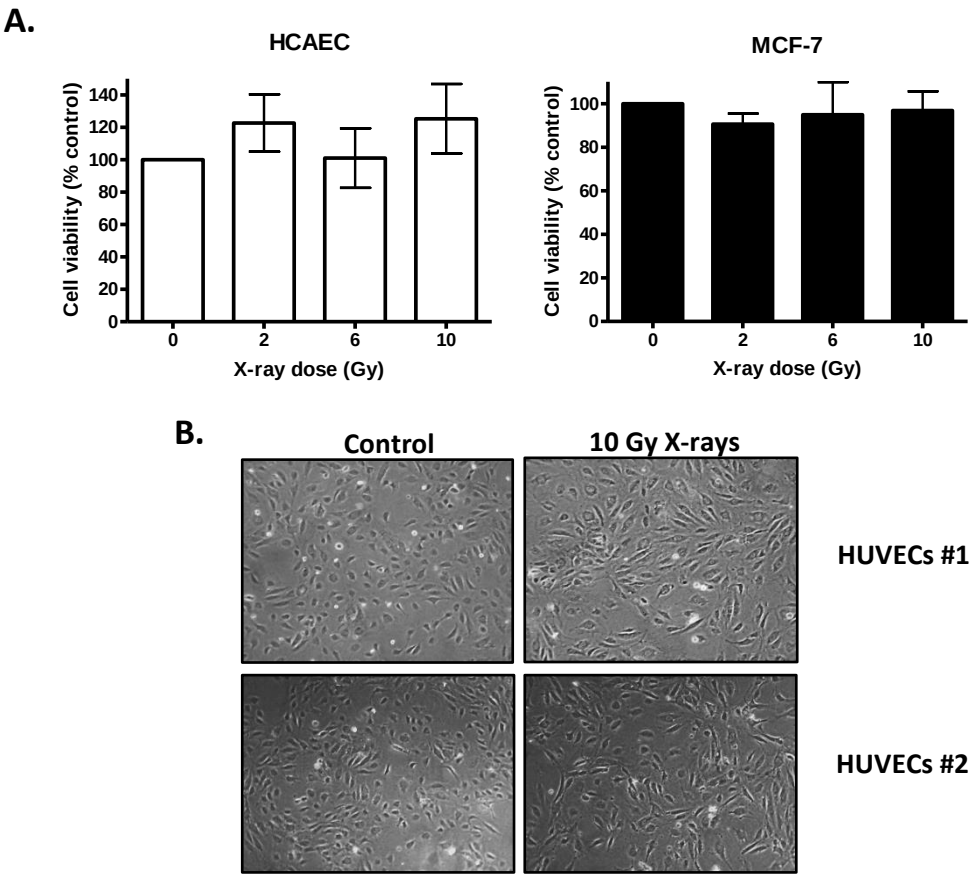

Figure 4.1: Viability of X-irradiated endothelial cells and MCF-7 cells. A. HCAECs and MCF-7 cells were exposed to X-rays and cell viability assessed by MTT assays 24 hours post-irradiation, as outlined in section 2.2.4. Values are representative of three separate experiments (n=3) ± S.E. mean, where means of triplicates were obtained for each individual experiment. **B.** A brightfield microscope (10X magnification) was used to capture the morphological differences between non-irradiated HUVECs (Control) and HUVECs irradiated with 10 Gy X-rays 24 hours post-exposure. The images were taken from the centre of each 6 cm dish.

compare the clonogenic survival of cancer cells and primary endothelial cells, plus provide a positive control. As illustrated in Figure 4.2 A, cancer cells formed defined, circular colonies whereas HUVECs developed larger, less dense colonies owing to the flatter morphology of HUVECs which form a monolayer in *in vitro* culture systems, as demonstrated in Figure 4.2 B, and within blood vessels. A dose-dependent reduction in the surviving fraction of both cell types was observed, 1 Gy caused a statistically significant, almost 50% reduction in HUVEC colony formation [surviving fraction: 1Gy. HUVEC, 0.52 ± 0.10, $p<0.01$, n=3] (Figure 4.2 C). Notably, HUVECs were more radiosensitive than UVW cells [surviving fraction: 3 Gy. HUVEC, 0.17 ± 0.04, $p<0.01$, n=3. UVW, 0.43 ± 0.09, $p<0.01$, n=3]. For each cell type, 200 cells were plated for colony formation during the clonogenic assay, however the plating efficiency for HUVECs was markedly lower than UVW cells [plating efficiency: Control. HUVEC, 25.66 ± 4.99%, UVW, 73.28 ± 3.92%, n=3]. Therefore, for subsequent experiments examining the clonogenic survival of HCAECs, the number of endothelial cells plated was increased to 350.

Having demonstrated that HUVECs are radiosensitive, with even 1 Gy X-rays significantly attenuating HUVEC clonogenic survival, HCAECs were exposed to lesser doses of X-irradiation to examine the effects of low-dose X-irradiation on HCAEC clonogenic survival. As depicted in Figure 4.3 A, HCAECs also successfully formed colonies after irradiation and re-plating for clonogenic assays. A dose-dependent reduction in colony formation was observed in HCAECs, with a modest reduction in HCAEC clonogenic survival with doses up to 1 Gy [surviving fraction: 0.5 Gy. 0.86 ± 0.13] (Figure 4.3 C). There was a drastic and significant difference between the survival of HCAECs treated with 1 and 2 Gy X-rays. An approximate 20% reduction in colony formation was detected with 1 Gy X-rays but 2 Gy reduced clonogenic survival by almost 80% [surviving fraction: 1 Gy. 0.78 ± 0.05 vs. 2 Gy. 0.22 ± 0.03, $p<0.01$, n=4]. The effect of 1.5 Gy X-rays on HCAEC clonogenic survival should have also been assessed as the reduction in HCAEC survival between 1 and 2 Gy may not be completely linear. However, these findings confirm that HCAECs are radiosensitive to low, therapeutically relevant doses of X-rays.

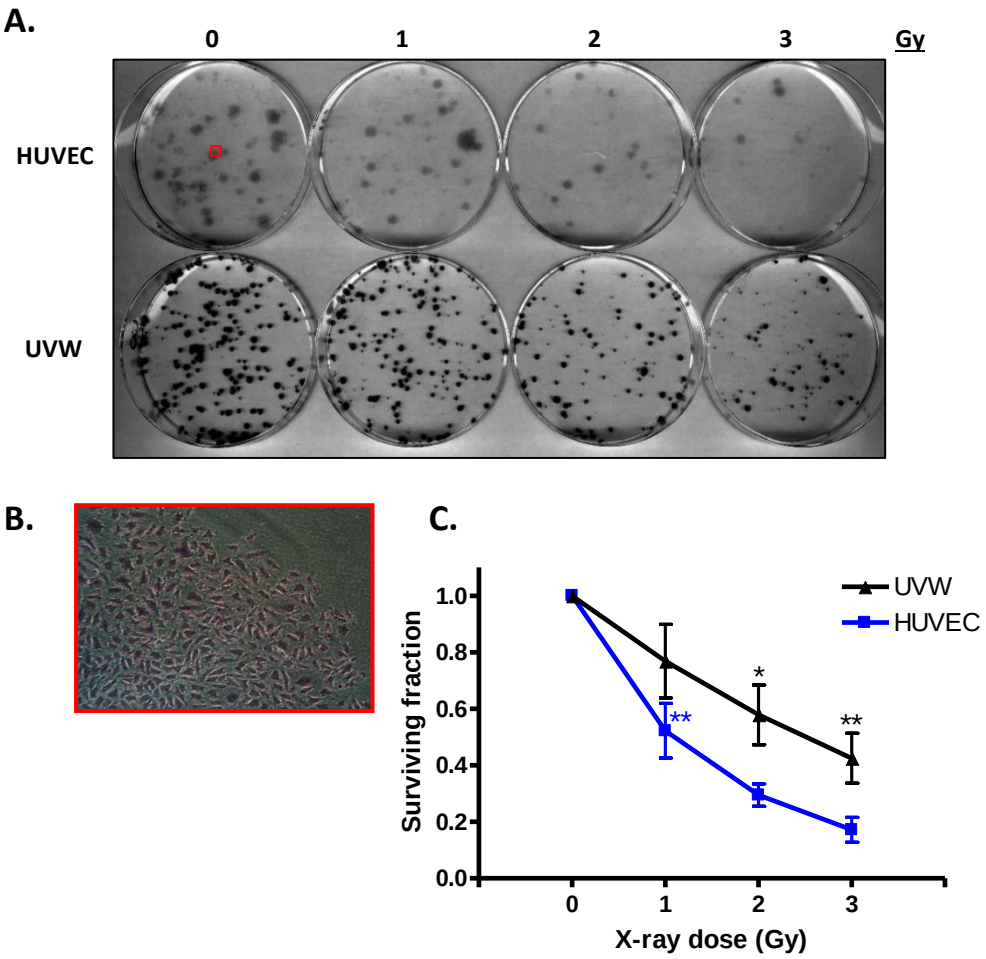

Figure 4.2: Clonogenic survival of HUVECs and UVW cells post-irradiation. HUVECs and UVW cells were X-irradiated with the indicated doses. After a 24-hour incubation period the cells were subject to clonogenic assay analysis as described in section 2.2.5. **A.** Colonies visible post-staining. **B.** A portion of a stained HUVEC colony was visualised using a brightfield microscope (10X magnification) (red box). **C.** Surviving fractions were calculated as outlined in section 2.2.5.2 and depicted as mean ± S.E. mean, n=3. *$p<0.05$, **$p<0.01$ compared to 0 Gy.

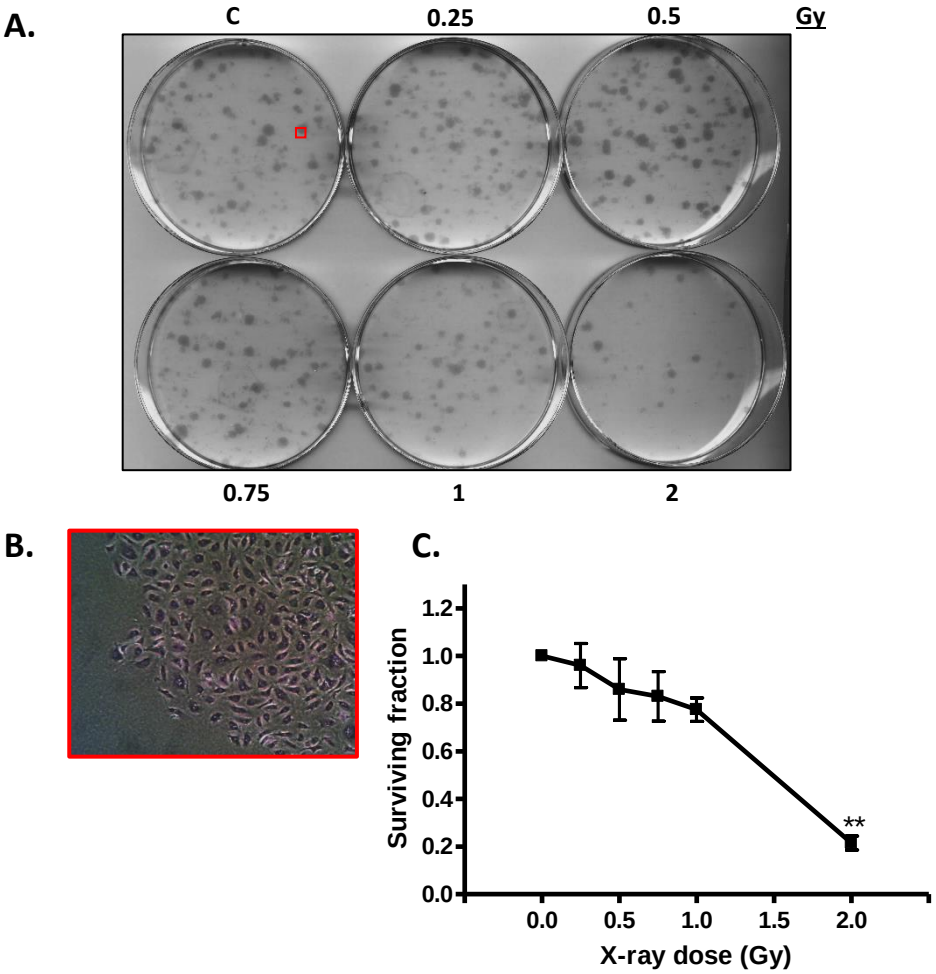

Figure 4.3: Inhibition of HCAEC colony formation by low X-ray doses. HCAECs were irradiated with increasing doses of X-rays and incubated for 24 hours before a clonogenic assay was performed as outlined in section 2.2.5. **A.** Stained colonies. **B.** A brightfield microscope (10X magnification) was used to visualise a section of a stained HCAEC colony (red box). **C.** Surviving fractions were calculated as described in section 2.2.5.2 and shown as mean ± S.E. mean, n=4. **p<0.01 compared to 1 Gy.

To gain a greater understanding of the cellular events leading to the reduced replicative ability of irradiated HCAECs, extra cells remaining at the time of trypsinisation and re-plating during the clonogenic assay (i.e. 24 hours post-irradiation) were retained and analysed by FACs to determine their cell cycle profile. Differences in cell cycle distribution were observed as a dose-dependent reduction in the percentage of cells in the S phase of the cell cycle [surviving fraction: 0.75 Gy. 0.68 ± 0.06, $p<0.01$, $n=4$] (Figure 4.4). The decrease in S phase cells was associated with a minor dose-dependent reduction of cells in G2/M and an increase in G1 cells. Hence, X-irradiation appears to hinder G1 to S phase transition thus resulting in a reduced number of cells undergoing DNA replication and impairing colony formation by HCAECs in the long-term. Despite the marked difference in HCAEC colony formation by 1 and 2 Gy X-rays, both doses reduced the number of S phase, replicating HCAECs equally by 37%, suggesting further detrimental effects beyond 24 hours post-irradiation resulting in hindered proliferation of cells exposed to these X-ray doses.

A key consideration for experiments involving irradiation of cells in culture was the potential for ionizing radiation to alter the chemistry of the cell culture media and consequently influence cellular function. Previous studies have demonstrated that irradiated media had no effect on the surviving fraction of non-irradiated cells thus the culture media was not compromised by ionizing radiation (Potter *et al*., 2011, Zhou *et a*l., 2002). Despite these findings, a single experiment was performed to confirm that the inhibition of HCAEC clonogenic survival observed was indeed a consequence of direct irradiation of the HCAECs. As illustrated in Figure 4.5, irradiated cells lost their ability to replicate whereas HCAECs incubated in irradiated media maintained their ability to form colonies, verifying that the detrimental effects of X-irradiation on HCAEC survival are attributed to X-ray effects on the cells themselves.

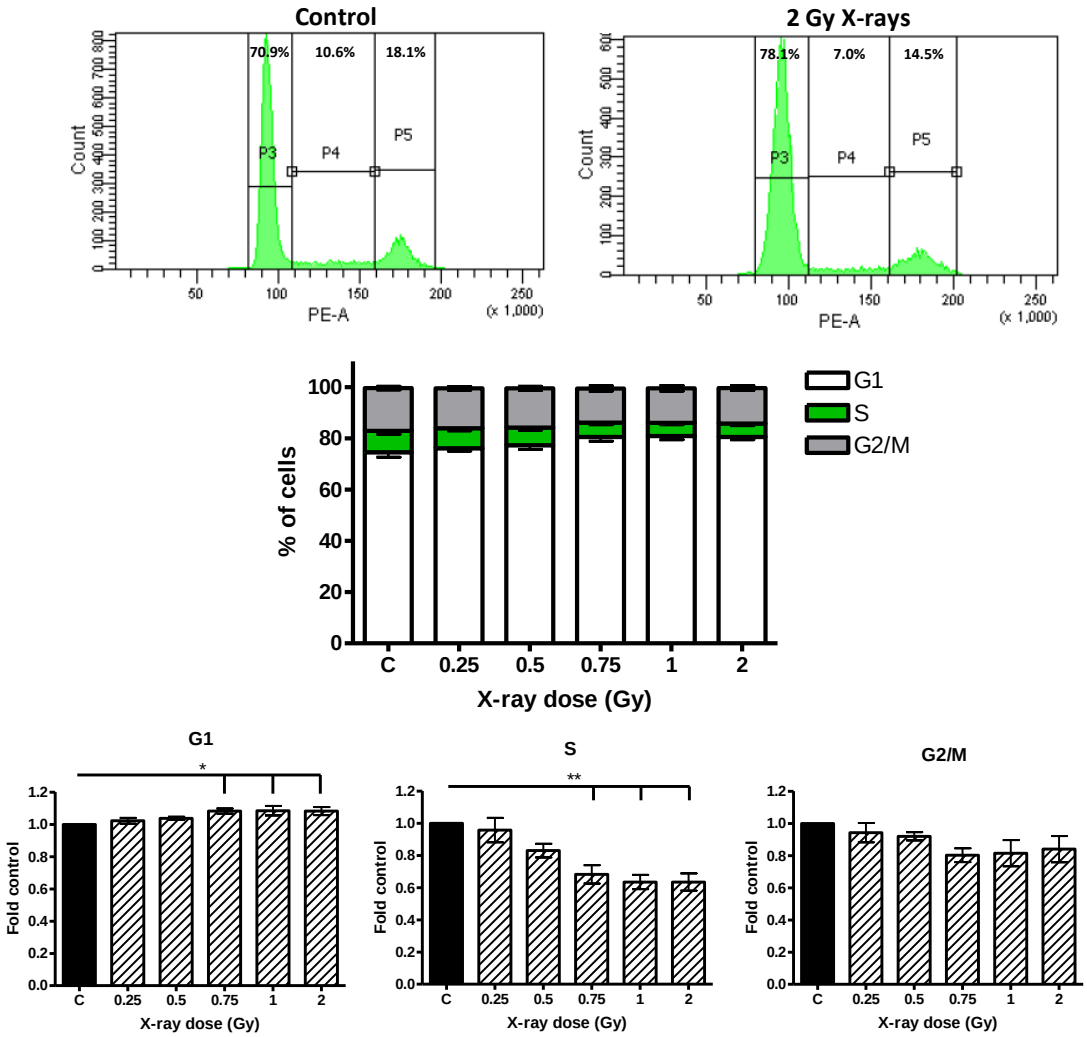

Figure 4.4: Cell cycle distribution of HCAECs exposed to low X-ray doses. Surplus HCAECs remaining at the time of re-plating for the clonogenic assay (24 hours post-irradiation) were subject to cell cycle analysis as outlined in section 2.2.7. Intervals P3, P4 and P5 represent cell cycle stages G1, S and G2/M respectively. Values depict mean ± S.E. mean, n=4. *p<0.05, *p<0.01 compared to control (C).

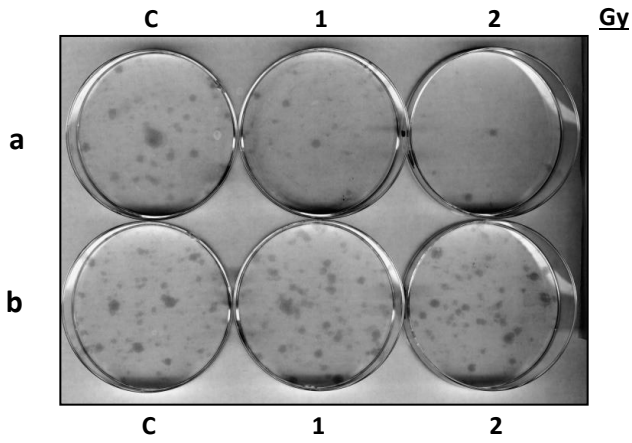

Figure 4.5: Effect of X-irradiated media on HCAEC colony formation. HCAECs were either directly X-irradiated in the presence of media (a) or the media maintaining HCAECs was removed and X-irradiated media was transferred onto the non-irradiated HCAECs (b). Cells were incubated for 24 hours after irradiation or transfer of irradiated media and a clonogenic assay was performed as outlined in section 2.2.5. n=1.

4.2.2 JNK activation in X-irradiated endothelial cells

The role of JNK in endothelial cell deregulation in response to genotoxic chemotherapeutic drug doxorubicin was previously examined in chapter 3. Following the observations that DNA-damaging X-rays inhibit the clonogenic survival of endothelial cells, experiments were performed to elucidate whether X-irradiation promotes JNK activation in endothelial cells.

The kinetics of JNK phosphorylation were assessed in X-irradiated HUVECs. Unlike the sustained JNK phosphorylation observed in doxorubicin-treated endothelial cells (chapter 3, figure 3.8), following exposure of HUVECs to 10 Gy X-rays, both phosphorylated p54 JNK and p46 JNK were transiently up-regulated with maximum phosphorylation of JNK achieved after 4 hours [fold control: p54 JNK, 3.20 ± 0.85, n=3. p46 JNK, 3.96 ± 1.09, $p<0.01$, n=3] (Figure 4.6). Assessing JNK phosphorylation by Western blotting only provides information about the phosphorylation state of JNK, therefore kinase activity assays were utilised to examine the functional activity of JNK in response to X-irradiation. HUVECs were exposed to increasing doses of X-rays and JNK-mediated phosphorylation of downstream transcription factor c-Jun, at serine residues 63 and 73, was investigated 4 hours post-exposure. Phosphorylation of c-Jun appeared to be dose-dependent [fold control: 10 Gy. 2.39 ± 0.81, n=3] (Figure 4.7). However, the increase in c-Jun phosphorylation by high X-ray doses was not deemed statistically significant, likely due to the variations between repetitions of the experiment; the representative blot in Figure 4.7 shows the strongest c-Jun phosphorylation observed. Thus, JNK was not activated in HUVECs by low doses of X-rays and appeared to be only modestly activated by higher doses.

JNK activation by X-irradiation was further characterised in HCAECs, which also responded to X-irradiation by reduced clonogenic survival, as reported in Figure 4.3. The culture media used to maintain endothelial cells contains excessive growth factors to promote cell survival throughout multiple sub-cultivations. Therefore, experiments were performed to compare phosphorylation of c-Jun by JNK in HCAECs which were growing in full medium (non-starved) and HCAECs starved of growth factors and FCS, to establish whether the JNK response would be altered when HCAECs are less

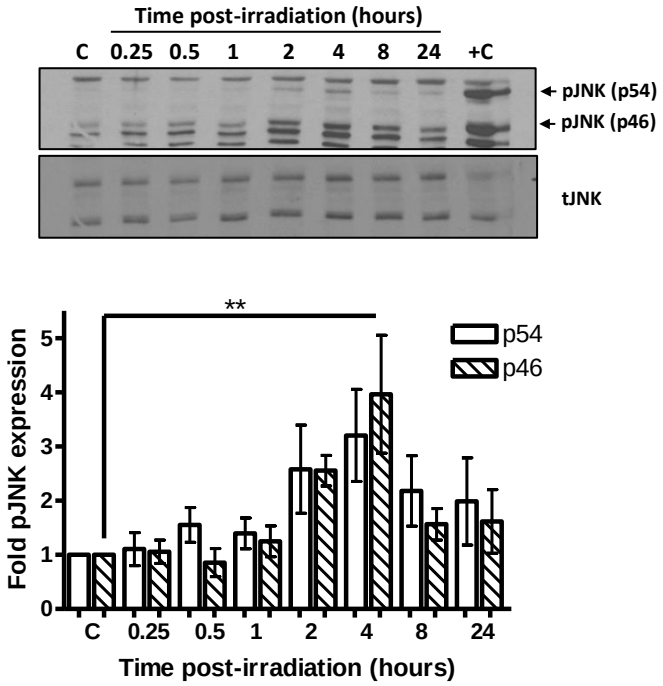

Figure 4.6: Phosphorylation of JNK in X-irradiated HUVECs. HUVECs grown in T_{25} flasks were exposed to 10 Gy X-rays and phosphorylated JNK expression detected at the indicated timepoints post-exposure by Western blotting as outlined in section 2.2.8. Non-irradiated control cells (C) were harvested after 24 hours and TNFα (10 ng/ml, 15 minutes)-treated HUVECs provided a positive control (+C). Values are representative of mean ± S.E. mean, n=3. **$p<0.01$ compared to control (C).

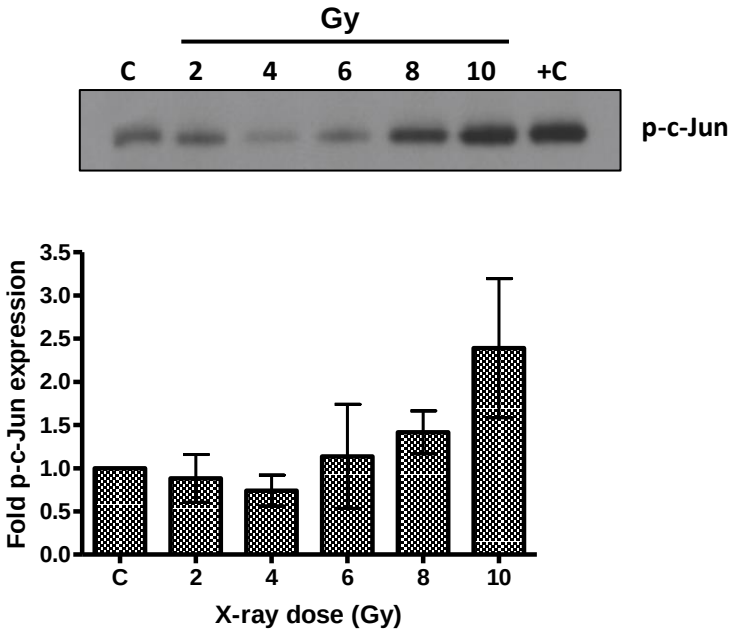

Figure 4.7: The effect of HUVEC X-irradiation on JNK kinase activity. HUVECs confluency were exposed to X-rays (2 to 10 Gy) and JNK-mediated phosphorylation of c-Jun assessed by an *in vitro* kinase assay 4 hours post-radiation exposure, as detailed in section 2.2.9.3**.** TNFα-treated (20 ng/ml, 15 minutes) HUVECs provided a positive control. Values are representative of mean ± S.E. mean, n=3.

protected. Notably, basal phosphorylated c-Jun levels were higher in the non-starved HCAECs and X-irradiation did not promote increased phosphorylation of c-Jun (Figure 4.8). Conversely, basal phosphorylated c-Jun levels in the starved HCAECs were low and phosphorylated c-Jun expression was significantly increased 4 hours following exposure of HCAECs to 10 Gy X-rays [fold starved control: 10 Gy. 3.54 ± 0.72, $p<0.01$, $n=3$] (Figure 4.8). Thus, the condition of the growth medium affected c-Jun phosphorylation in response to X-irradiation, starvation of cells enabled a more distinct up-regulation of phosphorylated c-Jun to be observed. Nonetheless, JNK activity in the starved HCAECs was extremely weak relative to the robust JNK-induced phosphorylation of c-Jun observed in IL-1β-treated HCAECs (Figure 4.8). Due to the poor JNK activation in both HUVECS and HCAECs in response to X-irradiation, the role of JNK in X-ray-induced cell death was not explored further.

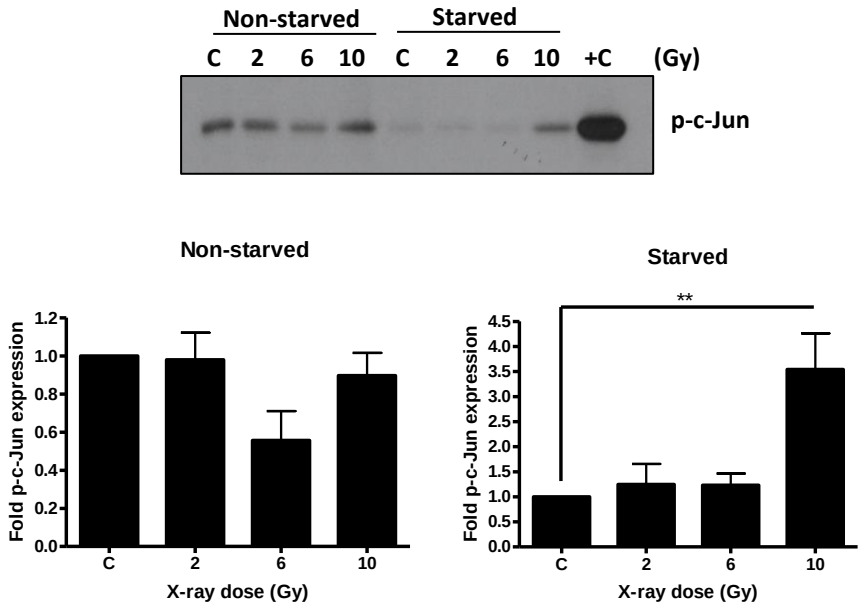

Figure 4.8: The effect of growth factor starvation on JNK activation in X-irradiated HCAECs. HCAECs were plated and incubated in full media, thereafter the media was replaced with either fresh full media, containing 2% FCS (non-starved), or media containing 0.5% FCS and lacking growth factors (starved) 18 hours prior to X-ray exposure. HCAECs were treated with the identified doses of X-rays and JNK-mediated phosphorylation of c-Jun detected after 4 hours by an *in vitro* kinase assay, as outlined in section 2.2.9.3. Results are depicted as fold of control (sham-irradiated, C) for either non-starved or starved (± S.E. mean). IL-1β-stimulated HCAECs (10 ng/ml, 30 minutes) provided a positive control (+C). n=3. **p<0.01 compared to control (C).

4.3 Discussion

The vasculature is an extensive network throughout the body hence radiation therapy for any type of cancer is likely to hit endothelial cells, potentially resulting in vascular damage. Exposure of the coronary arteries during radiotherapy to the chest area, in particular left-sided breast cancer radiotherapy, is concerning. Sato *et al.*, studied women treated with external beam radiation therapy for either left- or right-sided breast cancer, the mean doses to the left anterior descending coronary artery (LAD) were 2.13 ± 0.11 Gy and 0.37 ± 0.02 Gy for left and right breast cancer radiotherapy respectively (Sato *et al*., 2015). It is also recognised that the LAD receives a greater dose of X-rays during left breast radiotherapy than the heart (Sardaro *et al*., 2012). The mean total dose to the heart was 2.4 Gy in left-sided breast cancer patients who received respiratory-gated adjuvant radiotherapy to breast surgery but the mean total dose to the LAD was 9.3 Gy (Becker-Schiebe *et al*., 2016), highlighting the potential for radiation-induced cardiotoxicity to be exacerbated by damage to the surrounding coronary arteries. Thus, this chapter aimed to elucidate the effects of X-rays on HCAECs, as well as recognised radiosensitive HUVECs.

Clonogenic assays, also referred to as colony forming assays, are a useful method to study the cellular effects of radiation over multiple population doublings and are routinely performed to assess the sensitivity of cancer cell lines to radiation. In this chapter, clonogenic assays were utilised to study the replicative ability of X-irradiated endothelial cells and compare the effects of X-irradiation on endothelial and cancer cells. Clonogenic assays are not a typical method to study the survival of primary cells including endothelial cells, therefore the clonogenic assay protocol was carefully considered as two methods can be applied: 1) plating cells at a very low density then irradiating or 2) irradiating a sub-confluent monolayer of cells then re-plating the cells post-irradiation (Franken *et al*., 2006). The first method, plating then irradiation, would expose the endothelial cells to radiation at an extremely low cell density resulting in a poor survival rate and possible overestimation of the toxic effects of X-irradiation on endothelial cells. This method was used by Park *et al*., to study the differing radiosensitivities of endothelial cells from distinct organs to γ-radiation and compare the sensitivity of endothelial cells from normal and cancerous breast tissue. (Park *et al*., 2012[1], Park *et al*., 2012[2]). However, the alternative clonogenic assay protocol,

plating cells post-irradiation, is the preferred method by most studies which employ clonogenic assays to examine long-term endothelial cell survival post-irradiation. Both Zhang *et al*., and Panganiban *et al*., X-irradiated sub-confluent endothelial cells (HUVECs or bovine PAECs respectively) and performed delayed re-plating (16 to 24 hours post-irradiation) (Panganiban *et al*., 2013, Zhang *et al*., 2011). Delayed re-plating enables DNA repair processes to proceed providing more information about aberrations in cellular repair post-irradiation (Buch *et al*. 2012). Using this method, a greater proportion of cells are likely to survive and form colonies, achieving a greater plating efficiency, thus this method was chosen to study the clonogenic survival of HUVECs and HCAECs. Franken *et al*., suggested some useful techniques to improve the survival of primary cells, which may have plating efficiencies less than 0.5% during colony forming assays, such as: incubation of cells with conditioned media from a proliferating culture of cells, seeding cells onto a feeder layer of non-proliferating but growth factor-producing cells or growing cells on soft agar (Franken *et al*. 2006). In this study, HCAECs successfully formed colonies without the additional measures described by Franken *et al*., the plating efficiency for non-irradiated HCAECs was 12.76 ± 2.53%, hence the effects of X-rays on HCAEC clonogenic survival were able to be elucidated.

Both HCAEC and HUVEC clonogenic survival was significantly attenuated with low, therapeutically relevant doses of radiation. An X-ray dose of 2 Gy considerably inhibited HCAEC colony formation, the surviving fraction was 0.2 as reported in Figure 4.3. Likewise, Panganiban *et al*., who also performed delayed re-plating similar to this study, observed a surviving fraction of 0.28 for bovine PAEC exposed to 2 Gy X-rays (Panganiban *et al*., 2013). As depicted in Figure 4.2, the survival of 2 Gy irradiated HUVECs correlated well with these findings as a surviving fraction of 0.30 was observed. Despite using a different type of ionizing radiation, the study by Park *et al*, devised to compare the radiosensitivities of endothelial cells from different vascular regions, found that the most radiosensitive endothelial cells, HDMECs, displayed approximately 20% colony formation after exposure to 2 Gy γ-rays (Park *et al*., 2012[1]). Clearly low doses of X-rays, and γ-rays, have a detrimental effect on the ability of endothelial cells to proliferate.

Although inhibition of HCAEC and HUVEC replication in response to X-irradiation was identified, clonogenic assays do not reveal the exact cellular mechanisms leading to defective cell proliferation and survival (Panganiban *et al*., 2013). Loss of HCAEC and HUVEC survival may be due to the cytotoxic effects of X-rays on endothelial cells such as apoptotic death. The localisation of phosphorylated H2AX (γH2AX) at DNA strand breaks, associated with apoptosis, has been identified in HUVECs and EA.hy926 cells post-X-irradiation, occurring rapidly within 30 minutes post-exposure in a dose-dependent manner (Cervelli *et al*., 2014, Rombouts *et al*., 2013). Cervelli *et al.,* found that at least 98% of HUVECs were positive for γH2AX 30 minutes after exposure to very low doses of X-rays (0.125 to 0.5 Gy) (Cervelli *et al*., 2014). In addition to observing γH2AX recruitment at DNA lesions, Rombouts *et al*., observed a dose-dependent increase in apoptotic HUVECs and EA.hy926 cells by flow cytometric analysis of Annexin V-FITC/PI dual-stained cells, 5 Gy promoted significant HUVEC apoptosis after 24 hours while 0.5 Gy induced apoptotic death after 48 hours (Rombouts *et al*., 2013). While not relevant to the X-rays doses utilised for the clonogenic experiments in this chapter, Panaganiban *et al*., detected HUVEC apoptosis with very high X-ray doses (≥ 10 Gy) 24 hours after exposure using neutral comet assays (Panganiban *et al*., 2013). Panganiban *et al*., identified transient, elevated caspase-3 activity, expression of cleaved caspase-3 plus caspase 8 and 9 activity 6 hours following irradiation of HUVECs with 50 Gy X-rays, suggesting caspase-dependent apoptosis of endothelial cells in response to very high X-ray doses; this has not been investigated in endothelial cells exposed to low doses of X-rays. Evidently, programmed cell death is induced in X-irradiated endothelial cells, even at low doses such as those used in this chapter and may be responsible for loss of HCAEC and HUVEC clonogenic survival.

Studies have also investigated non-apoptotic mechanisms of cell death in response to ionizing radiation. Having observed reduced bovine PAEC clonogenic survival and the induction of apoptosis in some irradiated cells, Panganiban *et al*., also examined the release of lactate dehydrogenase (LDH) from X-irradiated cells into the culture media. This is a marker for the induction of necrosis, a mode of cell death characterised by swelling of intracellular organelles and bursting of the cell membrane with

subsequent expulsion of cellular components (Panganiban *et al*., 2013). X-irradiated PAECs did not exhibit LDH release at any dose studied (up to 50 Gy) 24 or 72 hours post-exposure, showing a lack of necrotic death in X-irradiated PAECs (Panganiban *et al*., 2013). However, Rombouts *et al*., observed a reduction in the percentage of HUVECs with a cell membrane 24 hours after irradiation with 0.5 Gy X-rays, indicating potential necrotic death (Rombouts *et al*., 2013). Rombouts *et al*., also suggested mitotic catastrophe, which can occur independently of apoptosis, as an alternative intracellular process leading to loss of endothelial cell proliferation post-irradiation (Rombouts *et al*., 2013). Mitotic catastrophe is defined by aberrant cytokinesis and ineffective chromosome separation resulting in enlarged cells with numerous micronuclei (Castedo *et al*., 2004). Riquier *et al*, detected micronuclei formation in immortalized EA.hy926 cells 24 hours after exposure to 5 Gy X-rays, with subsequent formation of inflated cells with multiple nuclei after 48 hours, mitotic catastrophe was occurring in 43% of cells after 48 hours (Riquier *et al*. 2013). Similarly, Rombouts *et al*., found that X-irradiated EA.hy926 cells displayed increased cell size, several nuclei and the presence of nuclear bodies, confirming the occurrence of mitotic catastrophe in X-irradiated immortalized endothelial cells (Rombouts *et al*., 2013). Polynucleated primary HUVECs were also identified post-irradiation (5 Gy X-rays), indicating mitotic catastrophe in X-irradiated primary endothelial cells too (Rombouts *et al*., 2013). A number of studies have investigated the death responses of irradiated endothelial cells and have identified several modes of cell death (apoptosis, necrosis and mitotic catastrophe) which may account for the loss of HCAEC and HUVEC colony formation observed in this chapter.

The attenuated colony formation by radiation-exposed endothelial cells may also be a result of growth arrest and the induction of cellular senescence. Panganiban *et al*., identified a senescent phenotype in X-irradiated (50 Gy) PAECs characterised by a time-dependent increase in the presence of senescence-associated β-galactosidase and increased p21 expression (Panganiban *et al*., 2013). Palayoor *et al*., identified significant alteration of cell cycle regulatory genes involved at various cell cycle stages, including up-regulation of ATM and p21 plus down-regulation of CDK1/2 and Cdc25A/B/C in X-irradiated HCAECs (Palayoor *et al*., 2014). Consequently, Palayoor *et al*., investigated the cell cycle distribution of HCAECs 24 hours post exposure to 10

Gy X-rays, a reduction in the G1 and S populations was observed with an increase in G2 phase cells (Palayoor *et al*., 2014). Exposure of HUVECs to lower X-ray doses (5 and 3 Gy) for 24 hours has also demonstrated this distinct cell cycle re-distribution (Rombouts *et al*., 2013, Zhang *et al*., 2011). Thus DNA damage by X-rays arrests cells in G2, preventing transition to mitosis until DNA repair process have been executed correctly or cellular apoptosis has been triggered (Palayoor *et al*., 2014). Ionizing radiation is recognized to induce G2 checkpoint arrest via the characteristic ATM-CHK1-Cdc25-cdc2 pathway but ATM-mediated CHK2 activation, induced by DNA damage, is also linked to G1 checkpoint arrest (Lapenna and Giordano, 2009). Unlike the previously discussed studies which identified G2 accumulation in endothelial cells exposed to X-rays, irradiated HCAECs displayed a modest but statistically significant G1 arrest, as depicted in Figure 4.4. Indeed, γ-radiation (4 Gy) has been shown to increase the expression of phosphorylated ATM, phosphorylated p53 and p21 in HUVECs, key players in G1 phase arrest (Kim *et al*., 2014). Microarray analysis also identified the down-regulation of genes responsible for G1 to S transition including cyclin E and CDK2 in HUVECs expressing a senescent phenotype induced by 8 Gy γ-radiation (Igarashi *et al*., 2012). Ionizing radiation appears to affect cell cycle regulatory proteins instrumental in both G1 or G2 phase progression or obstruction. A definitive finding in irradiated endothelial cells is a reduction in the number of S phase cells undergoing DNA replication. A dose-dependent reduction in the percentage of replicating, S phase HCAECs was identified in this chapter 24 hours post-irradiation, attributed to the DNA damaging effects of X-rays, γH2AX was still detectable up to 24 hours after irradiation of HUVECs (Rombouts *et al*., 2013). Thus it can be concluded that the reduced clonogenic survival of irradiated HCAECs was partly due to fewer replicating HCAECs when the cells were re-plated for colony formation. Further research is required to establish whether DNA damaged HCAECs subsequently undergo: apoptosis, necrosis, mitotic catastrophe or senescence resulting in diminished clonogenic survival.

The clonogenic assays performed in this chapter yielded successful colony formation, however a limitation of the protocol used in this study is the requirement for irradiated endothelial cells to re-attach to a new culture surface. X-irradiation may affect the adhesive properties of endothelial cells resulting in poor re-attachment, this

would be interpreted as reduced colony formation. However, ionizing radiation is primarily recognised to promote adhesion molecule expression on endothelial cells linked to the pathogenesis of atherosclerosis; γ-irradiated HUVECs have displayed increased ICAM-1, CD44 and CD31 expression (Kim *et al*., 2014, Prabhakarpandian *et al*., 2001, Quarmby *et al*., 1999). Furthermore, urinary endothelial cells from female mice (C3H/Neu strain from Dresden breeding colony, 8 to 12 weeks old) exposed to lower abdominal X-irradiation (20 Gy single dose) displayed early, elevated ICAM-1 expression with increased leukocyte infiltration 2 days post-irradiation (Jaal and Dorr, 2005). This suggests that endothelial cells would retain their ability to adhere post-irradiation. Nevertheless, the adhesion of irradiated endothelial cells re-plated during the clonogenic assay is an area lacking consideration and should be investigated further.

Intracellular transducers are the determinants of cellular fate, having investigated JNK activation in doxorubicin-treated HCAECs, experiments were performed to further extrapolate the role of JNK in the response of endothelial cells to DNA damaging X-rays. Knowledge regarding the effects of X-irradiation on JNK activation in endothelial cells is poor. Two decades ago Verheij *et al*., identified dose-dependent JNK-mediated phosphorylation of c-Jun 20 minutes after exposure of BAECs to 5 Gy X-rays and greater, utilising kinase activity assays (Verheij *et al*., 1998). In an earlier study, Verheij *et al*., observed apoptosis in wild-type U937 human monoblastic leukaemia cells 12 hours post-exposure to 5 Gy X-irradiation but apoptosis was prevented in cells transfected with a dominant-negative c-Jun construct lacking the N-terminal domain which harbours the serine 63 and 73 residues phosphorylated by JNK (U937/TAM-67 cells), showing a role for JNK in X-ray induced apoptosis (Verheij *et al*., 1996). Enomoto *et al*., also identified a correlation between JNK activation and cell death, highly radiosensitive human T-cell leukaemia (MOLT-4) cells displayed sustained JNK phosphorylation in response to 10 Gy X-rays, however this was not comprehensively characterised as only up to 4 hours post-irradiation was investigated, while human Rh-1a T-cell leukaemia cells which are less sensitive to the death-promoting effects of X-rays demonstrated transient JNK phosphorylation, maximum JNK phosphorylation was achieved 1 hour post-IR (Enomoto *et al*., 2000). As discussed previously, sustained JNK activation promotes cell death whereas transient

JNK activity is linked to cell survival. Interestingly, JNK phosphorylation in HUVECs exposed to 10 Gy X-rays was transient, implying a pro-survival role for JNK in irradiated endothelial cells. Single, high doses of radiation, such as 10 Gy, are still regarded useful therapeutically, with improved tumour killing observed relative to low-dose fractionated therapy (Panganiban, *et al*., 2013). Cancers in the thoracic region, including primary and metastasised lung cancers were successfully controlled with a 30 Gy individual dose of radiation (Fritz *et al*., 2006). Additionally, tissues are exposed to a high dose of radiation during administration of intraoperative electron radiation therapy (IOERT). IOERT delivers a high dose of radiation, 21-23 Gy, directly following surgery to remove a tumour, such as a breast tumour, with the intention of killing any residual cancer cells (Bravata *et al*., 2015). Hamasu *et al*, employed 15 Gy X-irradiation in a further study investigating the effects of X-rays on JNK signalling in MOLT-4 cells (Hamasu *et al*., 2005). The authors observed transient JNK phosphorylation in irradiated cells, elevated phosphorylated JNK expression was detected between 1.5 and 6 hours post -irradiation, with levels returning to basal after 9 hours (Hamasu *et al*., 2005). In this study, antioxidant N-acetylcysteine (NAC) attenuated JNK phosphorylation induced by 7.5 Gy X-rays and significantly reduced apoptosis incited by 7.5 Gy after 9 hours, implicating oxidative stress-induced JNK activation in the apoptosis of MOLT-4 cells (Hamasu *et al*., 2005). Reactive oxygen species have been linked to endothelial cell dysfunction *in vivo* by examining total-body X-irradiated (2.5 Gy fractions) Sprague-Dawley rats (Hatoum *et al*., 2006). Hatoum *et al*., found increased generation of superoxide anions and peroxides in irradiated rats compared to sham-irradiated rats and acetylcholine-induced relation of gut submucosal microvessels, which was impaired in irradiated rats, improved when the vessels were treated with a superoxide-dismutase mimetic (MnTBAP) (Hatoum *et al*., 2006). As discussed previously in chapter 1, section 1.7.3, ROS generation is a precursor for JNK activation but the association between ROS and JNK activation in endothelial cells exposed to ionizing radiation remains undefined. However, oxidative stress has been linked to JNK activation in normal human fibroblasts (MRC5CV1) exposed to ionising radiation (Lee *et al*., 2001). NAC pre-treatment reduced levels of nuclear phosphorylated c-Jun at serine residue 73 in MRRC5CV1 cells 2 hours after exposure to 20 Gy γ-rays (Lee *et al*., 2001). The normal human fibroblasts in this

study, demonstrated transient c-Jun phosphorylation post-exposure to 20 Gy X-rays, peak expression was detected after at 2 hours, but no observable c-Jun phosphorylation was detected in ATM-deficient fibroblasts (AT5BIVA) from patients with ataxia telangiectasia (AT), thus further proving ATM-dependent JNK cascade activation in cells exposed to ionizing radiation (Lee *et al*., 2001).

Despite numerous studies identifying transient JNK activation in X-irradiated cells, including this thesis, FAS-mediated death has been characterised in cells exposed to ionizing radiation with a contributory role for JNK. JNK-regulated c-Jun forms homo- or -heterodimers resulting in the formation of AP-1 transcription factors, known to regulate FAS ligand gene expression (Karin and Gallagher, 2005). Kuwabara *et al*., identified increased FAS expression on MOLT-4 cells 4 hours after exposure to 7.5 Gy X-rays (Kuwabara *et al*., 2003). Both JNK inhibition and a FAS receptor antagonist significantly reduced apoptosis of Jurkat T lymphocytes and RPMI8226 human multiple myeloma B cells 72 hours after exposure to 10 or 12 Gy γ-rays, implicating FAS and JNK signalling in death induced by γ-rays (Praveen and Saxena, 2013). JNK inhibition resulted in reduced FAS ligand surface expression on Jurkat T cells while FAS receptor inhibition reduced JNK phosphorylation in Jurkat T cells 72 hours after exposure to 10 or 12 Gy X-rays, the authors concluded that FAS was essential for maintained JNK activation while JNK itself was a regulator of FAS ligand expression, establishing a self-perpetuating loop in response to ionizing radiation (Praveen and Saxena, 2013). These studies provide an insight into the regulation of JNK activation in response to ionizing radiation in various cancer cell types but the methods of JNK cascade induction in X-irradiated endothelial remain to be addressed.

Overall, the findings from this chapter prove that HCAECs are radiosensitive and lose their ability to replicate post-irradiation, this was found to involve hindrance of G1 to S phase cell cycle transition. The contribution of JNK to the loss of HCAEC survival post-irradiation remains unverified but the weak response of JNK in irradiated HUVECs and HCAEC imply that JNK is not a dominant signalling intermediate involved in deregulation and death of coronary artery endothelial cells exposed to X-rays.

Chapter 5:

Combinatory effects of doxorubicin and X-irradiation on endothelial cell function

5.1 Introduction

Having investigated the independent effects of doxorubicin and X-rays on endothelial cell function, the toxic effects of doxorubicin and X-irradiation in combination were researched.

Anticancer therapies which generate similar cellular effects, such as the DNA damaging properties of doxorubicin and X-rays, are often administered in combination to promote therapy interactions and thus improve treatment efficacy (Tallarida. 2011). Interactions between therapeutic agents are recognised as either supra-additive (synergistic), additive or infra-additive (antagonistic) (Tallarida. 2011). Synergy occurs between agents when their combined effect is greater than their individual potencies in summation while an interaction is merely additive when the combined action of both agents is consistent with the individual actions of each drug (Tallarida. 2011). An ideal therapy combination would utilise agents which display synergy for the desired effect but antagonism, where the effect of one or more than one agent is reduced, for the unwanted effects (Tallarida. 2011).

Experimental studies have facilitated understanding of the interaction between doxorubicin and radiation. Supiot *et al.*, observed an additive effect on DNA strand break formation in RPMI 8226 myeloma cells treated with doxorubicin plus α-radioimmunotherapy, tail DNA content (representative of the number of DNA lesions and determined by comet assays) was 2.86 compared to 1.30 and 1.95 for doxorubicin and α-radioimmunotherapy alone respectively (Supiot *et al*., 2005). However, analysis of the clonogenic survival of combinatory treated myeloma cells revealed a synergistic effect between doxorubicin and α-radioimmunotherapy, radiation enhancement ratios (REF) of 1.17, 1.20 and 1.19 were obtained for LP1, RPM1 8226 and U266 cell lines respectively (Supiot *et al*., 2005). REF values greater than 1 are indicative of radiosensitization thus synergy between anticancer therapies (Supiot *et al*., 2005). Interestingly, doxorubicin accumulated all three human myeloma cell lines studied in the highly radiosensitive G2/M phase of the cell cycle. Hence Supiot *et al.*, concluded that promotion of G2/M cell cycle synchronisation was a mechanism responsible for synergy between doxorubicin and radiation (Supiot *et al*., 2005). The damaging combinatory effects of doxorubicin and radiation have also been observed in breast

cancer cell lines. Pre-treatment of HeLa S3 cells with 10 µg/ml doxorubicin 2 hours before γ-irradiation reduced cell survival in an additive manner (Jagetia and Nayak, 2000). Jagetia and Nayak, also observed increased presence of micronuclei in combinatory-treated HeLa cells compared to solely irradiated cells and a correlation between micronuclei frequency and cell survival was discerned (Jagetia and Nayak, 2000). In addition, there was a reduced incidence of binucleate cells post-combinatory treatment (doxorubicin plus 0 Gy = 458.33, doxorubicin plus 3 Gy = 196.00), indicating a decline in cancer cell proliferation (Jagetia and Nayak, 2000). Thus, the genotoxic effects of doxorubicin and radiation were greater in combination compared to either treatment alone.

Several decades ago initial research was performed to understand the interactions between doxorubicin and X-irradiation, X-ray and doxorubicin combinatory treatment *in vitro* was shown to have an additive effect on DNA single-strand breakage (Byfield *et al*., 1977). Interestingly, doxorubicin did not interfere with repair of DNA lesions induced by X-irradiation (Byfield *et al*., 1977, Cantoni *et al*., 1985). Belli and Piro, also reported that treatment of mammalian V79-182 lung cells with doxorubicin (0.4 µg/ml) 1 hour prior to X-irradiation attenuated the accumulation of sub-lethal injury caused by radiation (Belli and Piro, 1977). Since then, little research has been performed to further understand the biochemistry and cellular fates of doxorubicin and X-irradiation interactions. In particular, the combinatory effects of doxorubicin and X-irradiation on the endothelium have yet to be defined.

The set of experiments in this chapter investigated the effects of combinatory treatment with doxorubicin and X-irradiation on endothelial cells by specifically assessing HCAEC survival and determining whether the interactions between doxorubicin and X-irradiation are synergistic, additive or antagonistic in endothelial cells.

5.2 Results

5.2.1 Clonogenic survival of doxorubicin-treated endothelial cells

Clonogenic assays, having been successfully used to demonstrate the cytotoxicity of X-irradiation to endothelial cells in chapter 4, were performed to experimentally evaluate the effects of doxorubicin and X-irradiation in combination on HCAEC replication and survival. Combinatory experiments employ sub-lethal concentrations/doses of anticancer treatment to enable observation of an enhanced detrimental effect when drug and radiation are used in combination.

Since the effects of doxorubicin alone on HCAEC clonogenic survival had yet to be investigated, experiments were performed to elucidate a sub-lethal dose which could be applied for combinatory clonogenic assays. Doxorubicin promoted a concentration-dependent reduction in HCAEC colony formation as depicted in Figure 5.1 A, with concentrations ≥ 0.01 μM causing a significant reduction in the surviving fraction of HCAECs [surviving fraction: 0.01 μM. 0.447 ± 0.159, $p<0.01$, $n=3$]. An IC_{50} value of 0.016 ± 0.005 μM was obtained for doxorubicin-mediation inhibition of HCAEC colony formation from the sigmoidal concentration-response curve depicted in Figure 5.1 C. Evidently, doxorubicin, at concentrations lower than those which showed cytotoxicity in MTT assays (chapter 3, section 3.2.1), greatly impaired longer-term HCAEC clonogenic growth.

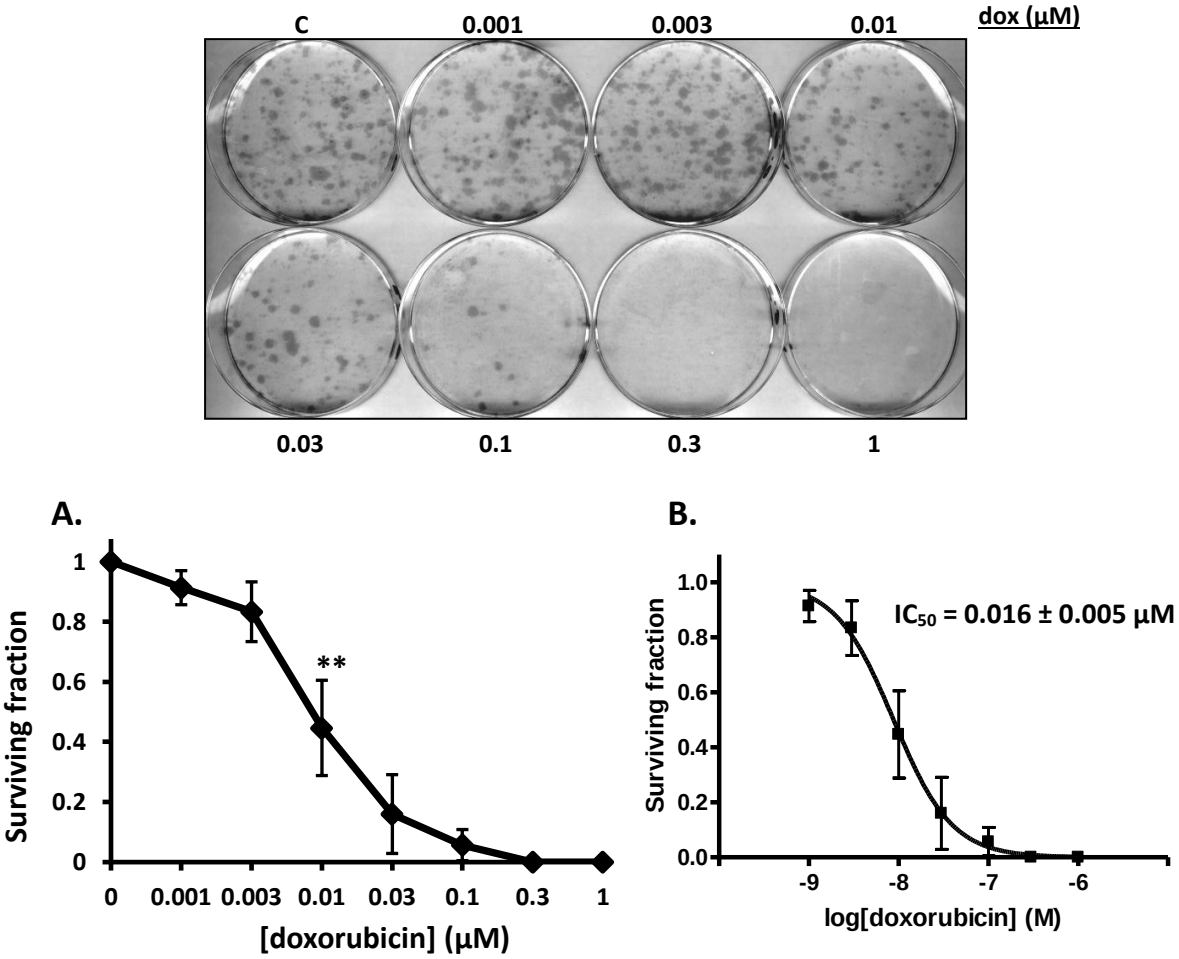

Figure 5.1: Inhibition of HCAEC colony formation by doxorubicin. A. HCAECs were treated with doxorubicin (dox) at the indicated concentrations for 48 hours, followed by a clonogenic assay and calculation of surviving fraction as described in section 2.2.5. Values represent mean ± S. E. mean, n=3. **p<0.01 compared to control (0 µM). **B.** Concentration-response curves were generated from 3 separate experiments and IC_{50} values calculated as outlined in section 2.2.11. Each IC_{50} was averaged to determine the mean IC_{50} ± S.E.mean. Graph B depicts the average curve from the 3 separate curves. An upper constraint of 1 and lower constraint of 0 were applied to each response curve.

5.2.2 Survival of endothelial cells treated with doxorubicin and X-rays in combination

Due to time constraints, complex combination experiments utilising an extensive range of doxorubicin concentrations and radiation doses could not be assessed. Thus, a single dose of X-radiation and concentration of doxorubicin which reduced the HCAEC surviving fraction by approximately 70%, were chosen for assessment of the combinatory effects of each anticancer agent, 1 Gy and 0.005 µM respectively. As observed previously in chapter 3, section 3.2.2, 24-hour treatment of HCAECs with low doxorubicin concentrations promoted G2/M phase arrest, suggesting radiosensitization of the cells. Therefore, to evaluate the combinatory toxic effects of both treatments, HCAECs were treated with doxorubicin for 24 hours prior to X-irradiation. Once irradiated, the endothelial cells were incubated for a further 24 hours before re-plating for clonogenic growth.

Surprisingly, 0.005 µM doxorubicin reduced endothelial cell death induced by 1 Gy X-rays, observed as an increase in the surviving fraction of HCAECs [surviving fraction: 1 Gy. 0.505 ± 0.091, 0.005 µM +1 Gy. 0.651 ± 0.085, n=3] (Figure 5.2). However, the difference between the surviving fraction of irradiated and irradiated plus doxorubicin-treated (i.e. combinatory-treated) cells was not statistically significant, demonstrating a lack of interaction between 0.005 µM doxorubicin and 1 Gy X-irradiation.

To further understand the molecular mechanisms altered in combinatory-treated cells compared to cells treated with single anticancer agents, cell cycle analysis of treated HCAECs was also performed 24 hours post-irradiation, when cells were re-plated for clonogenic growth. Exposure of HCAECs to doxorubicin plus radiation reduced the percentage of S phase replicating cells to the same extent as radiation alone [Fold control: 1 Gy. 0.690 ± 0.038, 0.005 µM + 1 Gy. 0.660 ± 0.029, n=3] (Figure 5.3). Thus doxorubicin (0.005 µM) had little effect on the cellular effects of X-rays.

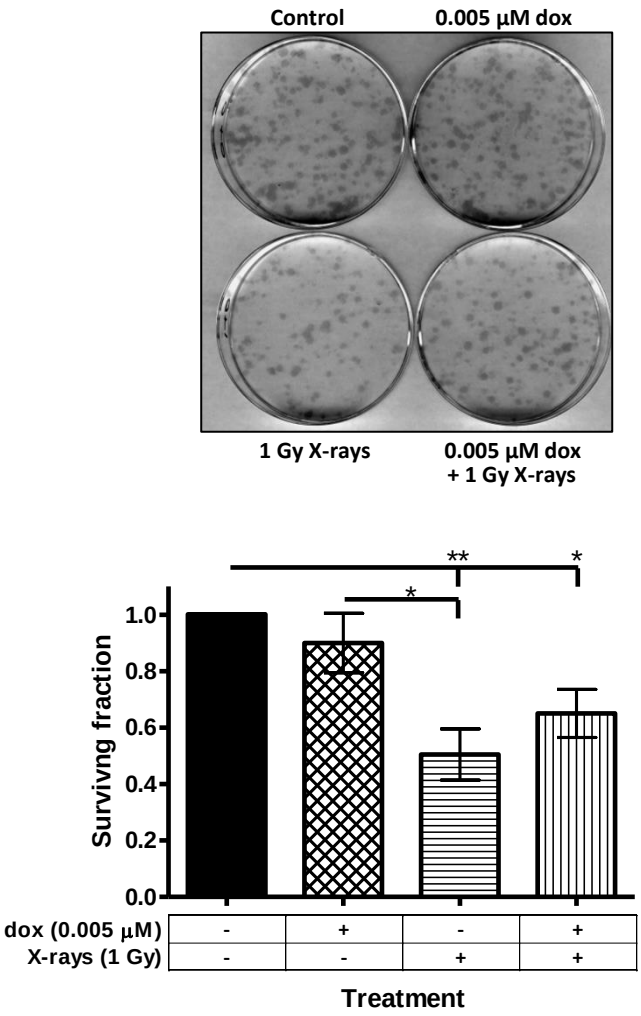

Figure 5.2: Combinatory effect of doxorubicin (0.005 µM) and X-irradiation (1 Gy) on HCAEC clonogenic survival. HCAECs were treated with doxorubicin (dox) for 24 hours prior to X-irradiation. HCAECs were incubated for a further 24 hours post-irradiation then subject to a clonogenic assay as outlined in section 2.2.5. HCAECs which did not receive doxorubicin, were treated with dH_20 and non-irradiated cells were sham-irradiated as described in section 2.2.3. Values depict mean ± S.E. mean, n=3. *$p<0.05$, **$p<0.01$.

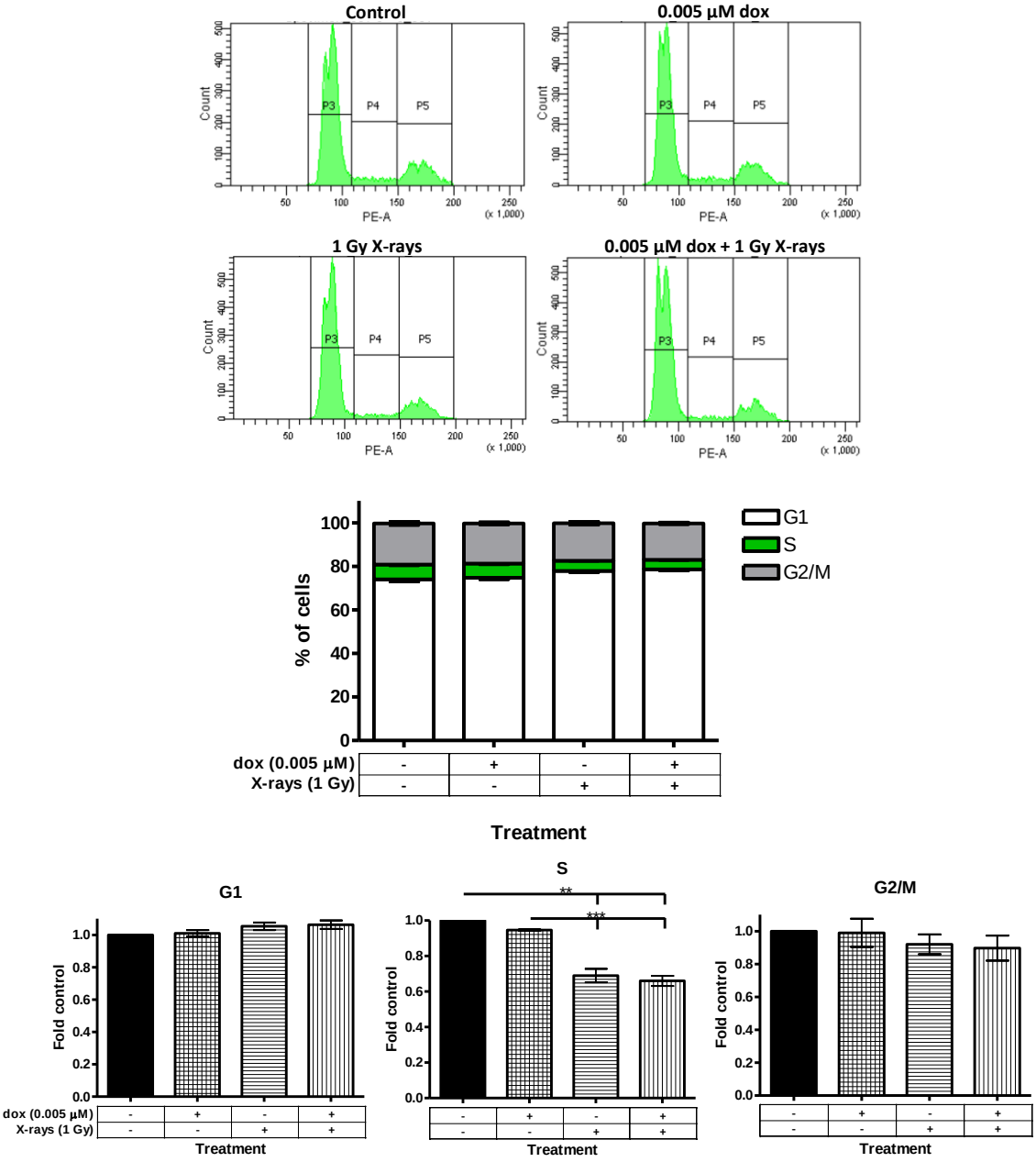

Figure 5.3: Cell cycle status of HCAECs treated with doxorubicin (0.005 µM) and X-irradiation (1 Gy). HCAECs treated with doxorubicin for 24 hours prior to X-irradiation and incubation for a further 24 hours were retained during re-plating for the clonogenic assay (results Figure 5.2) and analysed by FACs to determine cell cycle profile, as described in section 2.2.7. Intervals P3, P4 and P5 represent cell cycle stages G1, S and G2/M respectively. Values denote mean ± S.E. mean, n=3. **p<0.01, ***p<0.001.

To determine whether a greater concentration of doxorubicin would be required to generate a synergistic effect with X-irradiation, further combinatory treatment experiments were performed using 0.01 µM doxorubicin, which reduced the surviving fraction of HCAECs by approximately 55% as depicted previously in Figure 5.1. However, as demonstrated in Figure 5.4, the effect of doxorubicin (0.01 µM) and X-irradiation (1 Gy) in combination was found to be additive. Doxorubicin (0.01 µM) alone reduced the clonogenic survival of HCAECs by 74.83% and when used in combination with X-irradiation, reduced the clonogenic survival of X-ray-exposed HCAECs by 76.91% (Figure 5.4). Likewise, X-ray-treatment alone reduced clonogenic survival by 55.7% and X-rays caused a 59.12% reduction in the surviving fraction of doxorubicin-treated HCAECs when used in combination (Figure 5.4). Unpaired, two-tailed t-tests proved that the reduction caused by doxorubicin or X-rays alone and in combination treatment was not significantly different and indeed additive. Analysis of the cell cycle profile of the treated HCAECs did not reveal any additive effects regarding cell cycle distribution when doxorubicin and radiation were used in combination rather than independently [S phase, Fold control: 0.01 µM 0.533 ± 0.018, 0.01 µM + 1 Gy. 0.553 ± 0.033, n=4] (Figure 5.5). Therefore, although an additive effect on clonogenic survival was observed with 0.01 µM doxorubicin and 1 Gy X-rays, cell cycle stage analysis did not provide further information concerning the intracellular response in combinatory-treated endothelial cells.

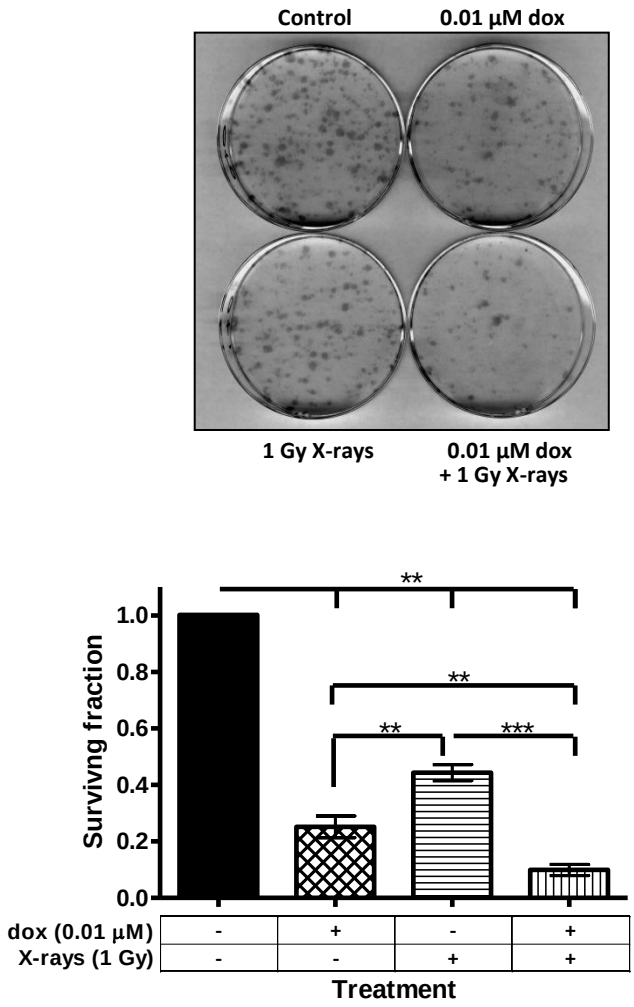

Figure 5.4: Combinatory effect of doxorubicin (0.01 µM) and X-irradiation (1 Gy) on HCAEC clonogenic survival. HCAECs were treated with doxorubicin (dox) for 24 hours, then X-irradiated and incubated for a further 24 hours post-irradiation. A clonogenic assay was performed on control and treated HCAECs as detailed in section 2.2.5. HCAECs which did not receive doxorubicin, were treated with dH_20 and non-irradiated cells were sham-irradiated as outlined in section 2.2.3. Values represent mean ± S. E. mean, n=4. **p<0.01, ***p<0.001.

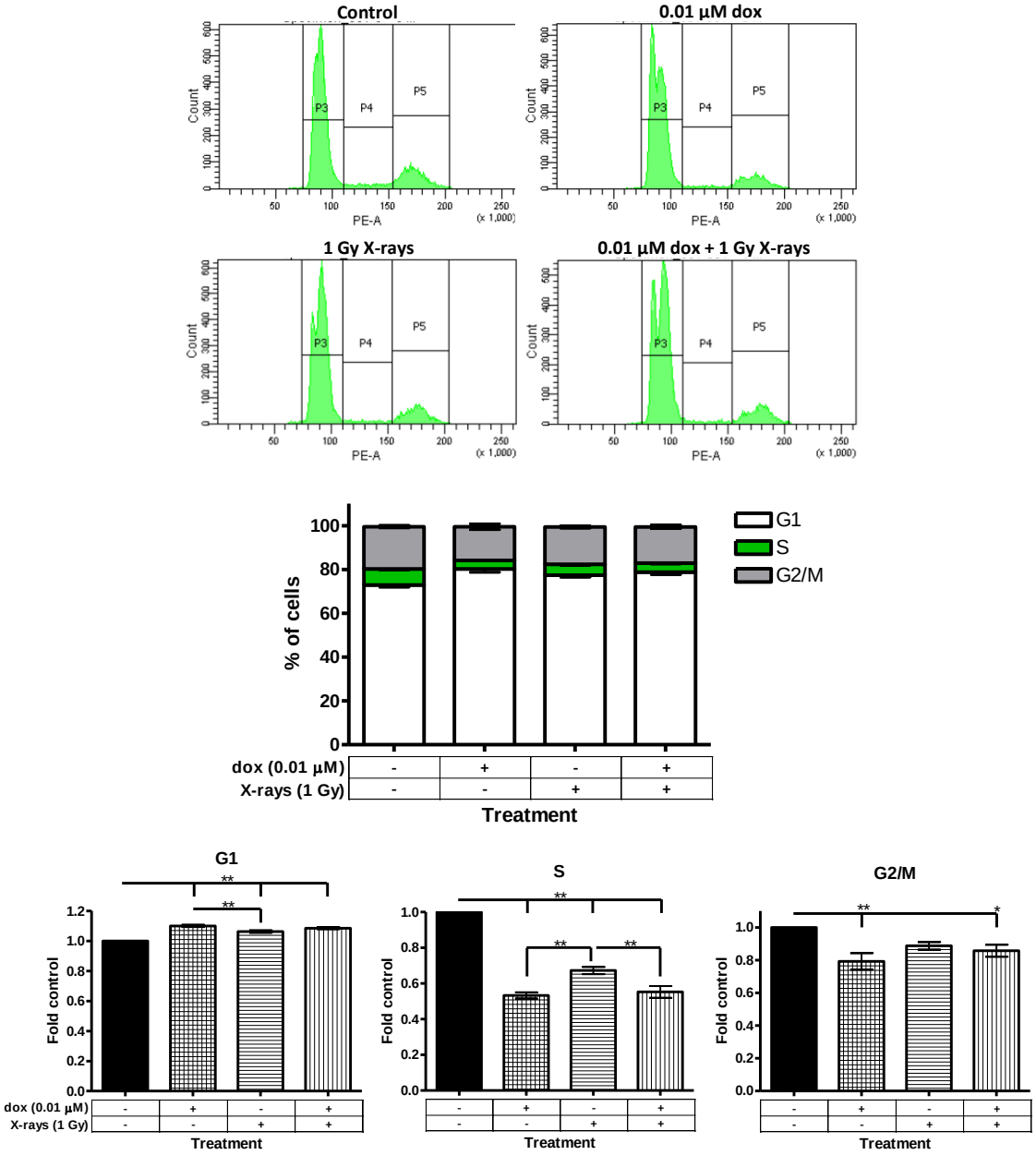

Figure 5.5: Effect of combinatory treatment with doxorubicin (0.01 µM) and X-irradiation (1 Gy) on HCAEC cell cycle profile. Post-combination treatment of HCAECs as described in Figure 5.4, HCAECs were retained during the clonogenic assay and analysed by FACs to determine cell cycle status, as described in section 2.2.7. Intervals P3, P4 and P5 represent cell cycle stages G1, S and G2/M respectively. Values represent mean ± S.E. mean, n=4. *p<0.05 **p<0.01.

5.3 Discussion

Combination anticancer therapy is a strategic method applied clinically to improve cancer cell killing and patient outcome. This chapter explored the effects of doxorubicin and X-rays in combination on endothelial cells of the coronary artery to compare the adverse vascular effects of combination therapy relative to mono-therapy. The scheduling of doxorubicin and X-ray combination treatment is patient-specific. Radiation can be delivered post-chemotherapy, for example, early-stage plasmablastic lymphoma (PLB), a type of diffuse large B-cell lymphoma, has been effectively treated by intense doxorubicin-based chemotherapy and subsequent consolidative external beam radiation therapy (30 to 50 Gy total dose) (Pinnix *et al*., 2016). Zhang *et al*, also reported improved survival of adult stage I/II systemic anaplastic large-cell lymphoma (ALCL) patients administered doxorubicin-containing chemotherapy followed by radiotherapy, patients who displayed a complete response post-chemotherapy were delivered a total dose of 40 Gy in 2 Gy fractions whereas patients with residual disease were treated with 45 to 50 Gy (Zhang *et al*., 2013). Alternatively, chemotherapeutic drugs, such as doxorubicin, can be administered post-radiotherapy but X-rays have been suggested to interfere with intracellular doxorubicin distribution by decreasing the intranuclear pH thus hindering doxorubicin-DNA interactions and altering nuclear and cytoplasmic membrane structures promoting doxorubicin efflux (Chevillard *et al*., 1992). Additionally, radiation recall, typified by acute inflammation localised to a previously irradiated site, is a problem associated with the use of systemic chemotherapeutic drugs post-radiotherapy (Burris and Hurtig, 2010).

Most frequently, doxorubicin and radiation therapy are administered concurrently such as therapy for anaplastic thyroid cancer (ATC). ATC patients receive weekly doxorubicin (10 mg/m^2) administration plus daily radiotherapy treatment, post-2002 patients were administered radiotherapy one times per day, 5 days per week in 1.8 to 2 Gy fractions resulting in a total dose of 70 Gy (Sherman *et al*., 2011). Invasive bladder cancer can also be treated with concurrent doxorubicin (20 mg/m^2) plus hypoACR, an aggressive radiation therapy regime (daily fractions of 3.4 Gy to bladder, total of 15 fractions) (Panteliadou *et al*., 2011). In this chapter, the radiosensitizing properties of doxorubicin were examined therefore endothelial cells were treated with

doxorubicin prior to X-ray exposure. As discussed previously in chapter 3, doxorubicin treatment for 24 hours caused significant arrest of HCAECs in the G2/M phase of the cell cycle, a characteristic of radiosensitizing chemotherapeutic drugs. Chevillard *et al*., have reported the varying outcomes of different doxorubicin and radiation scheduling *in vitro* (Chevillard *et al*., 1992). Using organotypic cultures (i.e. nodules) of A549 human lung carcinoma cells, Chevillard *et al*., found that administration of doxorubicin (0.1 µg/ml) 24 hours before X-irradiation (5 Gy) reduced nodule growth by approximately 80% at day 10 post-treatment (Chevillard *et al*., 1992). Whereas, exposure of cells to X-rays (5 Gy) 24 hours prior to doxorubicin treatment only resulted in an approximate 30% reduction in nodule growth (Chevillard *et al*., 1992), thus demonstrating a greater effect when cells were treated with doxorubicin prior to X-irradiation and showing the importance of the order of combination therapy.

Chevillard *et al*., analysed the pharmacokinetics of doxorubicin during the combined treatment of A549 cells and observed a correlation between drug pharmacokinetics and their experimental findings. Intracellular and intranuclear doxorubicin concentrations remained constant in cells treated with doxorubicin then exposed to X-rays 24 hours later, however exposure of cells to X-irradiation 24 hours prior to doxorubicin significantly diminished drug uptake and retention (Chevillard *et al*., 1992). Primary X-irradiation affects intracellular doxorubicin concentration thus influencing the magnitude of cytotoxicity incurred and it is unlikely that X-irradiation with subsequent, delayed doxorubicin treatment would have an enhanced detrimental effect on endothelial cells. As shown by Chevillard *et al*., doxorubicin concentration was sustained in cells exposed to X-irradiation 24 hours post-doxorubicin treatment, resulting in an enhanced cytotoxic effect when both treatments were used together than independently (Chevillard *et al*., 1992). Similarly, Petznek *et al*., observed improved killing of a feline fibrosarcoma cell line treated with doxorubicin (0.25 µmol) 24 hours prior to X-irradiation (3.5 Gy) rather than 4 hours (Petznek *et al*., 2014). Furthermore, utilising a mouse xenograft model to assess doxorubicin and radiation combinatory effects *in vivo*, Petznek *et al*., found that combination therapy attenuated tumour growth more greatly and improved mice survival relative to mono-therapy (Petznek *et al*., 2014). The median survival of mice treated with doxorubicin or X-irradiation alone

were 66 and 59.5 days respectively however treatment with doxorubicin and two 3.5 Gy doses of X-rays at intervals of 24 hours post-doxorubicin treatment increased median survival to 73 days (Petznek *et al*., 2014). Studies have therefore demonstrated the superior killing of cancer cells using a scheduling method of doxorubicin then X-irradiation but the combinatory effects of this regime on endothelial cells remained to be ascertained.

In this chapter, examining the interactive effects between doxorubicin and X-irradiation on endothelial cell clonogenic survival, 0.005 µM doxorubicin did not enhance inhibition of HCAEC growth caused by radiation (1 Gy). However, a twofold greater concentration of doxorubicin (0.01 µM) displayed additivity with X-irradiation as shown in Figure 5.4. Doxorubicin and ionizing radiation are known to execute greatest DNA damage at differential cell cycle stages, S and G2/M respectively which may account for the additivity between doxorubicin and X-irradiation in combination treatment (Seiwert *et al*., 2007). Nevertheless, synergy between agents is known to be dependent on the concentration/dose of each agent in combination, thus synergy between doxorubicin and radiation with concentrations/doses not examined in this study may occur (Tallarida. 2011). Synergy between doxorubicin and radiation has been reported to arise via two principle mechanisms. Firstly, doxorubicin synchronizes cells in the G2/M phase of the cell cycle; optimum DNA damage in response to radiation occurs during mitosis resulting in synergy between the anticancer therapies (Supiot *et al*., 2005). Additionally, the locality of doxorubicin within the DNA double helix, such as neighbouring a single-stand break induced by radiation, can impede repair of the DNA lesion (Seiwert *et al*., 2007, Supiot et al., 2005). In a study of combinatory-treated Chinese hamster lung fibroblast V97 cells, doxorubicin (1.5 µg/ml before irradiation) prevented the repair of radiation-induced DNA double-stand breaks attributed to the ability of doxorubicin to intercalate within the DNA helix and prevent repair enzymes from recognizing and correcting DNA adducts effectively (Bonner and Lawrence, 1990). Further investigations by Agahee *et al*., comparing the effects of combination therapy and mono-therapy on intracellular signalling intermediates surprisingly discovered that p53 mRNA expression was reduced by 83% in SK3 breast cancer cells treated with doxorubicin (1 µM) 24 hours prior to X-irradiation (1 Gy) relative to doxorubicin treatment only (Agahee *et al*., 2013).

Conversely, mRNA expression of phosphatase and tensin homologue (PTEN), a phosphatase that antagonizes AKT survival pathway signalling was increased in combinatory-treated SK3 cells (Agahee *et al*., 2013). The effects of doxorubicin and radiation on intracellular signalling cascades, resulting in enhanced cell death, is undoubtedly multi-factorial, the JNK pathway may be involved in synergy between doxorubicin and X-irradiation but this has yet to be investigated. Clearly, combinatory treatment with doxorubicin and radiation therapy provides superior therapeutic treatment of tumours but, as demonstrated in this chapter, adverse endothelial cell damage is consequential and there is the potential for synergy between doxorubicin and X-rays during endothelial cell injury.

The combination experiments performed in this chapter were insightful but rudimentary, the nature of drug and radiation interactions can be more comprehensively quantified by the calculation of combination indices (CI). Combination index analysis is applied to examine the interactions between a drug and radiation which are toxic independently and have distinct mechanisms of action (Gorodetsky *et al*., 1998). Survival curves are generated for radiation only, drug only and radiation plus drug. The mathematical equation, **CI = D/Dx + C/Cx + (D/Dx * C/Cx)**, is thereafter used to analyse drug and radiation interactive effects on cell survival and was devised from a method outlined by Chou and Talalay in the 1980s for drug combination studies (Chou and Talalay, 1984). Dx and Cx are a dose/concentration of radiation and drug respectively which reduce survival to a specific level when both are used independently. D and C represent the dose of radiation and concentration of drug respectively which result in the same reduction in survival when both are used in combination (Gorodetsky et al., 1998). CI values less than, equal to or greater than one represent synergistic, additive or antagonistic effects of combination treatment respectively (Gorodetsky et al., 1998). Combination index analysis was used by Gorodetsky *et al*., to study the interactive effects of cisplatin and X-irradiation on murine mammary adenocarcinoma EMT-6 cells (Gorodetsky *et al*., 1998). Pre-treatment of cells with cisplatin (0.16 µg/ml) for 24 hours prior to irradiation (2 Gy) attained a CI of 1.26 indicating a marginally infra-additive (antagonistic) interaction (Gorodetsky *et al*., 1998). The authors proposed that the antagonism was a result of modified cellular oxygenation and intracellular levels of

thiol groups, potentially hindering X-ray-mediated DNA base oxidation and strand breakage (Gorodetsky *et al*., 1998). Furthermore, the combinatory treatment of EMT-6 cells with radiation and subsequent cisplatin increased the number of S phase cells relative to radiation alone, therefore the authors concluded that DNA repairs enzymes which are most active during the S phase of the cell cycle may contribute to the infra-additive effect (Gorodetsky *et al*., 1998). In this chapter, no correlation was observed between cell-cycle re-distribution and the additive interaction between doxorubicin and X-irradiation. Doxorubicin applied in combination with X-irradiation reduced the percentage of S phase cells to the same extent as doxorubicin alone, signifying that the additive interaction between doxorubicin and X-rays is not due to a reduction in DNA repair activity during the S phase of the cell cycle. A greater understanding of the effects of combination treatment on cell cycle progression, with relation to doxorubicin and X-irradiation interactions, is required. Moreover, further experimental work on the combinatory effects of doxorubicin and X-irradiation on endothelial cell survival would have utilised combination index analysis to fully characterise doxorubicin and radiation interactions.

The results in this chapter provide a novel understanding of the combinatory effects of doxorubicin and X-irradiation on endothelial cell survival, an additive detrimental effect on cell survival was observed when both therapies were administered in combination. However this is a very limited investigation and further characterisation is required to identify potential synergy between doxorubicin and X-rays in endothelial cells and the subsequent effect on HCAEC function such as vasodilator properties and barrier function.

Chapter 6:

General discussion

6.1 Overview

The adverse effects of anticancer therapies on the cardiovascular system are well documented in patient studies. Thus, researchers are aiming to define the principal vascular changes during and post-cancer therapy. This thesis aimed to understand the effects of two widely administered treatment modalities for neoplastic disease, X-rays and doxorubicin, on endothelial cells from within the vasculature.

Anticancer agents cause heart failure by damage of cardiac tissue including cardiomyocytes however it is highly probable that injury of vascular endothelial cells by antineoplastic agents can have a consequential effect on the heart promoting cardiac failure (Maney *et al*., 2011). Indeed, vascular endothelial cells are more sensitive to the damaging effects of anticancer agents than endocardial endothelial cells lining the lumen of the heart (Maney *et al*., 2011). Primary porcine endocardial endothelial cells were found to be more resistant to apoptosis induced by the chemotherapeutic drugs doxorubicin, camptothectin (topoisomerase-I inhibitor) and thapsigargin (inhibits sarco/endoplasmic reticulum Ca^{2+}-ATPase (SERCA) pump) compared to human umbilical vein endothelial cells (Maney *et al*., 2011). Employing immortalised endocardial endothelial cells (hTERT-EECs), Maney *et al*., demonstrated that the lack of endocardial endothelial cell death was attributable to resistance against mitochondrial transmembrane potential loss and consequential hindrance of caspase-dependent and caspase-independent apoptosis (Maney *et al*., 2011). More recently, the superior resistance of endocardial endothelial cells relative to vascular endothelial cells was reported to be due to a greater endogenous expression of ATP-binding cassette transporter subfamily G member 2 (ABCG2), critical for maintaining cellular homeostasis including expulsion of anticancer drugs (Ajithkumar *et al*., 2016). Furthermore, the resistance of primary cardiac endothelial cells, isolated from the ventricles of 4 to 6-week old mice, to X-irradiation was found to be mediated by p53 which induced mitotic arrest of the irradiated cardiac endothelial cells, preventing radiation-triggered mitotic catastrophe and death (Lee *et al*., 2012). It is evident that endocardial cells are more protected against the damaging effects of anticancer therapies than endothelial cells from the vasculature. Therefore, it was important to investigate the potential role of vascular endothelium dysfunction in therapy-induced cardiovascular disease.

As demonstrated in this thesis, both X-rays and doxorubicin independently had an adverse effect on the survival of human coronary artery endothelial cells. Low doses of doxorubicin were cytostatic whereas high doxorubicin concentrations were cytotoxic, as discussed in chapter 3. This phenomenon has also been observed in NIH 3T3 fibroblasts treated with the topoisomerase-II inhibitor danorubicin (Stein *et al*., 2003). Low concentrations of danorubicin (up to 80 ng/ml) were cytostatic promoting reversible G2/M arrest while high danorubicin concentrations (above 160 ng/ml) induced irreversible arrest in the S or G1 phases and cell death (Stein *et al*., 2003). It is noteworthy that doxorubicin at low concentrations provoked G2/M arrest of HCAECs which serves as a radiosensitizing property of chemotherapeutic drugs. Following radiotherapy alone for primary tumours, local failure rates are high therefore chemotherapeutic drugs are administered to enhance the response in the irradiated volume (Nishimura. 2004). However, the molecular targets of doxorubicin, DNA and topoisomerase II, are ubiquitously expressed resulting in an enhancement of radiation damage in normal tissues too (Agahee *et al*., 2013, Brunner. 2016). A therapeutic benefit is only acquired during chemoradiotherapy when enhancement of the tumour response is superior to the enhancement of damage to normal tissue (Brunner. 2016). Spatial co-operation between radiotherapy and chemotherapeutic drugs is an additional means to improve cancer control rates, no interaction between the radiation and drug is needed but both require differential toxicities to enable both modalities to be administered at effective doses (Nishimura. 2004). As demonstrated in chapter 5, doxorubicin and X-irradiation displayed additive toxicity when used in combination to treat human coronary artery endothelial cells. This indicates that doxorubicin and X-rays used in combination at effective doses would increase endothelial cell cytotoxicity. The lack of synergy between doxorubicin and X-irradiation on endothelial cells is encouraging as it insinuates that radiation damage is not heightened by doxorubicin beyond the additive toxicity of both agents, whether a higher doxorubicin concentration would promote radiation and drug synergy and an enhanced toxic effect needs to be established.

Considering the correlation between the toxic effects of doxorubicin and X-rays on vascular endothelial cells and cardiovascular disease in treated patients, it is essential to identify pharmacological targets for drug-directed alleviation of therapy-mediated

cardiovascular disease. This thesis focused on JNK, a well-established regulator of cellular responses to stress. Indeed, JNK appears to be moderately activated in endothelial cells exposed to doxorubicin, JNK was found to have a minor contributory role in G2/M arrest induced by low-dose doxorubicin and may be involved in doxorubicin-mediated HCAEC death with higher drug concentrations, as discussed in chapter 3. Meanwhile JNK responded poorly upon X-irradiation, as demonstrated in chapter 4. Hence, JNK is not a prime target for pharmacological intervention and aberration of vascular damage.

While interfering with JNK activity may not be therapeutically beneficial to prevent therapy-mediated injury to the vasculature, other MAPKs may serve as useful pharmacological targets. Spallarossa *et al*., identified p38 MAPK as a preferred target to prevent doxorubicin-mediated endothelial cell injury (Spallarossa *et al*., 2010). The authors of this study found that p38 induced senescence, identified by increased SA-β-galactosidase and $p16^{INK4A}$ expression, and cytoskeletal remodelling of cord blood endothelial progenitor cells (EPCs) exposed to low-dose doxorubicin (0.25 μM) (Spallarossa *et al*., 2010). However, JNK antagonized p38-mediated senescence and promoted survival of doxorubicin-treated EPCs, thus p38 inhibition over JNK would be preferable to prevent doxorubicin-mediated damage of EPCs (Spallarossa *et al*., 2010). Indeed, lentiviral knockdown of p38 in the cultured human endothelial cell line E.A.hy926 (EC^{DNp38}) or co-treatment with p38 pharmacological inhibitor SB203580 reduced caspase-3 activation and doxorubicin-mediated cytotoxicity (Grethe *et al*., 2006). Apoptosis induced by doxorubicin was found to be a result of p38-mediated inhibition of Bad phosphorylation, surprisingly mediated by PI3K/Akt, plus down-regulation of pro-survival Bcl-xl (Grethe *et al*., 2006). Grethe *et al*., also reported that ERK had a pro-apoptotic role in doxorubicin-treated wild-type EA.hy926 cells, ERK pharmacological inhibition decreased doxorubicin-triggered caspase-3 activity and cell death by 73% and 49% respectively (Grethe *et al*., 2006). ERK has also been implicated in the aberration of endothelial barrier function in H_2O_2-treated HUVECs, ERK was involved in loss of occludin at cellular junctions with consequential increased endothelium permeability, promoting a pro-atherosclerotic setting (Kevil *et al*., 2000). Nevertheless, due the substantial experimental evidence for a pro-survival role of ERK in response to chemotherapeutics and the role of ERK in cellular

radioresistance, ERK would not be an effective target to lessen therapy-induced endothelium damage (Munshi and Ramesh, 2013). Clearly targeting MAPK would be challenging due to the multifaceted nature of MAPK responses to anticancer therapies, targeting a single MAPK may not be sufficiently effective to prevent vascular damage. An alternative approach would be to employ antioxidants such as, vitamin E or N-acetylcysteine (NAC), because oxidative stress is key for intracellular damage and MAPK pathway activation post-cancer therapy (Mangge *et al*., 2014, Morbidell *et al*., 2016). However, inhibition of oxidative stress is likely to impair the cancer-killing efficacy of doxorubicin and X-rays (Morbidell *et al*., 2016). Thus, patients should have a pre-existing risk of cardiovascular disease to justify drug intervention.

The concomitant use of a drug to prevent cardiovascular damage during anticancer therapy is controversial due to the potential adverse effects of the intervening drug itself (Morbidell *et al*., 2016). A more radical option would be to switch to a wholly different treatment in individuals at risk of cardiovascular disease but changing to a different therapy strategy is not always feasible due to the nature of the cancer being treated. Hence, liposome-encapsulated formulations of doxorubicin have been prepared and trialled in cancer patients (Gabizon *et al*., 2003). Doxorubicin is entrapped within a liposome to aid drug delivery to the tumour site and reduce normal tissue toxicity (Gabizon *et al*., 2003). Liposomes harbouring doxorubicin extravasate across the leaky tumour vasculature into the interstitial fluid surrounding tumour tissue; normal vessels possess less permeations than tumour vessels thus liposomes are maintained within the intravascular space (Davies *et al*., 2004, Gabizon *et al*., 2003). This promotes selective localization of liposomal doxorubicin within tumour tissue and reduced doxorubicin-mediated toxicity to normal tissue (Davies *et al*., 2004). Ren *et al*., found that intratumoral injection of liposomal doxorubicin (20 mg/kg) in murine H22-hepatoma-bearing mice increased the tumour mean residence time 1.3-fold relative to free doxorubicin (Ren *et al*., 2014). Commercial liposomal doxorubicin formulations used clinically (trade names Doxil and Caelyx in the US and Europe respectively) are coated with polyethylene glycol (PEG), a synthetic hydrophilic polymer, to impair uptake by cells of the reticulo-endothelial system, thus extending the half-life of liposomal doxorubicin to approximately 45 hours in the human circulation (Davies *et al*., 2004). This enables prolonged tumour uptake plus liposomes

exhibit a larger surface area than free doxorubicin thus hindering drug clearance (Panteliadou *et al*., 2011). Pegylated liposomes are rarely endocytosed by tumour cells thus doxorubicin is released from the liposomes, mediated by phospholipases, into the interstitial fluid where it can target tumour cells (Gabizon *et al*., 2003). Kaushal *et al*., performed a comparative study on the toxic effects of equimolar concentrations (0.5 μM) of Doxil and free doxorubicin on human coronary artery endothelial cells (Kaushal *et al*., 2004[2]). Several observations were described in this study: Doxil reduced HCAEC viability to a lesser extent than free doxorubicin after 72 hours (85 and 45% viable cells respectively), HCAECs treated with Doxil did not stain positive for DNA fragmentation using TUNEL staining but 25.21% of cells were TUNEL positive 24 hours post-free doxorubicin treatment, Doxil did not activate caspase-3 activity as greatly as free doxorubicin and did not initiate proteolytic cleavage of caspase-3 whereas free doxorubicin promoted the formation of caspase-3 17 kDa and 12 kDa sub-units which form an active complex (Kaushal *et al*., 2004[2]). The authors distinguished that Doxil conserves anti-apoptotic Mcl-1 expression in HACECs, defending HCAECs from death (Kaushal *et al*., 2004[2]). Thus, Doxil is a better tool for doxorubicin delivery to reduce endothelial damage.

The effects of radiation used in combination with liposomal doxorubicin have also been researched. Interestingly, using confocal laser scanning microscopy (CLSM) Davies *et al*., identified that radiation promoted uptake of doxorubicin released from liposomes into the central region of the tumour (Davies *et al*., 2004). Caelyx (16 mg/kg) administered alone to athymic mice bearing human osteosarcoma xenografts was found to accumulate primarily at the periphery of the tumour, however when irradiation was delivered 24 hours post-Caelyx treatment (8 Gy or 3 x 3.6 Gy fractions) a greater distribution of doxorubicin was found around vessels within the centre of the tumour (Davies *et al*., 2004). Panteliadou *et al*., reported that 3-year survival rates of bladder cancer patients (T2-T4 stage) improved significantly when patients received concurrent pelvic hypoARC (14 x 2.7 Gy to the pelvis and 15 x 3.4 Gy to the bladder) and Caeylex (20 mg/m2 every 2 weeks for 3 cycles) compared to hypoARC alone, 72.1% survival versus 58.7% survival respectively (Panteliadou *et al*., 2011). Therefore, there is clinical evidence for the success of liposomal doxorubicin and radiation combinations in cancer patients. The findings in this thesis verify the need

for the innovation and use of new doxorubicin formulations, in combination with radiation therapy, to prevent therapy-related vascular disease.

6.2 Future work

Having examined the effects of doxorubicin and X-rays independently or in combination on HCAECs and HUVECs, investigations beyond single cell-type cultures and therapy regimes more clinically relevant are required.

This thesis addressed the effects of single dose X-rays, alone or in combination with doxorubicin, on endothelial cell function but fractionated radiotherapy is often implemented for radiotherapy treatment of cancer patients. Radiation therapy used for the treatment of breast and lung cancer is commonly delivered to the thoracic area in around 2 Gy fractions resulting in a cumulative dose of between 30 and 70 Gy at the cessation of radiotherapy treatment (Panganiban *et al*., 2013, Stewart *et al*., 2013). Despite the effectiveness of single, high dose radiotherapy for the induction of tumour death, fractionated radiotherapy generates less normal tissue damage, such as injury to the lungs or remodelling of fibrotic tissue in the heart (Panganiban *et al*., 2013). Cervelli *et al*., performed a comparative study of the effects of single low-dose X-irradiation (0.125, 0.25 and 0.5 Gy) and fractionated doses (2 x 0.125 Gy, 2x 0.25 Gy) on HUVEC function (Cervelli *et al*., 2014). Single dose X-irradiation increased ROS generation dose-dependently but when HUVECs were exposed to fractionated doses, ROS generation was not increased relative to the respective single doses (Cervelli *et al*., 2014). The authors concluded that this was due to the ability of HUVECs to re-establish their physiological redox status during the 24-hour period between each fraction (Cervelli *et al*., 2014). However, ICAM-1 surface and mRNA expression was increased more greatly in HUVECs exposed to fractionated doses than single doses and significantly increased adhesion of human polymorphonuclear leukocytes (PMN) to HUVECs was observed when cells were exposed to fractionated doses compared to single doses (Cervelli *et al*., 2014). This suggests that fractionated therapy has the potential to amplify pro-atherosclerotic events at the vessel wall. Investigations are therefore required to establish the effects of fractionated radiation therapy on HCAEC function and identify the interactions between fractionated X-ray doses and

doxorubicin to elucidate the effect of more clinically practiced therapy regimes on coronary artery damage.

Endothelial cells reside at the surface of the vascular wall but are part of a dynamic vessel structure comprising of macrophages and smooth muscle cells. Cell-cell communication is a key feature of vascular remodelling post-injury (Milliat *et al*., 2006). This thesis did not explore the co-operation between endothelial cells and macrophages or vascular smooth muscle cells (VSMCs) post-irradiation or drug treatment, this is a key issue that should be investigated. Smooth muscle cells and endothelial cells are known to interact via myoendothelial junctions, superoxide anions generated from VSMCs diffuse into endothelial cells resulting in eNOS uncoupling and reduced NO expression. This results in attenuated NO-mediated control of vascular tone and contributes to the pathogenesis of pulmonary hypertension (Gao *et al*., 2016). During hypertension, endothelial cells can influence VSMCs via paracrine signalling, ET-1 released from endothelial cells binds to endothelin receptors, chiefly via the endothelin A receptor (ET_A), on smooth muscle cells causing elevated intracellular Ca^{2+} concentration and resultant vasoconstriction (Gao *et al*., 2016). Vascular smooth muscle proliferation, migration and differentiation is vital for remodelling of the vascular wall during atherogenesis (Milliat *et al*., 2006). Milliat *et al*., discovered that irradiated (^{137}Cs) dermal human microvascular endothelial cells promoted aortic human smooth muscle cells to display a fibrogenic phenotype using an *in vitro* co-culture transwell system (Milliat *et al*., 2006). In the presence of irradiated endothelial cells, irradiated VSMCs displayed increased mRNA expression of connective tissue growth factor (CTGF), a profibrogenic cytokine which enhances TGF-β1 receptor binding, and plasminogen activator inhibitor type 1 (PAI-1), which hinders fibrinolysis and matrix degradation by inhibition of plasmin-dependent activation of matrix metalloproteinases (MMPs) (Milliat *et al*., 2006). Likewise, co-culture with irradiated endothelial cells increased mRNA expression of collagen type 1 (COL1A2) and type 3 (COL3A1) in vascular smooth muscle cells contributing to a profibrogenic phenotype (Milliat *et al*., 2006). This was indeed due to co-culture with irradiated endothelial cells as VSMC irradiated alone did not display changes in the target genes examined; endothelial cells appear to release paracrine factors which influence the intracellular molecular machinery of VSMC during radiation-mediated

vascular injury (Milliat *et al*., 2006). The cross-talk between VSMC/macrophages and endothelial cells requires exploration to determine whether the response of endothelial cells to X-irradiation and doxorubicin would differ in a complex cell system.

The release of nutrient-rich exosomes from cells and their influence on the function of other cells is an area of scientific research gaining significant interest. In the field of oncology, experimental studies investigating bystander signalling between cancer cells have gathered increasing attention. Various studies have observed that irradiation of cells has elicited a damaging response in neighbouring cells which have not been targeted with radiation. This has been termed a 'bystander response'. In addition to ionizing radiation, other therapeutic agents utilised in cancer treatment are able to initiate a bystander effect in nearby cells such as photodynamic therapy and chemotherapeutic drugs (Prise and O'Sullivan, 2009). Bystander responses have not only been detected in cells adjoining irradiated cells but also cells a significant distance away from radiation-exposed cells (Chaudhry. 2006). Bystander signals are either transported through gap junctions between adjacent cells or factors are expelled from irradiated cells into the extracellular environment (Rzeszowska-Wolny *et al*., 2009). The latter mechanism was initially identified in 1922 when lymphoid cells were incubated with serum from animals exposed to radiation. This experiment found that lymphoid cell growth was provoked by factors found in the serum of animals exposed to radiation but growth was not stimulated by serum from non-irradiated animals (Murphy *et al*., 1922). Messengers released from irradiated cells are able to travel and target non-irradiated bystander cells, this is identified as an abscopal or out-of-field bystander effect (Prise and O'Sullivan, 2009). This may be responsible for the development of atherosclerotic plaques in vessels a significant distance from the cancer-treated site.

Intranuclear bystander damage was demonstrated by Khan *et al*., as localised irradiation of rat lung caused an increased presence of micronuclei, a marker of non-rejoined DNA damage, in lung regions not exposed to radiation (Khan *et al*., 1998). The principal characteristics of the harmful bystander response include damage to DNA structure and DNA mutations, altered gene expression and ultimately cell death (Prise and O'Sullivan, 2009). Yang *et al*., observed that X-irradiation of normal human skin fibroblasts with 0.1 Gy resulted in a 2-fold elevation in micronucleus formation

in bystander fibroblast cells. This study also detected a 2-fold increase in γ-H2AX foci formation, an indicator of DNA double-strand breaks in bystander cells (Yang *et al*., 2005). Hence there is much evidence detailing a harmful, DNA-damaging bystander effect in non-irradiated cells.

Several methods can be undertaken to assess bystander effects. A simple technique involves the transfer of media from irradiated cells, termed 'conditioned media' which contains any factors released by the irradiated cells, to non-treated cells (bystander cells) (Rzeszowska-Wolny *et al*., 2009). Bystander cells are incubated with the conditioned media and desired cellular changes analysed. This method was trialled to observe bystander signalling between radiosensitive UVW cells, as depicted in Figure 6.1, and MCF-7 cells, as illustrated in Figure 6.2. As shown in Figures 6.1 and 6.2 the media-transfer technique successfully demonstrated a bystander effect, a dose-dependent reduction in clonogenic survival of non-irradiated UVW cells and MCF-7 cells was observed. The aim was to determine whether irradiated breast cancer cells (MCF-7) would cause bystander damage of endothelial cells (HCAECs) contributing to vascular damage and coronary artery disease. This setup models possible bystander effects post-cancer therapy as breast cancer tissue treated with radiotherapy may cause bystander injury of local or distant vessels. Unfortunately, this area of research was not able to be explored but should be investigated in the future to provide an insight into bystander damage of endothelial cells in response to cancer therapy.

Having attained an understanding of the effects of X-irradiation and doxorubicin on endothelial cells *in vitro*, as set-out in this thesis, it is crucial to establish whether these findings are corroborated *in vivo*. No published studies have yet detailed the combinatory effects of doxorubicin and X-irradiation on the vasculature in an *in vivo* setting. Once a greater understanding of how cell-cell interactions and bystander signalling affects endothelial dysfunction post-cancer therapy, these studies should also be extended to *in vivo* experiments.

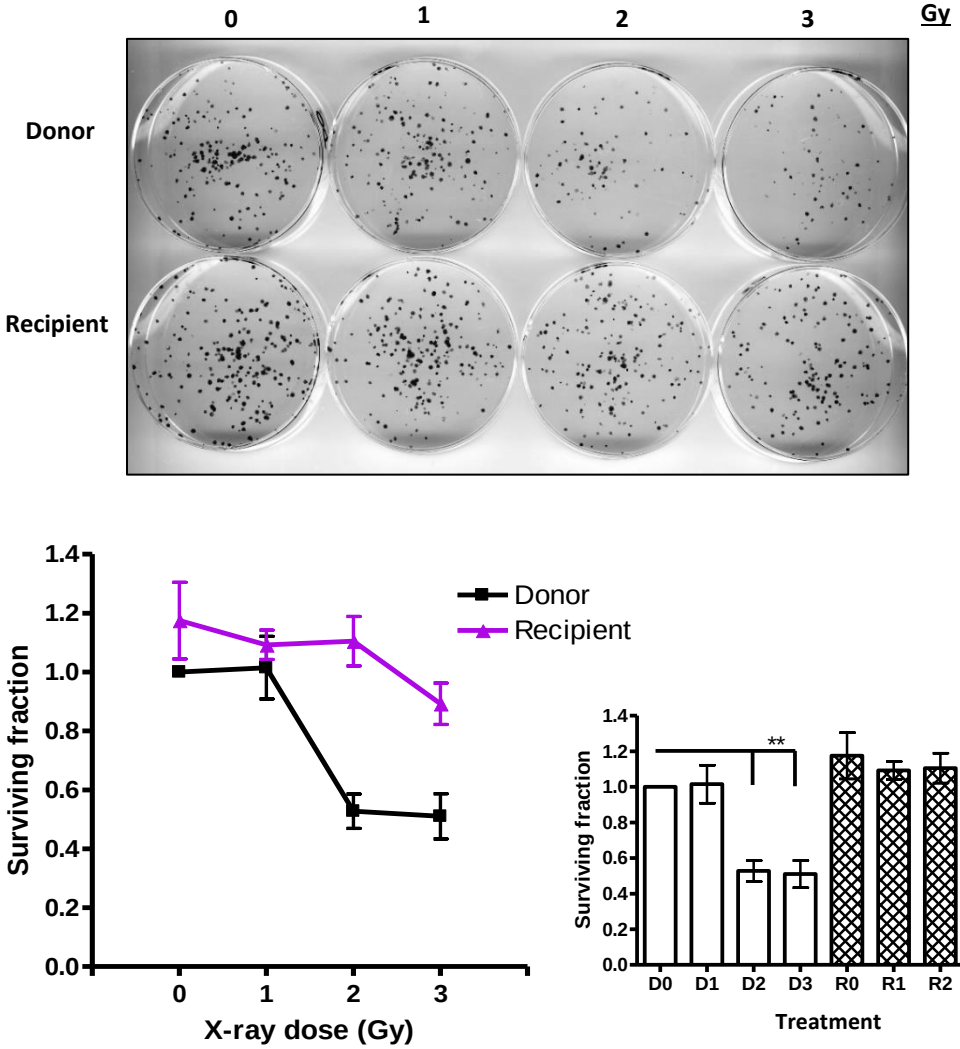

Figure 6.1: Bystander-mediated inhibition of UVW colony formation. The media from X-irradiated UVW cells (Donor, D) was transferred to non-irradiated UVW cells (Recipient, R) and colony formation assessed as outlined in section 2.2.10. Values represent mean ± S.E. mean, n=4. **p<0.01 compared to control (0 Gy).

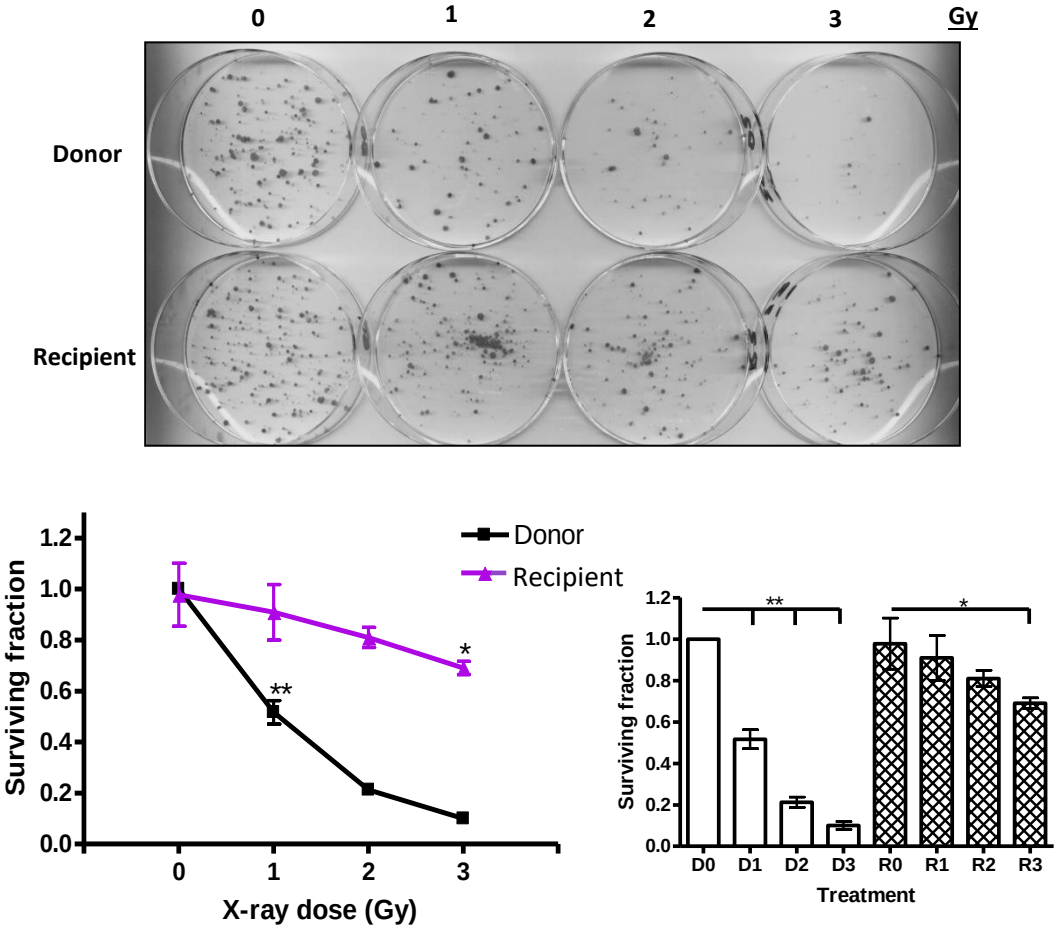

Figure 6.2: Inhibition of MCF-7 colony formation due to by bystander signalling. The conditioned media from X-irradiated MCF-7 cells (Donor, D) was transferred to non-irradiated MCF-7 cells (Recipient, R), following 24 hours incubation a colony assay was performed as described in section 2.2.10. Values show mean ± S.E. mean, n=4. *p<0.05, **p<0.01 compared to control (0 Gy).

6.3 Concluding remarks

There is clear clinical evidence for an increased risk of cardiovascular disease in patients previously administered radiation therapy or chemotherapeutic drugs for cancer. This thesis has presented findings implicating endothelial cell dysfunction in vascular damage caused by X-rays and doxorubicin, hence stressing the contribution of damage to the vasculature in therapy-mediated cardiovascular disease. Although cell-based assays were employed throughout this thesis providing an insight into acute cellular events post-therapy, acute damage to the vasculature fosters chronic atherosclerosis and cardiovascular-associated morbidity. Consideration should therefore be taken when patients require X-irradiation or doxorubicin administration as anticancer therapy, and the appropriate treatment and associated risks should be deliberated. This is particularly true when administration of both therapies in combination is required due to the increased endothelial cell dysfunction and consequential vascular damage relative to single therapy, as outlined in this thesis. When X-rays and/or doxorubicin are the chosen treatment modalities for cancer eradication, the patient's cardiovascular health should be monitored post-cancer therapy to prevent late-onset cardiovascular disease-related death.

Chapter 7:

References

Adams, M. J., Lipsitz, S. R., Colan, S. D., Tarbell, N. J., Treves, S. T., Diller, L., Greenbaum, N., Mauch, P. and Lipshultz, S. E. (2004). Cardiovascular status in long-term survivors of Hodgkin's disease treated with chest radiotherapy. *J Clini Oncol.* **22**(15), 3139–3148.

Agahee, F., Islamian, J. P., Baradaran, B., Mesbahi, A., Mohammadzadeh, M. and Jafarabadi, M. A. (2013). Enhancing the Effects of Low Dose Doxorubicin Treatment by the Radiation in T47D and SKBR3 Breast Cancer Cells. *J Breast Cancer*. **16**(2), 164-170.

Ajithkumar, G. S., Vinitha, A., Binil Raj, S. S. and Kartha, C. C. (2016). Drug Resistance of Endocardial Endothelial Cells is Related to Higher Endogenous ABCG2. *Cardiovasc Toxicol.* **16**(4), 390–405.

Al-Mutairi, M., Al-Harthi, S., Cadalbert, L., and Plevin, R. (2010). Over-expression of mitogen-activated protein kinase phosphatase-2 enhances adhesion molecule expression and protects against apoptosis in human endothelial cells. *Br J Pharmacol,* **161**(4), 782–798.

Amini, N., Boyle, J. J., Moers, B., Warboys, C. M., Malik, T. H., Zakkar, M., Francis, S. E., Mason, J. C., Haskard, D. O. and Evans, P. C. (2014). Requirement of JNK1 for endothelial cell injury in atherogenesis. *Atherosclerosis.* **235**(2), 613–8.

Barjaktarovic, Z., Anastasov, N., Azimzadeh, O., Sriharshan, A., Sarioglu, H., Ueffing, M., Tammio, H., Hakanen, A., Leszczynski, D., Atkinson, M. J. and Tapio, S. (2013). Integrative proteomic and microRNA analysis of primary human coronary artery endothelial cells exposed to low-dose gamma radiation. *Radiat Environ Biophys*. **52**(1), 87–98.

Bar-on, O., Shapira, M. and Hershko, D. D. (2007). Differential effects of doxorubicin treatment on cell cycle arrest and Skp2 expression in breast cancer cells. *Anticancer Drugs*. **18**(10), 1113–1121.

Barpe, D. R., Rosa, D. D. and Froehlich, P. E. (2010). Pharmacokinetic evaluation of doxorubicin plasma levels in normal and overweight patients with breast cancer and simulation of dose adjustment by different indexes of body mass. *Eur J Pharm Sci.* **41**(3-4), 458–463.

Bartelink, H., Schellens, J. H. M. and Verheij, M. (2002). The combined use of radiotherapy and chemotherapy in the treatment of solid tumours. *Eur J Cancer*. **38**(2), 216–222.

Baker, J. E., Moulder, J. E. and Hopewell, J. W. (2011). Radiation as a Risk Factor for Cardiovascular Disease. *Antioxid Redox Signal*. **15**(7), 1945-1956.

Barpe, D. R., Rosa, D. D. and Froehlich, P. E. (2010). Pharmacokinetic evaluation of doxorubicin plasma levels in normal and overweight patients with breast cancer and simulation of dose adjustment by different indexes of body mass. *Eur J Pharm Sci*. **41**(3-4), 458-463.

Becker-Schiebe, M., Stockhammer, M., Hoffmann, W., Wetzel, F. and Franz, H. (2016). Does mean heart dose sufficiently reflect coronary artery exposure in left-sided breast cancer radiotherapy? Influence of respiratory gating. *Strahlenther Onkol*. **192**(9), 624–631.

Belli, J., A. and Piro, A., J. (1977). The Interaction between Radiation and Adriamycin Damage in Mammalian Cells. *Cancer Res.* **37**(6), 1624-1630.

Benjamin, E. J., Blaha, M. J., Chiuve, S. E., Cushman, M., Das, S. R., Deo, R., de Ferranti, S. D., Floyd. J., Fornage, M., Gillespie, C., Isasi, C.R., Jiménez, M. C., Jordan, L. C., Judd, S. E., Lackland, D., Lichtman, J. H., Lisabeth, L., Liu, S., Longenecker, C. T., Mackey, R. H., Matsushita, K., Mozaffarian, D., Mussolino, M. E., Nasir, K., Neumar, R. W., Palaniappan, L., Pandey, D. K., Thiagarajan, R. R., Reeves, M. J., Ritchey, M., Rodriguez, C. J., Roth, G. A., Rosamond, W. D., Sasson, C., Towfighi, A., Tsao, C. W., Turner, M. B., Virani, S. S., Voeks, J. H., Willey, J. Z., Wilkins, J. T., Wu, J. H., Alger, H. M., Wong, S. S. and Muntner, P. (2017). Heart Disease and Stroke Statistics-2017 Update: A Report From the American Heart Association. *Circulation*. **135**(10), e146-e603

Bennett, B. L., Sasaki, D. T., Murray, B. W., O'Leary, E. C., Sakata, S. T., Xu, W., Leisten, J. C., Motiwala, A., Pierce, S., Satoh, Y., Bhagwat, S. S., Manning, A.M. and Anderson, D. W. (2001). SP600125, an anthrapyrazolone inhibitor of Jun N-terminal kinase. *Proct Natl Acad Sci U S A.* **98**(24), 13681–13686.

Brenner, D. J. and Hall, E. J. (2007). Computed tomography--an increasing source of radiation exposure. *N Engl J Med.* **357**(22), 2277–2284.

Bode, A. M. and Dong, Z. (2007). The Functional Contrariety of JNK. *Mol Carcinog*. **46**(8), 591-598.

Bonner, J. A. and Lawrence, T. S. (1990). Doxorubicin decreases the repair of radiation-induced DNA damage. *Int J Radiat Biol*. **57**(1), 55-64.

Bogoyevitch, M. A. and Kobe, B. (2006). Uses for JNK: The Many and Varied Substrates of the c-Jun N-terminal Kinases. *Microbiol Mol Biol Rev*. **70**(4), 1061-1095.

Borghini, A., Gianicolo, E. A. L., Picano, E. and Andreassi, M. G. (2013). Ionizing radiation and atherosclerosis: Current knowledge and future challenges. *Atherosclerosis*. **230**(1), 40-47.

Brouwer, C. A., Postma, A., Hooimeijer, H. L., Smit, A. J., Vonk, J. M., van den Berg, M. P., Dolsma, W. V., Lefrandt, J. D., Bink-Boelkens, M. T., Zwart, N., de Vries, E. G., Tissing, W. J. and Gietema, J. A. (2013). Endothelial Damage in Long-Term Survivors of Childhood Cancer. *J Clin Oncol.* **31**(31), 3906-3913.

Boyd, M., Ross, S. C., Dorrens, J., Fullerton, N. E., Tan, K. W., Zalutsky, M. R. and Mairs, R. J. (2006). Radiation-induced biologic bystander effect elicited in vitro by targeted radiopharmaceuticals labeled with alpha - beta - and auger electron – emitting radionuclides. *J Nucl Med*. **47**(6), 1007–1015.

Bozulic, L., Surucu, B., Hynx, D. and Hemmings, B. A. (2008). PKBα/Akt1 Acts Downstream of DNA-PK in the DNA Double-Strand Break Response and Promotes Survival. *Mol Cell.* **30**(2), 203-213.

Brantley-Finley, C., Lyle, C. S., Du, L., Goodwin, M. E., Hall, T., Szwedo, D., Kaushal, G. P. and Chambers, T. C. (2003). The JNK, ERK and p53 pathways play distinct roles in apoptosis mediated by the antitumour agents vinblastine, doxorubicin, and etoposide. *Biochem Pharmacol.* **66**(3), 459-469.

Bravatà, V., Minafra, L., Russo, G., Forte, G. I., Cammarata, F. P., Ripamonti, M., Casarino, C., Augello, G., Costantini, F., Barbieri, G., Messa, C. and Gilardi, M. C. (2015). High-dose Ionizing Radiation Regulates Gene Expression Changes in the MCF7 Breast Cancer Cell Line. *Anticancer Res*. **35**(5), 2577–2591.

Brunner, T. B. (2016). The rationale of combined radiotherapy and chemotherapy - Joint action of Castor and Pollux. *Best Pract Res Clin Gastroenterol.* **30**(4), 515–528.

Bruynzeel, A. M., Abou El Hassan, M. A., Torun, E., Bast, A., van der Vijgh, W. J. and Kruyt, F. A. (2007). Caspase-dependent and -independent suppression of apoptosis by monoHER in Doxorubicin treated cells. *Br J Cancer*. **96**(3), 450–456.

Buch, K., Peters, T., Nawroth, T., Sänger, M., Schmidberger, H. and Langguth, P. (2012). Determination of cell survival after irradiation via clonogenic assay versus multiple MTT Assay - A comparative study. *Radiat Oncol*. **7**:1.

Bulavin, D. V., Higashimoto, Y., Popoff, I. J., Gaarde, W. A., Basrur, V., Potapova, O., Apella, E. and Fornace Jr, A. J. (2001). Initiation of a G2/M checkpoint after ultraviolet radiation requires p38 kinase. *Nature*. **411**(6833), 102-107.

Burris, H. A. 3rd. and Hurtig, J. (2010). Radiation Recall with Anticancer Agents. *Oncologist*. **15**(11), 1227–1237.

Byfield, J. E., Lee, Y. C. and Tu, L. (1977). Molecular interactions between Adriamycin and x-ray damage in mammalian tumour cells. *Int J Cancer*. **19**(2), 186-193.

Cantoni, O., Sestili, P. and Cattabeni, F. (1985). Adriamycin does not affect the repair of X-ray induced DNA single strand breaks. *Cancer Lett.* **27**(2), 215-219.

Carvalho, F. S., Burgeiro, A., Garcia, R., Moreno, A., Carvalho, R. A. and Oliveira, P. J. (2014). Doxorubicin-Induced Cardiotoxicity: From Bioenergetic Failure and Cell Death to Cardiomyopathy. *Med Res Rev*. **34**(1), 106-135.

Castedo, M., Perfettini, J., Roumier, T., Andreau, K., Medema, R. and Kroemer, G. (2004). Cell death by mitotic catastrophe: a molecular definition. *Oncogene*. **23**(16), 2825–2837.

Cervelli, T., Panetta, D., Narvarra, T., Andreassi, M. G., Basta, G., Galli, A., Salvadori, P. A., Picano, E. and Del Turco, S. (2014). Effect sof single and fractionated low-dose irradiation on vascular endothelial cells. *Atherosclerosis.* **235**(2), 510-518.

Chang, W. T., Li, J., Huang, H. H., Liu, H., Han, M., Ramachandran, S., Li, C. Q., Sharp, W. W., Hamann, K. J., Yuan, C. S., Hoek, T. L. V. and Shao, Z. H. (2011). Baicalein Protects Against Doxorubicin-Induced Cardiotoxicity by Attenuation of Mitochondrial Oxidant Injury and JNK Activation. *J Cell Biochem*. **112**(10), 2873-2881.

Chaudhry, M. A. (2006). Bystander effect: Biological endpoints and microarray analysis. *Mutat Res*. **597**, 98-112.

Chaudhury, H., Zakkar, M., Boyle, J., Cuhlmann, S., van der Heiden, K., Luong, L., A., Davis, J., Platt, A., Mason, J. C., Krams, R., Haskard, D. O., Clark, A. R. and Evans, P. C. (2010). c-Jun N-terminal kinase primes endothelial cells at atheroprone sites for apoptosis. *Arterioscler. Thromb. Vasc. Biol.* **30**(3), 546–53.

Chen, Y., Wang, X.,Templeton, D., Davis, R. J. and Tan, T. (1996). The Role of c-Jun N-terminal Kinase in Apoptosis Induced by Ultraviolet C and γ Radiation: Duration of JNK Activation May Determine Cell Death and Proliferation. *J Biol Chem.* **271**(50), 31929-31936.

Chen, Y. L., Tsai, Y. T., Lee, C. Y., Lee, C. H., Chen, C. Y., Liu, C. M., Chen, J. J., Loh, S. H. and Tsai, C. S. (2014). Urotensin II Inhibits Doxorubicin-Induced Human Umbilical Vein Endothelial Cell Death by Modulating ATF Expression and via the ERK and Akt Pathway. *PLos One*. **9**(9), e106812.

Cheng, X., Bennett, R. L., Liu, X., Byrne, M. and Stratford May, W. (2013). PKR negatively regulates leukemia progression in association with PP2A activation, Bcl-2 inhibition and increased apoptosis. *Blood Cancer J*. **3**, e144.

Chieng, C. K. and Say, Y. (2015). Cellular prion protein contributes to LS 174T colon cancer cell carcinogenesis by increasing invasiveness and resistance against doxorubicin-induced apoptosis. *Tumour Biol*. **36**(10). 8107–8120.

Chevillard, S., Philippe, V., Campana, F., Bastian, G. and Coppey, J. (1992). Cytotoxic effects and pharmacokinetic analysis of combined adriamycin and X-ray treatments in human organtypic cell cultures. *Anticancer Drugs*. **3**(2), 133-137.

Chorna, I., Bilyy, R., Datsyuk, L. and Stoika, R. (2004). Comparative study of human breast carcinoma MCF-7 cells differing in their resistance to doxorubicin: effect of ionizing radiation on apoptosis and TGF-beta production. *Exp Oncol.* **26**(2), 111–117.

Chou, T. and Talalay, P. (1983). Analysis of combined drug effects: a new look at a very old problem. *TIPS.* **4**, 450–454.

Curran,W. J. Jr., Paulus, R., Langer, C. J., Komaki, R., Lee, J. S., Hauser, S., Movsas, B., Wasserman, T., Rosenthal, S. A., Gore, E., Machtay, M., Sause, W. and Cox, J. D. (2011). Sequential vs Concurrent Chemoradiation for Stage III Non – Small Cell Lung Cancer: Randomized Phase III Trial RTOG 9410. *J Natl Cancer Inst.* **103**(19), 1452-1460.

Darby, S., McGale, P., Peto, R., Granath, F., Hall, P. and Ekbom, A. (2003). Mortality from cardiovascular disease more than 10 years after radiotherapy for breast cancer: nationwide cohort study of 90 000 Swedish women. *BMJ.* **326**(7383), 256–257.

Davis, R. J. (2000). Signal Transduction by the JNK Group of MAP Kinases. *Cell.* **103**(2), 239-252.

Davies, C. D. L., Lundstrøm, L. M., Frengen, J., Eikenes, L., Bruland, Ø. S., Kaalhus, O., Hjelstuen, M. H. and Brekken, C. (2004). Radiation Improves the Distribution and Uptake of Liposomal Doxorubicin (Caelyx) in Human Osteosarcoma Xenografts. *Cancer Res.* **64**(2), 547–553.

Damrot, J., Nübel, T., Epe, B., Roos, W. P., Kaina, B. and Fritz, G. (2006). Lovastatin protects human endothelial cells from the genotoxic and cytotoxic effects of the anticancer drugs doxorubicin and etoposide. *Br J Pharmacol*, **149**(8), 988–997.

de Lange, J. H., Schipper, N. W., Schuurhuis, G. J., Kate, T. K., van Heijningen, T. H., Pinedo, H. M., Lankelma, J. and Baak, J. P. (1992). Quantification by Laser Scan Microscopy of Intracellular Doxorubicin Distribution. *Cytometry*. **13**(6), 571–576.

DiPaola, R. S. (2002). To arrest or not to G(2)-M Cell-cycle arrest : commentary re: A. K. Tyagi et al., Silibinin strongly synergizes human prostate carcinoma DU145 cells to doxorubicin-induced growth inhibition, G(2)-M arrest, and apoptosis. *Clin Cancer Res*. **8**(11), 3311-3314.

Du, L., Lyle, C. S., Obey, T. B., Gaarde, W. A., Muir, J. A., Bennett, B. L. and Chambers, T. C. (2004). Inhibition of Cell Proliferation and Cell Cycle Progression by Specific Inhibition of Basal JNK Activity: Evidence that Mitotic Bcl-2 Phosphorylation is JNK Independent. *J Biol Chem*. **279**(12), 11957-11966.

Dunn, C., Wiltshire, C., MacLaren, A. and Gillespie, D. A. F. (2002). Molecular mechanism and biological functions of c-Jun N-terminal kinase signalling via the c-Jun transcription factor. *Cell Signal*. **14**(7), 585-593.

Ennis, B. W., Fultz, K. E., Smith, K. A., Westwick, J. K., Zhu, D., Boluro-ajayi, M., Bilter, J. K. and Stein, B. (2005). Inhibition of Tumor Growth, Angiogenesis, and Tumor Cell Proliferation by a Small Molecule Inhibitor of c-Jun N-terminal Kinase. *J Pharmacol Exp Ther*. **313**(1), 325–332.

Enomoto, A, Suzuki, N., Hirano, K., Matsumoto, Y., Morita, A, Sakai, K. and Koyama, H. (2000). Involvement of SAPK/JNK pathway in X-ray-induced rapid cell death of human T-cell leukemia cell line MOLT-4. *Cancer Letters*. **155**(2), 137–144.

Fornari, F. A, Randolph, J. K., Yalowich, J. C., Ritke, M. K. and Gewirtz, D. A. (1994). Interference by doxorubicin with DNA unwinding in MCF-7 breast tumor cells. *Mol Pharmacol*. **45**(4), 649–656.

Forrest, R. A., Swift, L. P., Rephaeli, A., Nudelman, A., Kimura, K., Phillips, D. R. and Cutts, S. M. (2012). Activation of DNA damage response pathways as a consequence of anthracycline-DNA adduct formation. *Biochem Pharmacol*. **83**(12), 1602-1612.

Franken, N. A., Rodermond, H. M., Stap, J., Haveman, J. and van Bree, C. (2006). Clonogenic assay of cells in vitro. *Nat Protoc*. **1**(5), 2315–2319.

Fritz, P., Kraus, H. J., Mühlnickel, W., Hammer, U., Dölken, W., Engel-riedel, W., Chemaissani, A. and Stoelben, E. (2006). Stereotactic , single-dose irradiation of stage I non-small cell lung cancer and lung metastases. *Radiat Oncol.* **1**:30.

Gabizon, A., Shmeeda, H. and Barenholz, Y. (2003). Pharmacokinetics of Pegylated Liposomal Doxorubicin: Review of Animal and Human Studies. *Clin Pharmacokinet*. **42**(5), 419–436.

Gabriels, K., Hoving, S., Seemann, I., Visser, N. L., Gijbels, M. J., Pol, J. F., Daemen, M. J., Stewart, F. A. and Heeneman, S. (2012). Local heart irradiation of ApoE$^{-/-}$ mice induces microvascular and endocardial damage and accelerates coronary atherosclerosis. *Radiother Oncol*. **105**(3), 358-364.

Galis, Z. S., Sukhova, G. K., Lark, M. W. and Libby, P. (1994). Increased expression of matrix metalloproteinases and matrix degrading activity in vulnerable regions of human atherosclerotic plaques. *J Clin Invest*. **94**(6), 2493-2503.

Gao, Y., Chen, T. and Raj, J. U. (2016). Endothelial and Smooth Muscle Cell Interactions in the Pathobiology of Pulmonary Hypertension. *Am J Respir Cell Mol Biol*. **54**(4), 451–460.

Geenen, M. M., Bakker, P. J. M., Kremer, L. C. M., Kastelein, J. J. P. and van Leeuwen, F. E. (2010). Increased Prevalence of Risk Factors for Cardiovascular Disease in Long-Term Survivors of Acute Lymphoblastic Leukemia and Wilms Tumour Treated with Radiotherapy. *Pediatr Blood Cancer.* **55**(4), 690-697.

Ghosh, J., Das, J., Manna, P. and Sil, P. C. (2011). The protective role of arjunolic acid against doxorubicin induced intracellular ROS dependent JNK-p38 and p53-mediated cardiac apoptosis. *Biomaterials*. **32**(21), 4857–4866.

Grethe, S., Coltella, N., Di Renzo, M. F. and Porn-Ares, M. I. (2006). p38 MAPK downregulates phosphorylation of Bad in doxorubicin-induced endothelial apoptosis. *Biochem Biophys Res Commun.* **347**(3), 781–790.

Gorodetsky, R., Levy-Agababa, F., Mou, X. and Vexler, A. M. (1998). Combination of cisplatin and radiation in cell culture: Effect of duration of exposure to drug and timing of irradiation. *Int J Cancer.* **75**(4), 635–642.

Goss, V. L., Cross, J. V, Ma, K., Qian, Y., Mola, P. W. and Templeton, D. J. (2003). SAPK/JNK regulates cdc2 / cyclin B kinase through phosphorylation and inhibition of cdc25c. *Cell Signal.* **15**(7), 709–718.

Guo, R. M., Xu, W. M., Lin, J. C., Mo, L. Q., Hua, X. X., Chen, P. X., Wu, K., Zheng, D. D. and Feng, J. Q. (2013). Activation of the p38 MAPK/NF-κB pathway contributes to doxorubicin-induced inflammation and cytotoxicity in H9c2 cardiac cells. *Mol Med Rep*. **8**(2), 603-608.

Gururajan, M., Chui, R., Karuppannan, A. K., Ke, J., Jennings, C. D. and Bondada, S. (2005). c-Jun N-terminal kinase (JNK) is required for survival and proliferation of B-lymphoma cells. *Blood*. **106**(4), 1382–1391.

Gutierrez, G. J., Tsuji, T., Chen, M., Jiang, W. and Ronai, Z. A. (2010). Interplay between Cdh1 and JNK activity during the cell cycle. *Nat Cell Biol.* **12**(7), 686–695.

Hagtvet, E., Røe, K. and Olsen, D. R. (2011). Liposomal doxorubicin improves radiotherapy response in hypoxic prostate cancer xenografts. *Radiat Oncol.* **6**:135.

Hallahan, D., Kuchibhotla, J. and Wyble, C. (1996). Cell Adhesion Molecules Mediate Radiation-induced Leukocyte Adhesion to the Vascular Endothelium. *Cancer Res*. **56**(22), 5150–5155.

Hamasu, T., Inanami, O., Tsujitani, M., Yokoyama, K., Takahashi, E., Kashiwakura, I. and Kuwabara, M. (2005). Post-irradiation hypoxic incubation of X-irradiated MOLT-4 cells reduces apoptotic cell death by changing the intracellular redox state and modulating SAPK/JNK pathways. *Apoptosis*. **10**(3), 557–567.

Hartwell, L. H. and Weinert, T. A. (1989). Checkpoints: Controls That Ensure the Order of Cell Cycle Events. *Science*. **246**(4930), 629-634.

Hatoum, O. A, Otterson, M. F., Kopelman, D., Miura, H., Sukhotnik, I., Larsen, B. T., Selle, R. M., Moulder, J. E. and Gutterman, D. D. (2006). Radiation induces endothelial dysfunction in murine intestinal arterioles via enhanced production of reactive oxygen species. *Arterioscler Thromb Vasc Biol.* **26**(2), 287–94.

Haugnes, H. S., Oldenburg, J. and Bremnes, R. M. (2014). Pulmonary and cardiovascular toxicity in long-term testicular cancer survivors. *Urol Oncol.* **33**(9), 399–406.

Haugnes, H. S., Wethal, T., Aass, N., Dahl, O., Klepp, O., Langberg, C. W., Wilsgaard, T., Bremnes, R. M. and Fossa, S. D. (2010). Cardiovascular Risk Factors and Morbidity in Long-Term Survivors of Testicular Cancer: A 20-Year Follow-Up Study. *J Clin Oncol*. **28**(30), 4649-4657.

Hayashi, T., Morishita, Y., Kubo, Y., Kusunoki, Y., Hayashi, I., Kasagi, F., Hakoda, M., Nakachi, K. and Nakachi, K. (2005). Long-term effects of radiation dose on inflammatory markers in atomic bomb survivors. *Amn J Med.* **118**(1), 83–86.

Hempel, G., Flege, S., Wu, G., Wurthwein, G. and Boos, J. (2002). Peak plasma concentrations of doxorubicin in children with acute lymphoblastic leukemia or non-Hodgkin lymphoma. *Cancer Chemother Pharmacol*. **49**(2), 133–141.

Hochegger, H., Takeda, S. and Hunt T. (2008). Cyclin-dependent kinases and cell-cycle transitions: does one fit all? *Nat Rev Mol Cell Biol*. **9**(11), 910-916.

Igarashi, K., Sakimoto, I., Kataoka, K., Ohta, K. and Miura, M. (2007). Radiation-induced senescence-like phenotype in proliferating and plateau-phase vascular endothelial cells. *Exp Cell Res.* **313**(15), 3326–3336.

Jaal, J. and Dorr, W. (2005). Early and long-term effects of radiation on intercellular adhesion molecule 1 (ICAM-1) expression in mouse urinary bladder endothelium. *Int J Radiat Biol*. **81**(5), 387–395.

Jagetia, G. C. and Nayak, V. (2000). Effect of Doxorubicin on Cell Survival and Micronuclei Formation in HeLa Cells Exposed to Different Doses of Gamma-radiation. *Strahlenther Onkol*. **176**(9), 422–428.

Jang, W. Y., Lee, J. Y., Lee, S. T., Jun D, Y. and Kim, Y. H. (2014). Inhibition of JNK2 and JNK3 by JNK inhibitor IX induces prometaphase arrest-dependent apoptotic cell death in human Jurkat T cells. *Biochem Biophys Res Commun*. **452**(3), 845-851.

Jeremic, B., Shibamoto, Y., Milicic, B., Nikolic, N., Dagovic, A., Aleksandrovic, J., Vaskovic, Z. and Tadic, L. (2017). Hyperfractionated Radiation Therapy With or Without Concurrent Low-Dose Daily Cisplatin in Locally Advanced Squamous Cell Carcinoma of the Head and Neck: a prospective randomized trial. *J Clin Oncol*. **18**(7), 1458–1464.

Kaffas, E. A., Al-Mahrouki, Tran, W. T., Giles, A. and Czarnota, G. J. (2014). Sunitinib effects on the radiation response of endothelial and breast tumor cells. *Microvasc Res*. **92**, 1-9.

Kanno, S. I., Yomogida, S., Tomizawa, A., Yamazaki, H., Ukai, K., Mangindaan, R. E., Namikoshi, M. and Ishikawa, M. (2014). Combined effect of papuamine and doxorubicin in human breast cancer MCF-7 cells. *Oncol Lett.* **8**(2), 547–550.

Kaplon, J., van Dam, L. and Peeper, D. (2015). Two-way communication between the metabolic and cell cycle machineries: the molecular basis. *Cell Cycle*. **14**(13), 2022-2032.

Karin, M. and Gallagher, E. (2005). From JNK to Pay Dirt: Jun Kinases, their biochemistry, Physiology and Clinical Importance. *IUBMB Life*. **57**(4-5), 283-295.

Kaushal, G., Kaushal, G. P., Melkaveri, S. N. and Mehta, P. (2004). Thalidomide protects endothelial cells from doxorubicin-induced apoptosis but alters cell morphology. *J Thomb Haemost.* **2**(2), 327–334. [1]

Kaushal, V., Kaushal, G. R. and Mehta, P. (2003). Differential Toxicity of Anthracyclines on Cultured Endothelial Cells. *Endothelium*. **11**(5-6). 253–258. [2]

Keltai, K., Cervenak, L., Makó, V., Doleschall, Z., Zsáry, A. and Karádi, I. (2010). Doxorubicin selectively suppresses mRNA expression and production of endothelin-1 in endothelial cells. *Vascul Pharmacol*. **53**(5-6), 209–214.

Kevil, C. G., Oshima, T., Alexander, B., Coe, L. L. and Alexander, J. S. (2000). H(2)O(2)-mediated permeability: role of MAPK and occludin. *Am J Physiol Cell Physiol*. **279**(1), C21-30.

Khan M. A., Hill, R. P. and Van Dyk J. (1998). Partial volume rat lung irradiation: an evaluation of early DNA damage. *Int J Radiat Oncol Biol Phys*. **40**(2), 467–476.

Killander, F. Anderson, H. Kjellen, E. and Malmstrom, P. (2014). Increased cardio and cerebrovascular mortality in breast cancer patients treated with postmastectomy radiotherapy – 25 year follow-up of a randomised trial from the South Sweden Breast Cancer Group. *Eur J Cancer*. **50**(13), 2201-2210.

Kim, J. and Freeman, M. R. (2003). JNK/SAPK mediates doxorubicin-induced differentiation and apoptosis in MCF-7 breast cancer cells. *Breast Cancer Res Treat*. **79**(3), 321-328.

Kim, J., Kim, T. H., Kang, H. S., Ro, J., Kim, H. S. and Yoon, S. (2009). SP600125, an inhibitor of Jnk pathway, reduces viability pf relatively resistant cancer cells to doxorubicin. *Biochem Biophys Res Commun.* **387**(3), 450-455.

Kim, J. A., Lee, J., Margolis, R. L. and Fotedar, R. (2010). SP600125 suppresses Cdk1 and induces endoreplication directly from G2 phase, independent of JNK inhibition. *Oncogene*, **29**(11), 1702–1716.

Kim, K. S., Kim, J. E., Choi, K. J., Bae, S. and Kim, D. H. (2014). Characterization of DNA damage-induced cellular senescence by ionizing radiation in endothelial cells. *Int J Radiat Biol.* **90**(1), 71–80.

Kortzerke, J., Gertler, R., Buchmann, I., Baur, R., Hombach, V., Norbert Reske, S. and Voisard, R. (2000). Different radiosensitivity of smooth muscle cells and endothelial cells in vitro as demonstrated by irradiation from a Re-188 filled balloon catheter. *Atherosclerosis*. **152**(1), 35-42.

Korwek, Z., Sewastianik, T., Bielak-Zmijewska, A., Mosieniak, G., Alster, O., Moreno-Villanueva, M., Burkle, A. and Sikora, E. (2012). Inhibition of ATM blocks the etoposide-induced DNA damage response and apoptosis of resting human T cells. *DNA Repair*. **11**(11), 864-873.

Kumar, P., Miller, A. I. and Polverini, P. J. (2004). P38 MAPK Mediates γ-Irradiation-induced Endothelial Cell Apoptosis, and Vasular Endothelial Growth Factor Protects Endothelial Cells through the Phosphoinositide 3-Kinase-Akt-Bcl-2 Pathway. *J Biol Chem*. **279**(41), 43352-43360.

Kurz, E. U., Douglas, P. and Lees-Miller, S. P. (2004). Doxorubicin activates ATM-dependent phosphorylation of multiple downstream targets in part through the generation of reactive oxygen species. *J Biol Chem*, **279**(51), 53272–53281.

Kuwabara, M., Takahashi, K. and Inanami, O. (2003). Induction of Apoptosis through the Activation of SAPK/JNK Followed by the Expression of Death Receptor Fas in X-irradiated Cells. *J Radiat Res.* **44**(3), 203–209.

Kwak, M. S., Yu, S. J., Yoon, J. H., Lee, S. H., Lee, S. M., Lee, J. M., Kim, Y. J., Lee, H. S. and Kim, C. Y. (2015). Synergistic anti - tumor efficacy of doxorubicin and flavopiridol in an in vivo hepatocellular carcinoma model. *J Cancer Res Clin Oncol*. **141**(11), 2037–2045.

Lapenna, S. and Giordano, A. (2009). Cell cycle kinases as therapeutic targets for cancer. *Nat Rev Drug Discov*. **8**(7), 547-566.

Lau, P., Baumstark-Khan, C., Hellweg, C. E. and Reitz, G. (2010). X-irradiation-induced cell cycle delay and DNA double-strand breaks in the murine osteoblastic cell line OCT-1. *Radiat Environ Biophys*. **49**(2), 271-280.

Lee, S. A, Dritschilo, A. and Jung, M. (2001). Role of ATM in oxidative stress-mediated c-Jun phosphorylation in response to ionizing radiation and CdCl2. *J Biol Chem*. **276**(15), 11783–11790.

Lee, S. M., Youn, B., Kim, C. S., Kim, C. S., Kang, C. and Kim, J. (2005). Gamma-Irradiation and Doxorubicin Treatment of Normal Human Cells Cause Cell Cycle Arrest Via Different Pathways. *Mol Cells*. **20**(3), 331–338.

Lee, C.L., Moding, E. J., Cuneo, K. C., Li, Y., Sullivan, J. M., Mao, L., Washington, I., Jeffords, L. B., Rodriques, R. S., Ma, Y., Das, S., Kontos, C. D., Kim, Y., Rockman, H. A. and Kirsch, D. G. (2012). p53 functions in endothelial cells to prevent radiation-induced myocardial injury in mice. *Sci Signal.* **5**(234), ra52.

Leppa, S. and Bohmann, D. (1999). Diverse functions of JNK signalling and c-Jun in stress response and apoptosis. *Oncogene*. **18,** 6158-6162.

Li, H., Cybulsky, M. I., Gimbrone, M. A. Jr. and Libby, P. (1993). An Atherogenic Diet Rapidly Induces VCAM-1, a Cytokine-Regulatable Mononuclear Leukocyte Adhesion Molecule, in Rabbit Aortic Endothelium. *Arterioscler Thromb.* **13**(2), 197-204.

Li, X., Commane, M., Jiang, Z. and Stark, G. R. (2001). IL-1-induced NFκB and c-Jun N-terminal kinase (JNK) activation diverge at IL-1 receptor-associated kinase (IRAK). *Proc Natl Acad Sci U S A*. **98**(8), 4461–4465.

Li, C., Ma, D., Chen, M., Zhang, L., Zhang, L., Zhang, J., Qu, X. and Wang, C. (2016). Ulinastatin attenuates LPS-induced human endothelial cells oxidative damage through suppressing JNK/c-Jun signaling pathway. *Biochem Biophysl Resh Commun.* **474**(3), 572–578.

Libby, P. (2012). Inflammation in atherosclerosis. *Nature.* **420**(6917), 868–874.

Lorenzo, E., Ruiz-Ruiz, C., Quesada, A. J., Hernandez, G., Rodriguez, A., Lopez-Rivas, A. and Redondo, J. M. (2002). Doxorubicin Induces Apoptosis and CD95 Gene Expression in Human Primary Endothelial Cells through a p53-dependent Mechanism. *J Biol Chem*. **277**(13), 10883–10892.

Lu, X., Proctor, S. and Dickinson, A. M. (2008). The effect of cryopreservation on umbilical cord blood endothelial progenitor cell differentiation. *Cell Transplant*. **17**(12), 1423- 1428.

Lukas, J., Lukas, C. and Bartek, J. (2004). Mammalian cell cycle checkpoints: signalling pathways and their organization in space and time. *DNA Repair (Amst).* **3**(8-9), 997–1007.

Lüpertz, R., Wätjen, W., Kahl, R. and Chovolou, Y. (2010). Dose- and time-dependent effects of doxorubicin on cytotoxicity, cell cycle and apoptotic cell death in human colon cancer cells. *Toxicology*. **271**(3), 115–121.

Magne, N., Castadot, P., Chargari, C., Di Leo, A., Philippson, C. and Van Houtte, P. (2009). Special focus on cardiac toxicity of different sequences of adjuvant doxorubicin/docetaxel/CMF regimens combined with radiotherapy in breast cancer patients. *Radiother Oncol*. **90**(1), 116-121.

Makarenko, V., V., Usatyuk, P. V., Yuan, G., Lee, M. M., Nanduri, J., Natarajan, V., Kumar, G. K. and Prabhakar, N. R. (2014). Intermittent hypoxia-induced endothelial barrier dysfunction requires ROS-dependent MAP kinase activation. *Am J Physiol Cell Physiol*. **306**(8), C745-C752.

Mandilaras, V., Bouganim, N., Spayne, J., Dent, R., Arnaout, A., Boileau, J. F., Brackstone, M., Meterissian, S. and Clemons, M. (2015). Concurrent chemoradiotherapy for locally advanced breast cancer — time for a new paradigm?. *Curr Oncol*. **22**(1), 25–32.

Maney, S. K., Johnson, A. M., Sampath Kumar, A, Nair, V., Santhosh Kumar, T. R. and Kartha, C. C. (2011). Effect of apoptosis-inducing antitumor agents on endocardial endothelial cells. *Cardiovasc Toxicol*. **11**(3), 253–262.

Mansouri, A., Ridgway, L. D., Korapati, A. L., Zhang, Q., Tian, L., Wang, Y., Siddik, Z. H., Mills, G. B. and Claret, F. X. (2003). Sustained Activation of JNK/p38 MAPK Pathways in Response to Cisplatin Leads to Fas Ligand Induction and Cell Death in Ovarian Carcinoma Cells. *J Biol Chem*. **278**(21), 19245–19256.

Mangge, H., Becker, K., Fuchs, D. and Gostner, J. M. (2014). Antioxidants, inflammation and cardiovascular disease. *World J Cardiol*. **6**(6), 462–477.

Matsuda, N., Horikawa, M., Wang, L. H., Yoshida, M., Okaichi, K., Okumura, Y. and Watanabe, M. (2000). Differential Activation of ERK 1/2 and JNK in Normal Human Fibroblast-like Cells in Response to UVC Radiation Under Different Oxygen Tensions. *Photochem Photobiol*. **72**(3), 334–339.

Meng, Q. and Xia, Y. (2011). c-Jun, at the crossroad of the signalling network. *Protein Cell.* **2**(11)**,** 889-898.

Milliat, F., Francois, A., Isoir, M., Deutsch, E., Tamarat, R., Tarlet, G., Atfi, A., Validire, P., Bourhis, J., Sabourin, J. C. and Benderitter, M. (2006). Influence of endothelial cells on vascular smooth muscle cells phenotype after irradiation: implication in radiation-induced vascular damages. *Am J Pathol*. **169**(4), 1484-1495.

Min, W. and Pober, J. S. (1997). TNF initiates E-selectin transcription in human endothelial cells through parallel TRAF-NF-kappa B and TRAF-RAC/CDC42-JNK-c-Jun/ATF2 pathways. *J Immunol*. **159**(7), 3508-3518.

Mingo-Sion, A. M., Marietta, P. M., Koller, E., Wolf, D. M. and Van Den Berg, C. L. (2004). Inhibition of JNK reduces G2/M transit independent of p53, leading to endoreduplication, decreased proliferation, and apoptosis in breast cancer cells. *Oncogene*. **23**(2), 596–604.

Mitchel, R. E., Hasu, M., Bugden, M., Wyatt, H., Little, M. P., Gola, A., Hildebrandt, G., Priest, N. D. and Whitman, S. C. (2011). Low-dose radiation exposure and atherosclerosis in ApoE-/- mice. *Radiat Res*. **175**(5), 665-676.

Monti, M., Terzuoli, E., Ziche, M. and Morbidelli, L. (2013). The sulphydryl containing ACE inhibitor Zofenoprilat protects coronary endothelium from Doxorubicin-induced apoptosis. *Pharmacol Res*. **76**, 171–181.

Morbidelli, L., Donnini, S. and Ziche, M. (2016). Targeting endothelial cell metabolism for cardio-protection from the toxicity of antitumor agents. *Cardio-Oncology*. 2:3.

Munshi, A., and Ramesh, R. (2013). Mitogen-activated protein kinases and their role in radiation response. *Genes Cancer*, **4**(9-10), 401–408.

Muslin A. J. (2008). MAPK Signaling in Cardiovascular Health and Disease: Molecular Mechanisms and Therapeutic Targets. *Clin Sci*. **115,** 203-218.

Murphy, J. B., Liu, J. H. and Sturm, E. (1922). Studies on X-ray effects: IX The action of serum from X-rayed animals on lymphoid cells in vitro. J Exp Med. **35**(3), 373-384.

Neuner, G., Patel, A. and Suntharalingam, M. (2009). Chemoradiotherapy for esophageal cancer. *Gastrointest Cancer Res*. **3**(2), 57-65.

Nilsson, G., Witt Nystrom, P., Isacsson, U., Garmo, H., Duvernoy, O., Sjogren, I., Lagerqvist, B., Holmberg, L. and Blomqvist, C. (2016). Radiation dose distribution in coronary arteries in breast cancer radiotherapy. *Acta Oncol*. **55**(8), 959-963.

Nishimura, Y. (2004). Rationale for chemoradiotherapy. *Int J Clin Oncol*. **9**(6), 414-420.

Nurse, P. and Bissett, Y. (1981). Gene required in G1 for commitment to cell cycle and in G2 for control of mitosis in fission yeast. *Nature*. **292**(5823), 558-560.

Nurse, P. (2002). Cyclin Dependent Kinases and Cell Cycle Control (Noble Lecture). *Chembiochem*. **3**(7), 596-603.

Octavia, Y., Tocchetti, C. G., Gabrielson, K. L., Janssens, S., Crijns, H. J. and Moens, A. L. (2012). Doxorubicin-induced cardiomyopathy: From molecular mechanisms to therapeutic strategies. *J Mol CellCardiol.* **52**(6), 1213–1225.

Ohe, Y. (2004). Chemoradiotherapy for lung cancer: Current status and perspectives. *Intl J Clin Oncol.* **9(**6), 435–443.

O'Neill, L. A. J. and Dinarello, C. A. (2000). The IL-1 receptor/toll-like receptor superfamily: crucial receptors for inflammation and host defense. *Immunol Today*. **21**(5), 206-209.

Osman, A. M., Bayoumi, H. M., Al-Harthi, S. E., Damanhouri, Z. A, and Elshal, M. F. (2012). Modulation of doxorubicin cytotoxicity by resveratrol in a human breast cancer cell line. *Cancer Cell Int.* **12**(1):47.

Osto, E., Matter, C. M., Kouroedov, A., Malinski, T., Bachschmid, M., Camici, G. G., Kilic, U., Stallmach, T., Boren, J., Iliceta, S., Luscher, T. F. and Cosentino, F. (2008). c-Jun N-terminal kinase 2 deficiency protects against hypercholesterolemia-induced endothelial dysfunction and oxidative stress. *Circulation.* **118,** 2073–2080.

Palayoor, S. T., John-Aryankalayil, M., Makinde, A. Y., Falduto, M. T., Magnuson, S. R. and Coleman, C. N. (2014). Differential Expression of Stress and Immune Response Pathway Transcripts and miRNAs in Normal Human Endothelial Cells Subjected to Fractionated or Single-Dose Radiation. *Mol Cancer Res*. **12**(7). 1002–1015.

Panganiban, R. A. M., Mungunsukh, O. and Day, R. M. (2013). X-irradiation induces ER stress, apoptosis and senescence in pulmonary artery endothelial cells. *Int J Radiat Biol*. **89**(8), 656-667.

Panteliadou, M., Touloupidis, S., Giatromanolaki, A., Pistevou, K., Kyrgias, G. Tsoutsou, P., Kalaitzis, C. and Koukourakis, M. I. (2011). Concurrent administration of liposomal doxorubicin improves the survival of patients with invasive bladder cancer undergoing hypofractionated accelerated radiotherapy (HypoARC). *Med Oncol.* **28**(4), 1356–1362.

Park, M. T., Oh, E. T., Song, M. J., Lee, H. and Park, H. J. (2012). Radio-sensitivities and angiogenic signaling pathways of irradiated normal endothelial cells derived from diverse human organs. *J Radiat Res*. **53**(4), 570–580.[1]

Park, M. T., Oh, E. T., Song, M. J., Kim, W. J., Cho, Y. U., Kim, S. J., Han, J. Y., Suh, J. K., Choi, E. K., Lim, B. U., Song, C. W. and Park, H. J. (2012). The radiosensitivity of endothelial cells isolated from human breast cancer and normal tissue in vitro. *Microvasc Res.* **84**(2), 140–148.[2]

Parplys, A. C., Petermann, E., Petersen, C., Dikomey, E. and Borgmann, K. (2012). DNA damage by X-rays and their impact on replication processes. *Radiother Oncol.* **102**(3), 466–471.

Patel, K. J., Tredan, O. and Tannock, I. F. (2013). Distribution of the anticancer drugs doxorubicin, mitoxantrone and topotecan in tumors and normal tissues. *Cancer Chemother Pharmacol*. **72**(1), 127-138.

Peled, M., Shaish, A., Greenberger, S., Katav, A., Hodish, I., Ben-Shushan, D., Barshack, I., Mendel, I., Frishman, L., Tal, R., Bangio, L., Breitbart, E. and Harats, D. (2008). Antiangiogenic systemic gene therapy combined with doxorubicin administration induced caspase 8 and 9-mediated apoptosis in endothelial cells and an anti-metastasis effect. *Cancer Gene Ther*. **15**(8), 535–542.

Petznek, H., Kleiter, M., Tichy, A., Fuchs-Baumgartinger, A. and Hohenadl, C. (2014). Murine xenograft model demonstrates significant radio-sensitising effect of liposomal doxorubicin in a combination therapy for Feline Injection Site Sarcoma. *Res Vet Sci*. **97**(2), 386–390.

Pietenpol, J. A. and Stewart, Z. A. (2002). Cell cycle checkpoint signaling : Cell cycle arrest versus apoptosis. *Toxicology*. **182**, 475–481.

Pinnix, C. C., Shah, J. J., Chuang, H., Costelloe, C. M., Medeiros, L. J., Wogan, C. F., reed, V., Smoth, G. L., Milgrom, S., Patel, K., Huo, J., Turturro, F., Romaquera, J., Fayad, L., Oki, Y., Fanale, M. A,, Westin, J., Nastoupil, L., Hagemeister, F. B., Rodriquez, A., Qazilbash, M., Shan, N., Bashir, Q., Ahmed, S., Nieto, Y., Hosing, C., Prabhakarpandian, B., Goetz, D. J., Swerlick, R. A., Chen, X. and Kiani, M. F. (2001). Expression and Functional Significance of Adhesion Molecules on Cultured Endothelial Cells in Response to ionizing radiation. *Microcirculation*. **8**(5), 355–364.

Potapova, O., Basu, S., Mercola, D. and Holbrook, N. J. (2001). Protective Role for c-Jun in the Cellular Response to DNA Damage. *J Biol Chem*. **276**(30), 28546-28553.

Potter, M. D., Suchowerska, N., Rizvi, S. and McKenzie, D. R. (2011). Hidden stressors in the clonogenic assay used in radiobiology experiments. *Australas Phys Eng Sci Med*. **34**(3), 345-350.

Praveen, K. and Saxena, N. (2013). Crosstalk between Fas and JNK Determines Lymphocyte Apoptosis after Ionizing Radiation. *Radiat Res.* **179**(6), 725–736.

Prise, K. M. and O'Sullivan, J. M. (2009). Radiation-induced bystander signalling in cancer therapy. *Nat Rev Cancer*. **9**(5), 351-360.

Quarmby, S., Kumar, P. and Kumar, S. (1999). Radiation-induced normal tissue injury: role of adhesion molecules in leukocyte-endothelial cell interactions. *Int J Cancer*. **82**(3), 385–395.

Ramaswamy, N. T., Ronai, Z. and Pelling, J. C. (1998). Rapid activation of JNK1 in UV-B irradiated epidermal keratinocytes. *Oncogene*. **16**(11), 1501-1505.

Rahaman, S. O., Lennon, D. J., Febbraio, M., Podrez, E. A., Hazen, S. L. and Silverstein, R. L. (2006). A CD36-dependent signaling cascade is necessary for macrophage foam cell formation. *Cell Metab*. **4**(3), 211-221.

Rajendran, P., Rengarajan, T., Thangavel, J., Nishigaki, Y., Sakthisekaran, D., Sethi, G. and Nishigaki, I. (2013). The Vascular Endothelium and Human Diseases. *Int J Biol Sci*. **9**(10), 1057–1069.

Ren, S., Li, C., Dai, Y., Li, N., Wang, X., Tian, F., Zhou, S., Qiu, Z., Lu, Y., Zhao, D., Chen, X. and Chen, D. (2014). Comparison of pharmacokinetics, tissue distribution and pharmacodynamics of liposomal and free doxorubicin in tumour-bearing mice following intratumoral injection. *J Pharm Pharmacol*. **66**(9), 1231-1239.

Ricci, R., Sumara, G., Sumara, I., Rozenberg, I., Kurrere, M., Akhmedov, A., Hersberger,M., Eriksson, U., Eberli, F. R., Becher, B., Boren, J., Chen, M., Cybulsky, M. I., Moore, K. J., Freeman, M. W., Wagner, E. F., Matter, C. M. and Luscher, T. F. (2004). Requirement of JNK2 for scavenger receptor A-mediated foam cell formation in atherogenesis. *Science*. **306,** 1558–1561.

Riquier, H., Wera, A.C., Heuskin, A.C., Feron, O., Lucas, S. and Michiels, C. (2013). Comparison of X-ray and alpha particle effects on a human cancer and endothelial cells: survival curves and gene expression profiles. *Radiother Oncol.* **106**(3), 397–403.

Rohren, E. and Dabaja, B. (2016). Doxorubicin-Based Chemotherapy and Radiation Therapy Produces Favorable Outcomes in Limited-Stage Plasmablastic Lymphoma : A Single-Institution Review. *Clin Lymphoma Myeloma Leuk,* **16**(3), 122–128.

Rombouts, C., Aerts, A., Beck, M., De Vos, W. H., Van Oostveldt, P., Benotmane, M. A., and Baatout, S. (2013). Differential response to acute low dose radiation in primary and immortalized endothelial cells. *Int J Radiat Biol.* **89**(10), 841–50.

Ryu, R. J., Eyal, S., Kaplan, H. G., Akbarzadeh, A., Hays, K., Puhl, K., Easterling, T. R., Berg, S. L., Scorsone, K. A., Feldma, E. M., Umans, J. G., Miodovnik, M. and Hebert, M. F. (2014). Pharmacokinetics of doxorubicin in pregnant women. *Cancer Chemother Pharmacol.* **73**(4), 789–797.

Rzeszowska-Wolny, J., Przybyszewski, W. M. and Widel, M. (2009). Ionizing radiation-induced bystander effects, potential targets for modulation of radiotherapy. *Eur J Pharmacol.* **625**, 156-164.

Sanchez-Perez, I., Murquia, J. R. and Perona, R. (1998). Cisplatin induces a persistent activation of JNK that is related to cell death. *Oncogene*. **16**(4), 533-540.

Sardaro, A., Petruzzelli, M. F., D'Errico, M. P., Grimaldi, L., Pili, G. and Portaluri, M. (2012). Radiation-induced cardiac damage in early left breast cancer patients : Risk factors , biological mechanisms , radiobiology , and dosimetric constraints. *Radiother Oncol.* **103**(2), 133–142.

Sato, K., Mizuno, Y., Fuchikami, H., Kato, M., Shimo, T., Kubota, J., Takeda, N., Inoue, Y., Seto, H. and Okawa, T. (2015). Comparison of radiation dose to the left anterior descending artery by whole and partial breast irradiation in breast cancer patients. *J Contemp Brachytherapy.* **7**(1), 23-28.

Scalia, R., Appel, J. Z. 3rd. and Lefer, A. M. (1998). Leukocyte-Endothelium Interaction During the Early Stages of Hypercholesterolemia in the Rabbit. Role of P-selectin, ICAM-1, and VCAM-1. Arterioscler Thromb Vasc Biol. **18**(7), 1093-1100.

Seemann, I., te Poele, J. A., Song, J. Y., Hoving, S., Russell, N. S. and Stewart, F. A. (2013). Radiation- and anthracycline-induced cardiac toxicity and the influence of ErbB2 blocking agents. *Breast Cacer Res Treat*. **141**(3), 385-395.

Seiwert, T. Y., Salama, J. K. and Vokes, E. E. (2007). The concurrent chemoradiation paradigm — general principles. *Nat Clin Pract Oncol*. **4**(2), 86–100.

Senkus-Konefka, E. and Jassem, J. (2007). Cardiovascular effects of breast cancer radiotherapy. *Cancer Treat Rev*. **33**(6), 578-593.

Seok, J. H., Park, K. A., Byun, H. S., Won, M., Shin, S., Choi, B., Lee, H., Kim, Y., R., Hong, J. H., Park, J. and Hur, G. M. (2008). Long-term Activation of c-Jun N-terminal Kinase through Receptor Interacting Protein is Associated with DNA Damage-induced Cell Death. *Korean J Physiol Pharmacol*. **12**(4), 185–191.

Sherman, E. J., Lim, S. H., Ho, A. L., Ghossein, R. A., Fury, M. G., Shaha, A. R. Rivera, M., Lin, O., Wolden, S., Lee, N. Y. and Pfister, D. G. (2011). Concurrent doxorubicin and radiotherapy for anaplastic thyroid cancer : A critical re-evaluation including uniform pathologic review. *Radiother Oncol*. **101**(3), 425–430.

Shinoda, C., Maruyama, M., Fujishita, T., Dohkan, J., Oda, H., Shinoda, K., Yamada, T., Miyabayashi, K., Hayashi, R., Kawagishi, Y., Fujita, T., Matsui, S., Sugiyama, E., Muraguchi, A. and Kobayashi, M. (2005). Doxorubicin induces expression of multidrug resistance-associated protein 1 in human small cell lung cancer cell lines by the c-jun N-terminal kinase pathway. *Int J Cancer*. **117**(1), 21–31.

Sitia, S., Tomasoni, L., Atzeni, F., Cordiano, C., Catapano, A., Tramontana, S., Perticone, F., Naccarato, P., Camici, P., Cortigiani, L., Bevilacqua, M., Milazzo, L., Cusi, D., Barlassina, C., Sarzi-Puttini, P. and Turiel, M. (2010). From endothelial dysfunction to atherosclerosis. *Autoimmun Rev*. **9**(12), 830-834.

Spallarossa, P., Altieri, P., Barisione, C., Passalacqua, M., Aloi, C., Fugazza, G., Frassoni, F., Podesta, M., Canepa, M., Ghigliotti, G. and Brunelli, C. (2010). p38 MAPK and JNK antagonistically control senescence and cytoplasmic p16INK4A expression in doxorubicin-treated endothelial progenitor cells. *PLoS One*, **5**(12), e15583.

Stein, W. D., Robey, R., Cardarelli, C., Gottesman, M. M. and Bates, S. E. (2003). Low and High Concentrations of the Topo II Inhibitor Daunorubicin in NIH3T3 Cells: Reversible G2/M Versus Irreversible G1 and S Arrest. *Cell Cycle*. **2**(2), 134–142.

Stewart, Z. A., Westfall, M. and Pietenpol, J. A. (2003). Cell-cycle dysregulation and anticancer therapy. *Trends Pharmacol Sci*. **24**(3), 139-145.

Stewart, F. A., Heeneman, S., Te Poele, J., Kruse, J., Russell, N. S., Gijbels, M. and Daemen, M. (2006). Ionizing radiation accelerates the development of atherosclerotic lesions in ApoE-/- mice and predisposes to an inflammatory plaque phenotype prone to hemorrhage. *Am J Pathol*.**168**(2), 649–658.

Stewart, F. A., Seemann, I., Hoving, S. and Russell, N. S. (2013). Understanding Radiation-induced Cardiovascular Damage and Strategies for Intervention. *Clin Oncol*. **25**(10), 617-624.

Sugihara, T., Hattori, Y., Yamamoto, Y., Qi, F., Ichikawa, R., Sato, A., Liu, M. Y., Abe, K. and Kanno, M. (1999). Preferential Impairement of Nitric Oxide-Mediated Endothelium-Dependent Relaxation in Human Cervical Arteries After Irradiation. *Circulation*. **100**(6), 635-641.

Sumara, G., Belwal, M. and Ricci, R. (2005). "Jnking" atherosclerosis. *Cell. Mol. Life Sci.* **62**(21), 2487–94.

Sun, X., Belkin, N. and Feinberg, M. W. (2013). Endothelial MicroRNAs and Atherosclerosis. *Curr Atheroscler Rep*. **15**(2). doi: 10.1007/s11883-013-0372-2. [1]

Sun, Y., Tang, S., Jin, X., Zhang, C., Zhao, W. and Xiao, X. (2013). Involvement of the p38 MAPK signaling pathway in S-phase cell-cycle arrest induced by Furazolidone in human hepatoma G2 cells. *J Appl Toxicol*. **33**(12), 1500–1505. [2]

Supiot, S., Gouard, S., Charrier, J., Apostolidis, C., Chatal, J., Barbet, J. and Cherel, M. (2005). Mechanisms of Cell Sensitization to Alpha Radioimmunotherapy by Doxorubicin or Paclitaxel in Multiple Myeloma Cell Lines. *Clin Cancer Res*. **11**, 7047s–7052s.

Swystun, L. L., Shin, L. Y., Beaudin, S. and Liaw, P. C. (2009). Chemotherapeutic agents doxorubicin and epirubicin induce a procoagulant phenotype on endothelial cells and blood monocytes. *J Thromb Haemost.* **7**(4), 619–626.

Tallarida, R. J. (2011). Quantitative methods for assessing drug synergism. *Genes Cancer.* **2**(11), 1003-1008.

Taylor, C. W., Povall, J. M., McGale, P., Nisbet, A., Dodwell, D., Smith, J. T. and Darby, S. C. (2008). Cardiac dose from tangential breast cancer radiotherapy in the year 2006. *Int J Radiat Oncol Biol Phys*. **72**(2), 501-507.

Thorn. C. F., Oshiro, C., March, S., Hernandez-Boussard, T., McLeod, H., Klein, T. E. and Altman, R. B. (2011). Doxorubicin pathways: pharmacodynamics and adverse effects. *Pharmacogenet Genomics*. **21**(7), 440-446.

Tournier, C. (2013). The 2 Faces of JNK Signaling in Cancer. *Genes Cancer.* **4**(9-10), 397-400.

Trevisan, M. G. and Poppi, R. J. (2003). Determination of doxorubicin in human plasma by excitation-emission matrix fluorescence and multi-way analysis. *Anal Chim Acta*. **493**, 69-81.

Valagussa, P., Zambetti, M., Biasi, S., Moliterni, A., Zucali, R. and Bonadonna, G. (1994). Cardiac effects following adjuvant chemotherapy and breast irradiation in operable breast cancer. *Ann Oncol*. **5**(3), 209-216.

van den Belt-Dusebout, A. W., Nuver, J., De Wit, R., Gietema, J. A., ten Bokkel Huinink, W. W., Rodrigus, P. T., Schimmel, E. C., Aleman, B. M. and van Leeuwen, F. E. (2006). Long-term risk of cardiovascular disease in 5-year survivors of testicular cancer. *J Clin Oncol*. **24**(3), 467-475.

Veheij, M., Bose, R., Lin, X. H., Yao, B., Jarvis, W. D., Grant, S., Birrer, M. J., Szabo, E., Zon, L. I., Kyriakis, J. M., Haimovitz-Friedman, A., Fuks, Z. and Kolesnick, R. N. (1996). Requirement for ceramide-initiated SAPK/JNK signalling in stress-induced apoptosis. *Nature*. **380**(6569), 75-79.

Verheij, M., Ruiter, G. A., Zerp, S. F., van Blitterswijk, W. J., Fuks, Z., Haimovitz-Friedman, A. and Bartelink, H. (1998). The role of the stress-activated protein kinase (SAPK / JNK) signaling pathway in radiation-induced apoptosis. *Radiother Oncol.* **47**(3), 225–232.

Wang, S., Konorev, E. A., Kotamraju, S., Joseph, J., Kalivendi, S. and Kalyanaraman, B. (2004). Doxorubicin Induces Apoptosis in Normal and Tumor Cells via distinctly different mechanisms. intermediacy of H(2)O(2)- and p53-dependent pathways. *J Biol Chem*. **279**(24), 25535–25543.

Wang, J., An, F. S., Zhang, W., Gong, L., Wei, S. J., Qin, W. D., Wang, X. P., Zhao, Y. X., Zhang, Y., Zhang, C. and Zhang, M. X. (2011). Inhibition of c-Jun N-terminal kinase attenuates low shear stress-induced atherogenesis in apolipoprotein E-deficient mice. *Mol Med*.**17**(9-10), 990-999.

Wethal., T., Nedregaard, B., Andersen, R., Fossa, A., Lund, M. B., Gunther, A., Kvaloy, S., Fossa, S. D. and Kjekshus, J. (2014). Atherosclerotic lesions in lymphoma survivors treated with radiotherapy. *Radiother Oncol*. **110** (3), 448-454.

Weston, C. R. and Davis, R. J. (2002). The JNK signal transduction pathway. *Curr Opin Cell Biol*. **12,** 14-21.

Widel, M., Krzywon, A., Gajda, K., Skonieczna, M., and Rzeszowska-Wolny, J. (2014). Induction of bystander effects by UVA, UVB, and UVC radiation in human fibroblasts and the implication of reactive oxygen species. *Free Radic Biol Med*. **68**, 278–287.

Wilkinson, E. L., Sidaway, J. E. and Cross, M. J. (2016). Cardiotoxic drugs Herceptin and doxorubicin inhibit cardiac microvascular endothelial cell barrier formation resulting in increased drug permeability. *Biol Open*. **5**(10), 1362–1370.

Wojcik, T., Buczek, E., Majzner, K., Kolodziejczyk, A., Miszczyk, J., Kaczara, P., Kwiatek, W., Baranska, M., Szymonski, M. and Chlopicki, S. (2015). Comparative endothelial profiling of doxorubicin and daunorubicin in cultured endothelial cells. *Toxicol In Vitro*. **29**(3), 512–521.

Woodley-Cook, J., Shin, L. Y., Swystun, L., Caruso, S., Beaudin, S. and Liaw, P. C. (2006). Effects of the chemotherapeutic agent doxorubicin on the protein C anticoagulant pathway. *Mol Cancer Ther.* **5**(12), 3303–3311.

Wu, S., Ko, Y. S., Teng, M. S., Ko, Y. L., Hsu, L. A., Hsueh, C., Chou, Y. Y., Liew, C. C. and Lee, Y. S. (2002). Adriamycin-induced Cardiomyocyte and Endothelial Cell Apoptosis: *In Vitro* and *In Vivo* Studies. *J Mol Cell Cardiol*. **34**(12), 1595-1607.

Yamada, T., Egashira, N., Bando, A., Nishime, Y., Tonogai, Y., Imuta, M., Yano, T. and Oishi, R. (2012). Activation of p38 MAPK by oxidative stress underlying epirubicin-induced vascular endothelial cell injury. *Free Radic Biol Med.* **52**(8), 1285-1293.

Yang, H., Asaad, N. and Held, K. D. (2005). Medium-mediated intercellular communication is involved in bystander responses of X-ray-irradiated normal human fibroblasts. *Oncogene*. **24**(12), 2096-2103.

Yang, F., Chen, H., Liu, Y., Yin, K., Wang, Y., Li, X., Wang, G., Wang, S., Tan, X., Xu, C., Lu, Y. and Cai, B. (2013). Doxorubicin caused apoptosis of mesenchymal stem cells via p38, JNK and p53 pathway. *Cell Physiol Biochem.* **32**(4), 1072-1082.

Yang, F., Teves, S. S., Kemp, C. J. and Henikoff, S. (2014). Doxorubicin, DNA torsion, and chromatin dynamics. *Biochim Biophys Acta*. **1845**(1), 84-89.

Zambetti, M., Moliterni, A., Materazzo, C, Stefanelli, M., Cipriani, S., Valagussa, P., Bonadonna, G. and Gianni, L. (2001). Long-term cardiac sequelae in operable breast cancer patients given adjuvant chemotherapy with or without doxorubicin and breast irradiation. *J Clin Oncol*. **19**(1), 37-43.

Zembruski, N. C., Stache, V., Haefeli, W. E., and Weiss, J. (2012). 7-Aminoactinomycin D for apoptosis staining in flow cytometry. *Anal Biochem*. **429**(1), 79–81.

Zhang, S. H., Wang, W. Q. and Wang, J. L. (2009). Protective effect of tetrahydroxystilbene glucoside on cardiotoxicity induced by doxorubicin in vitro and in vivo. *Acta Pharmacologica Sin*. **30**(11), 1479–1487.

Zhang, H. P., Takayama, K., Su, B., Jiao, X. D., Li, R. and Wang, J. J. (2011). Effect of Sunitinib Combined with Ionizing Radiation on Endothelial Cells. *J Radiat Res*. **52**(1), 1-8.

Zhang, X. M., Li, Y. X., Wang, W. H., Jin, J., Wang, S. L., Liu, Y. P., Song, Y. W., Ren, H., Fang, H., Zhou, L. Q., Chen, B., Qi, S. N., Liu, Q. F., Lu, N. N., Liu, X. F. and Yu, Z. H. (2013). Favorable outcome with doxorubicin-based chemotherapy and radiotherapy for adult patients with early stage primary systemic anaplastic large-cell lymphoma. *Eur J Haematol*. **90**(3), 195–201.

Zhao, M., Liu, Y., Wang, X., New, L., Han, J. and Brunk, U. T. (2002). Activation of the p38 MAP kinase pathway is required for foam cell formation from macrophages exposed to oxidized LDL. *APMIS.* **110**(6), 458-468.

Zhou, H., Suzuki, M., Geard, C. R. and Hei, T. K. (2002). Effects of irradiated medium with or without cells on bystander cell responses. *Mutat Res*. **499**(2), 135-141.

Zingg, D., Riesterer, O., Fabbro, D., Glanzmann, C., Bodis, S. and Pruschy, M. (2004). Differential Activation of the Phosphatidylinositol 3'-Kinase/Akt Pathway by Ionizing Radiation in Tumour and Primary Endothelial Cells. *Cancer Res*. **64**(15), 5398-5406.